SIGNAL REPRESENTATION AND RECOVERY UNDER PARTIAL INFORMATION, REDUNDANCY, AND GENERALIZED FINITE EXTENT CONSTRAINTS

A THESIS

SUBMITTED TO THE DEPARTMENT OF ELECTRICAL AND

ELECTRONICS ENGINEERING

AND THE INSTITUTE OF ENGINEERING AND SCIENCES

OF BILKENT UNIVERSITY

IN PARTIAL FULFILLMENT OF THE REQUIREMENTS

FOR THE DEGREE OF

MASTER OF SCIENCE

By

Sevinç Figen Öktem

July 2009

I certify that I have read this thesis and that in my opinion it is fully adequate, in scope and in quality, as a thesis for the degree of Master of Science.

Prof. Dr. Haldun M. Özaktaş(Supervisor)

I certify that I have read this thesis and that in my opinion it is fully adequate, in scope and in quality, as a thesis for the degree of Master of Science.

Prof. Dr. Orhan Arıkan

I certify that I have read this thesis and that in my opinion it is fully adequate, in scope and in quality, as a thesis for the degree of Master of Science.

Asst. Prof. Dr. Çağatay Candan

Approved for the Institute of Engineering and Sciences:

Prof. Dr. Mehmet Baray
Director of Institute of Engineering and Sciences

ABSTRACT

SIGNAL REPRESENTATION AND RECOVERY UNDER PARTIAL INFORMATION, REDUNDANCY, AND GENERALIZED FINITE EXTENT CONSTRAINTS

Sevinç Figen Öktem
M.S. in Electrical and Electronics Engineering
Supervisor: Prof. Dr. Haldun M. Özaktaş
July 2009

We study a number of fundamental issues and problems associated with linear canonical transforms (LCTs) and fractional Fourier transforms (FRTs). First, we study signal representation under generalized finite extent constraints. Then we turn our attention to signal recovery problems under partial and redundant information in multiple transform domains. In the signal representation part, we focus on sampling issues, the number of degrees of freedom, and the time-frequency support of the set of signals which are confined to finite intervals in two arbitrary linear canonical domains. We develop the notion of bicanonical width product, which is the generalization of the ordinary time-bandwidth product, to refer to the number of degrees of freedom of this set of signals. The bicanonical width product is shown to be the area of the time-frequency support of this set of signals, which is simply given by a parallelogram. Furthermore, these signals can be represented in these two LCT domains with the minimum number of samples given by the bicanonical width product. We prove that with these samples the discrete LCT provides a good approximation to the continuous LCT due to the

underlying exact relation between them. In addition, the problem of finding the minimum number of samples to represent arbitrary signals is addressed based on the LCT sampling theorem. We show that this problem reduces to a simple geometrical problem, which aims to find the smallest parallelogram enclosing a given time-frequency support. By using this equivalence, we see that the bicanonical width product provides a better fit to the actual number of degrees of freedom of a signal as compared to the time-bandwidth product. We give theoretical bounds on the representational efficiency of this approach. In the process, we accomplish to relate LCT domains to the time-frequency plane. We show that each LCT domain is essentially a scaled FRT domain, and thus any LCT domain can be labeled by the associated fractional order, instead of its three parameters. We apply these concepts knowledge to the analysis of optical systems with arbitrary numbers of apertures. We propose a method to find the largest number of degrees of freedom that can pass through the system. Besides, we investigate the minimum number of samples to represent the wave at any plane in the system. In the signal recovery part of this thesis, we study a class of signal recovery problems where partial information in two or more fractional Fourier domains are available. We propose a novel linear algebraic approach to these problems and use the condition number as a measure of redundant information in given samples. By analyzing the effect of the number of known samples and their distributions on the condition number, we explore the redundancy and information relations between the given data under different partial information conditions.

Keywords: Linear canonical transform, fractional Fourier transform, bicanonical width product, linear canonical series, linear canonical domain, signal representation, signal recovery, sampling, finite extent, partial information, redundancy, condition number, optics

ÖZET

KISMİ BİLGİ, ARTIKLIK VE GENELLEŞTİRİLMİŞ SONLU KAPLAM KISITLARI ALTINDA SİNYAL TEMSİLİ VE GERİ ÇATILMASI

Sevinç Figen Öktem
Elektrik ve Elektronik Mühendisliği Bölümü Yüksek Lisans
Tez Yöneticisi: Prof. Dr. Haldun M. Özaktaş
Temmuz 2009

Bu tezde doğrusal doğal ve kesirli Fourier dönüşümleri ile ilgili bir çok temel konu ve problem ele alındı. İlk olarak, genelleştirilmiş sonlu kaplam kısıtları altında sinyalin temsil edilmesi üzerine çalışıldı. Sonra birden çok dönüşüm bölgesinde kısmi ve artık bilgiler verildiğinde, sinyalin geri çatılması problemiyle uğraşıldı. Sinyalin temsili kısmında, herhangi iki doğrusal doğal bölgede sonlu aralıklara hapis olan sinyallerin örnekleme, serbestlik derecesi, ve zaman-sıklık tanım alanı konularına odaklanıldı. Bu sinyallerin serbestlik derecesi için zaman-bant genişliği çarpımının genellenmesi olan ikili doğrusal doğal genişlik çarpımı kavramı geliştirildi. İkili doğrusal doğal genişlik çarpımının bu sinyallerin paralelkenar şeklindeki zaman-sıklık tanım alanına karşılık geldiği ispatlandı. Ayrıca, bu sinyaller ikili doğrusal doğal genişlik çarpımına eşit sayıdaki en az örnek sayısı ile bu iki doğrusal doğal bölgede temsil edilebilir. Bu örneklerle hesaplanan ayrık doğrusal doğal dönüşümünün, sürekli doğrusal dönüşüm için oldukça iyi bir yaklaşım verdiği aralarındaki tam ilişki verilerek ispatlandı. Bunun yanısıra, rastgele sinyallerin en az örnek ile temsil edilmesi problemine, doğrusal doğal dönüşüm örnekleme teoremi kullanılarak bakıldı. Bu problemin

zaman-sıklık tanım alanını içine alan en küçük paralelkenarı bulma problemine karşılık geldiği ispatlandı. Bundan yararlanılarak, ikili doğrusal doğal genişlik çarpımının sinyallerin serbestlik derecesine zaman-bant genişliği çarpımından daha çok yaklaştığı görüldü. Bu yaklaşımın temsili verimliliği için kuramsal sınırlar verildi. Ayrıca, doğrusal doğal bölgelerin zaman-sıklık düzlemi ile ilişkisi kuruldu. Her doğrusal doğal bölgenin aslında ölçeklenmiş kesirli Fourier bölgelerine karşılık geldiği ve herhangi bir doğrusal doğal bölgenin ilişkili olduğu kesir değeri ile etiketlenebileceği ispatlandı. Bu kavramlar açıklıklı optik sistemlerin incelenmesi konusunda kullanıldı. Sistemin serbestlik derecesinin bulanabilmesini sağlayan bir method geliştirildi. Bunun yanı sıra, dalganın herhangi bir düzlemde en az ne kadar örnek ile temsil edilebileceği araştırıldı. Tezin diğer kısmında ise, iki yada daha çok kesirli Fourier bölgelerinde kısmi bilgiler verildiğinde sinyalin geri çatılması üzerine çalışıldı. Bu problem için yeni bir doğrusal cebirsel yaklaşım sunuldu ve kararsızlık oranı verilen noktalar arasındaki artık bilgi miktarının ölçüsü olarak kullanıldı. Kararsızlık oranının bilinen nokta sayısı ve diziliminden nasıl etkilendiği incelenerek, verilen noktalar arasındaki artıklık ve bilgi ilişkileri araştırıldı.

Anahtar Kelimeler: Doğrusal doğal dönüşüm, kesirli Fourier dönüşümü, ikili doğrusal doğal genişlik çarpımı, doğrusal doğal dizisi, doğrusal doğal bölge, sinyal temsili, sinyalin geri çatılması, örnekleme, sonlu kaplam, kısmi bilgi, artıklık, kararsızlık oranı, optik

ACKNOWLEDGMENTS

I would like to express my sincere gratitude to my supervisor, Prof. Dr. Haldun Özaktaş for his invaluable guidance, support, and encouragement throughout my MS studies. It would be an understatement to say that I learnt a lot from him.

I am grateful to the members of my thesis committee, Prof. Dr. Orhan Arıkan and Asst. Prof. Çağatay Candan for reading and commenting on this thesis.

I am thankful to Department of Electrical and Electronics Engineering at Bilkent University, and TÜBİTAK, The Scientific and Technological Research Council of Turkey, for providing financial support during my MS studies.

I would like to thank my friends inside and outside the department, especially Ezgi, Hakan, Bora, Esra and Ata for their constant moral support during all of my endeavors.

Finally, I would like to give my special thanks to my family for their understanding, love and support throughout my life.

Contents

List of Figures

List of Tables

Dedicated to my lovely family

Chapter 1

INTRODUCTION

Linear canonical transforms (LCTs) are a three-parameter family of integral transforms with wide application in optical, acoustical, electromagnetic, and other wave propagation problems. The Fourier and fractional Fourier transforms, coordinate scaling, and chirp multiplication and convolution operations, are special cases of LCTs. In this thesis, we will study a number of fundamental issues and problems associated with linear canonical and fractional Fourier transforms. First, we will study signal representation under generalized finite extent constraints. Then we will turn our attention to signal recovery problems under partial and redundant information in multiple transform domains.

In the first part, we deal with signals which are confined to finite intervals in fractional Fourier domains or linear canonical domains. We investigate sampling issues, the number of degrees of freedom, and the time-frequency support of this set of signals. Earlier works in the literature deal with time- and band-limited signals. Thus, when the time and frequency extents of signals are specified, the sampling issues, number of degrees of freedom, and time-frequency support are well-established. The number of degrees of freedom of time- and band-limited

signals is given by the time-bandwidth product, which is of fundamental importance in many areas of signal processing, and this is simply the area of the time-frequency support of these signals given by a rectangular region.

However, it is always possible to specify the extent of a signal in other fractional Fourier or linear canonical domains. For instance, in applications where the underlying physics involves LCT type integrals as is the case with propagation problems, specification of the extents in the LCT domains may provide a much better fit to the set of signals we are dealing with.

We find an expression for the number of degrees of freedom of signals confined to finite intervals in two LCT domains, and refer to this new quantity as the *bicanonical width product*. This result is significant since it constitutes a generalization of the time-bandwidth product. Moreover, to find the time-frequency support of LCT-limited signals, we clearify the notion of LCT domains. FRT domains are well-defined in the time-frequency plane; from analogy with FRT domains, the term *LCT domains* has been used in the literature without reference to their relationship to the time-frequency plane. One of the contributions of this work is to figure out where LCT domains exist in the ordinary time-frequency plane. With this, we show that the time-frequency support of the set of signals we are dealing with is a parallelogram and its area is given by the bicanonical width product. Furthermore, we can represent these signals in the specified LCT domains with the minimum number of samples, which equals to the number of degrees of freedom. We prove that with these samples discrete LCT provides a good approximation to the continuous LCT due to the underlying exact relation between them.

We then turn our attention to arbitrary sets of signals with arbitrary time-frequency support. We investigate the minimum number of samples to represent an arbitrary signal based on the LCT sampling criteria and the LCT domains that we can represent the signal with that minimum number of samples. This

investigation reduces to a simple geometric problem, which aims to find the smallest parallelogram enclosing a given time-frequency support. We give theoretical bounds on the representational efficiency of this approach compared to the actual number of degrees of freedom of the signals and minimum number of samples given by the classical approach. We also extend this approach to represent signals at a specific domain.

Finally, we apply these concepts to the analysis of optical systems. We propose a method to find the largest number of degrees of freedom that can pass through the system without any information loss. Besides, we investigate the minimum number of samples to represent the physical signal at an arbitrary plane in the system and use these samples to simulate the optical system with discrete-time systems.

In the second part, instead of paying our attention to the number of samples, we are interested in their distribution to multiple domains. We mainly study a class of signal recovery problems where partial information in two or more fractional Fourier domains are available and the aim is to find the unknown signal values by consolidating the known information. These problems have been motivated by the existence of applications in optical, acoustical, electromagnetic, and other wave propagation problems. This is because, the propagation of waves can be considered as a process of continual fractional Fourier transformation.

Our purpose in this part is to investigate the redundancy and information relations between the given data under different partial information constraints. For this purpose, we propose a novel linear algebraic approach to these problems and formulate the problem as a linear system of equations. Then, we deal with the sensitivity issues of ill-posed problems and use the condition number as a measure of redundant information in given samples. By analyzing the effect of the number of known samples and their distributions on the condition number, we aim to explore the redundancy and information relations between the given

data and independently from the signal to be recovered. Then, we apply this approach to a number of distributions for cases when total number of knowns is equal to and more than the number of unknowns.

In the process, we investigate the influence or dependency of a point in one domain to the points in the other domain for both continuous-time and discrete-time systems. We observe that a point in one domain affects (or is affected by) more samples in the other domain as the fractional order increases. We use these concepts to interpret the simulation results.

In Chapter 2, we present the exact relation between the continuous and discrete linear transforms. Chapter 3 discusses the bicanonical width product and its relationship to space-frequency plane. In Chapter 4, we investigate the problem of finding the minimum number of samples to represent arbitrary signals based on the LCT sampling criteria. In Chapter 5, we apply these concepts to analyze optical systems with arbitrary number of apertures. Chapter 6 investigates the effect of one point in the input to the points in the output as a function of fractional order when the output is related to its input through a FRT. In Chapter 7, we provide a linear algebraic approach to the signal recovery problems under partial and redundant information in multiple transform domains. We conclude in Chapter 8.

Chapter 2

EXACT RELATION BETWEEN CONTINUOUS AND DISCRETE LINEAR CANONICAL TRANSFORMS

2.1 Introduction

Discrete counterparts of continuous transforms are not only of intrinsic interest, but are important for approximately computing the samples of continuous transforms. For instance, the discrete Fourier transform (DFT) is commonly used to obtain the samples of the Fourier transform (FT) of a function from the samples of the original function.

Linear canonical transforms (LCTs) are a three-parameter family of integral transforms with wide application in wave propagation problems [2] and have also found use in optimal filtering [3]. The Fourier and fractional Fourier transforms, coordinate scaling, and chirp multiplication and convolution operations,

are special cases of LCTs. In this letter, we derive the exact relation between the continuous LCT and the discrete LCT (DLCT) defined in [4] and implemented in [5]. This provides the underlying foundation for approximately computing the samples of the LCT of a continuous signal by replacing the transform integral with a finite sum, and constitutes a generalization of the exact relation between continuous and discrete FTs, which has been regarded as a fundamental theorem by Papoulis [6]. Consequently, the DLCT in this letter approximates the continuous LCT in the same sense that the DFT approximates the continuous FT.

To state the above mentioned theorem for FTs, let $f(u)$ and $F(\mu)$ be a continuous-time signal and its FT, and define the periodically replicated functions

$$\bar{f}(u) \equiv \sum_{n=-\infty}^{\infty} f(u - n\Delta u), \ \bar{F}(\mu) \equiv \sum_{n=-\infty}^{\infty} F(\mu - n\Delta\mu), \tag{2.1}$$

where Δu and $\Delta\mu$ are arbitrary. Then, the samples of these functions form a DFT pair as follows for any m:

$$\bar{F}(m\,\delta\mu) = \delta u \sum_{k\in<N>} \bar{f}(k\,\delta u) e^{-i2\pi mk/N}, \tag{2.2}$$

where $\delta u = 1/\Delta\mu$, $\delta\mu = 1/\Delta u$, $N = \Delta u \Delta\mu$, and $<N>$ denotes any interval of length N. This exact relation between the continuous and discrete ordinary Fourier transforms, provides the basis for approximately computing the samples of the continuous FT of a function by using the DFT.

In addition to generalizing the above fundamental theorem to LCTs, we also show that it can be expressed in terms of a new definition of the DLCT which, unlike certain earlier definitions, can be explicitly expressed without reference to the underlying continuous functions or their extents and sampling intervals. This new definition would be useful in studies which are formulated in a purely discrete setting and in developing fast transform algorithms. In the process we define the linear canonical series, which is the generalization of the ordinary Fourier series.

We also compare a computational algorithm based on these definitions of the DLCT, with earlier proposed algorithms. Furthermore, we find an expression for the number of degrees of freedom of signals confined to finite intervals in the time and LCT domains. This result is significant since it constitutes a generalization of the time-bandwidth product. We refer to this new quantity as the *time-canonical width product* or more generally the *bicanonical width product*. The results presented in this chapter has been recently published in [7].

2.2 Discrete Linear Canonical Transforms

The LCT with parameter matrix $\mathbf{M}$ is defined as [8]

$$f_{\mathbf{M}}(u) \equiv (\mathcal{C}_{\mathbf{M}} f)(u) \equiv \int_{-\infty}^{\infty} C_{\mathbf{M}}(u,u') f(u')\, du', \qquad (2.3)$$
$$C_{\mathbf{M}}(u,u') \equiv \sqrt{\beta}\, e^{-i\pi/4}\, e^{i\pi(\alpha u^2 - 2\beta u u' + \gamma u'^2)},$$

where $\mathcal{C}_{\mathbf{M}}$ is the LCT operator, and α, β, γ are real parameters. The transform is unitary and $C^{-1}_{\mathbf{M}}(u,u') = C_{\mathbf{M}^{-1}}(u,u') = C^{*}_{\mathbf{M}}(u',u)$. The unit-determinant matrix $\mathbf{M}$ is equivalent to the three parameters and either set of parameters can be obtained from the other [8]: $\mathbf{M} \equiv [\gamma/\beta,\ 1/\beta;\ \ -\beta + \alpha\gamma/\beta,\ \alpha/\beta]$. The LCT reduces to the ath-order fractional Fourier transform (FRT) when $\alpha = \cot(a\pi/2)$, $\beta = \csc(a\pi/2)$, $\gamma = \cot(a\pi/2)$ [2] . The FRT operator $\mathcal{F}^a$ is additive in index: $\mathcal{F}^{a_2}\mathcal{F}^{a_1} = \mathcal{F}^{a_2+a_1}$ and reduces to the ordinary FT and identity operators for $a = 1$ and $a = 0$ respectively.

The discrete LCT $\hat{f}_{\mathbf{M}}(m\,\delta u_{\mathbf{M}})$ of $\hat{f}(k\,\delta u)$ has been defined as follows for $m = -N/2, \ldots, N/2-1$ [4, 5]:

$$\hat{f}_{\mathbf{M}}(m\,\delta u_{\mathbf{M}}) \equiv \delta u \sum_{k=-N/2}^{N/2-1} \hat{f}(k\,\delta u)\, C_{\mathbf{M}}(m\,\delta u_{\mathbf{M}}, k\,\delta u), \qquad (2.4)$$

$$C_{\mathbf{M}}(m\,\delta u_{\mathbf{M}}, k\,\delta u) = \sqrt{\beta}\, e^{-i\pi/4} e^{i\pi \frac{1}{N|\beta|}(\alpha \frac{\delta u_{\mathbf{M}}}{\delta u} m^2 - 2\beta k m + \gamma \frac{\delta u}{\delta u_{\mathbf{M}}} k^2)},$$

where $\delta u_{\mathbf{M}} = (|\beta| N \delta u)^{-1}$. Here δu and $\delta u_{\mathbf{M}}$ are the sampling intervals in the time and LCT domains. N is the number of samples. The carets in (2.4) are to remind us that $\hat{f}_{\mathbf{M}}$ is not the continuous LCT of $\hat{f}$. The special case of (2.4) corresponding to the FRT has been defined in [9], but we note that this definition is different than the discrete FRT given in [10]. The definition in (2.4) can be made unitary by including an additional factor $\sqrt{\delta u_{\mathbf{M}}/\delta u}$ in front of the summation.

The definition in (2.4), while suitable for certain purposes, is not a usual way of defining a discrete transform, since the transform matrix exhibits the undesirable quality of depending on the sampling intervals, whereas ideally it would depend only on the number of samples N and the transform parameters α, β, γ. One of the contributions of this letter is to show that an interval-independent definition of the DLCT can still be used to approximately compute continuous LCTs with arbitrary sampling intervals.

We express the transform matrix of this interval-independent and unitary definition of the DLCT as follows:

$$\mathbf{C}_{\mathbf{M}}[m,k] = \frac{\sqrt{\beta}\, e^{-i\pi/4}}{\sqrt{N|\beta|}} e^{i\pi \frac{1}{N|\beta|}(\alpha m^2 - 2\beta km + \gamma k^2)}. \tag{2.5}$$

This corresponds to the matrix elements in (2.4) with $\delta u = \delta u_{\mathbf{M}}$. We will demonstrate in Section 2.3 how to use this interval-independent DLCT to exactly compute DLCTs as defined in (2.4), as well as to approximately compute continuous LCTs.

2.3 Fundamental Theorem for LCTs

Let $f(u)$ and $f_{\mathbf{M}}(u)$ be a continuous-time signal and its LCT with parameters α, β, γ. Define the following periodically replicated functions where each period has been modulated with varying phase terms:

$$\bar{f}(u)_{(\mathbf{M}^{-1},\Delta u)} \equiv \sum_{n=-\infty}^{\infty} f(u - n\Delta u) e^{-i\pi\gamma n\Delta u(2u - n\Delta u)}, \tag{2.6}$$

$$\bar{f}_{\mathbf{M}}(u)_{(\mathbf{M},\Delta u_{\mathbf{M}})} \equiv \sum_{n=-\infty}^{\infty} f_{\mathbf{M}}(u - n\Delta u_{\mathbf{M}}) e^{i\pi\alpha n\Delta u_{\mathbf{M}}(2u - n\Delta u_{\mathbf{M}})}, \tag{2.7}$$

where Δu and $\Delta u_{\mathbf{M}}$ are arbitrary. Both definitions are of identical form since the value of α for $\mathbf{M}^{-1}$ is $-\gamma$ [2]. It is also worth noting that the functions we have just defined are chirp-periodic in the sense of [9, 11].

The generalization of the exact relation between continuous and discrete FTs (2.2) to LCTs will be stated as a theorem:

Theorem: The samples of the functions defined in (2.6) and (2.7) are exactly related to each other through the samples of the continuous kernel (the DLCT matrix in (2.4)):

$$\bar{f}_{\mathbf{M}}(m\,\delta u_{\mathbf{M}})_{(\mathbf{M},\Delta u_{\mathbf{M}})} = \delta u \sum_{k\in<N>} \bar{f}(k\,\delta u)_{(\mathbf{M}^{-1},\Delta u)} C_{\mathbf{M}}(m\,\delta u_{\mathbf{M}}, k\,\delta u), \tag{2.8}$$

for any m, where

$$\delta u = \frac{1}{|\beta|\Delta u_{\mathbf{M}}}, \quad \delta u_{\mathbf{M}} = \frac{1}{|\beta|\Delta u}, \quad N = \Delta u \Delta u_{\mathbf{M}} |\beta|. \tag{2.9}$$

Postponing the proof, we also express this exact relation in terms of the interval-independent DLCT as a corollary:

Corollary:

$$\bar{f}_{\mathbf{M}}(m\,\delta u_{\mathbf{M}})_{(\mathbf{M},\Delta u_{\mathbf{M}})} = \sqrt{\frac{\Delta u}{\Delta u_{\mathbf{M}}}} \sum_{k\in<N>} \bar{f}(k\,\delta u)_{(\mathbf{M}^{-1},\Delta u)} \mathbf{C}_{\mathbf{M}'}[m,k], \tag{2.10}$$

where $\mathbf{M}'$ corresponds to $\alpha' = \alpha\Delta u_{\mathbf{M}}/\Delta u$, $\beta' = \beta$, $\gamma' = \gamma\Delta u/\Delta u_{\mathbf{M}}$. Thus, the interval-independent DLCT defined in (2.5) exactly relates the samples of the functions defined in (2.6) and (2.7) to each other. The parameters α', β', γ' differ from the original α, β, γ because using the interval-independent DLCT effectively involves a rescaling of the sampling intervals, and the LCT of a scaled version of a function, is a scaled version of the LCT of the original function with different parameters.

The definition of the functions in (2.6) and (2.7), and the theorem and corollary can easily be specialized to the FRT by replacing $\alpha \rightarrow \cot(a\pi/2)$, $\beta \rightarrow \csc(a\pi/2)$, $\gamma \rightarrow \cot(a\pi/2)$.

Proof of Theorem: Let $f_s(u)$ be the sampled version of a continuous signal $f(u)$ with sampling interval δu:

$$f_s(u) = \sum_{n=-\infty}^{\infty} f(n\,\delta u)\delta(u - n\delta u) = \frac{1}{\delta u}\sum_{n=-\infty}^{\infty} f(u)e^{i2\pi nu/\delta u}. \tag{2.11}$$

Then, apply the LCT operator $\mathcal{C}_{\mathbf{M}}$ to the equivalent expressions for $f_s(u)$ in (2.11) to obtain

$$\bar{f}_{\mathbf{M}}(u)_{(\mathbf{M},\Delta u_{\mathbf{M}})} = \delta u \sum_{n=-\infty}^{\infty} f(n\,\delta u)C_{\mathbf{M}}(u, n\,\delta u), \tag{2.12}$$

where $\Delta u_{\mathbf{M}} = (|\beta|\delta u)^{-1}$. This result is the generalization of the *Poisson sum formula* [6], and is related to the LCT sampling theorem [12, 13, 14]. The right-hand side of this expression defines the *discrete-time* LCT [5] and its special case for the FRT defines the *discrete-time* FRT [9].

Now, sample $\bar{f}_{\mathbf{M}}(u)_{(\mathbf{M},\Delta u_{\mathbf{M}})}$ in (2.12) with a sampling interval chosen as $\delta u_{\mathbf{M}} = (|\beta|N\delta u)^{-1}$ with N an arbitrary integer. Then write the integer n as $n = k + rN$, $k \in <N>$, where r is an integer running from $-\infty$ to ∞:

$$\bar{f}_{\mathbf{M}}(m\,\delta u_{\mathbf{M}})_{(\mathbf{M},\Delta u_{\mathbf{M}})} = \delta u \sum_{r=-\infty}^{\infty}\sum_{k\in<N>} f((k+rN)\delta u)C_{\mathbf{M}}(m\,\delta u_{\mathbf{M}}, (k+rN)\delta u) \tag{2.13}$$

After changing the order of summations and substituting

$$C_{\mathbf{M}}(m\,\delta u_{\mathbf{M}}, (k+rN)\delta u) = C_{\mathbf{M}}(m\,\delta u_{\mathbf{M}}, k\,\delta u)e^{i\pi\gamma rN\delta u^2(2k+rN)} \tag{2.14}$$

in (2.13), we collect all the terms that depend on r in a summation and recognize this summation as the sampled version of (2.6) with the sampling interval δu where $\Delta u = N\delta u$. This completes the proof of (2.8).

We will make a number of comments before proving the corollary. Had the derivation been carried out by applying the operator $\mathcal{C}_{\mathbf{M}}^{-1}$ to the sampled version

of $f_{\mathbf{M}}(u)$ instead of applying $\mathcal{C}_{\mathbf{M}}$ to the sampled version of $f(u)$, one would obtain the duals of (2.8) and (2.12):

$$\bar{f}(k\,\delta u)_{(\mathbf{M}^{-1},\Delta u)} = \delta u_{\mathbf{M}} \sum_{m\in<N>} \bar{f}_{\mathbf{M}}(m\,\delta u_{\mathbf{M}})_{(\mathbf{M},\Delta u_{\mathbf{M}})} C^{*}_{\mathbf{M}}(m\,\delta u_{\mathbf{M}}, k\,\delta u) \qquad (2.15)$$

$$\bar{f}(u)_{(\mathbf{M}^{-1},\Delta u)} = \delta u_{\mathbf{M}} \sum_{n=-\infty}^{\infty} f_{\mathbf{M}}(n\,\delta u_{\mathbf{M}}) C^{*}_{\mathbf{M}}(n\,\delta u_{\mathbf{M}}, u). \qquad (2.16)$$

Here (2.15) provides the exact relation for the inverse DLCT and (2.16) gives the expression for the linear canonical series, which is the generalization of ordinary Fourier series. The fractional Fourier series derived in [15, 16, 9] is a special case of this series. Just as periodic functions have Fourier series expansions, a function in the form of (2.6), which is chirp-periodic, has a linear canonical series expansion. Here the expansion coefficients of $\bar{f}(u)_{(\mathbf{M}^{-1},\Delta u)}$ are $\delta u_{\mathbf{M}} f_{\mathbf{M}}(n\,\delta u_{\mathbf{M}})$. Again in analogy with the ordinary Fourier case, linear canonical series can also be used to represent an aperiodic signal $f(u)$ with finite extent. But in this case, the series will give the periodically replicated and phase modulated extension of $f(u)$ outside its finite extent. Unlike the *discrete-time* LCTs, which take discrete signals to continuous signals [5, 16, 9], linear canonical series, which take continuous signals to discrete signals, do not seem to have received attention in the literature.

Just as periodicity and discreteness in either the time or frequency domain implies the dual property in the other domain [17], (2.12) and (2.16) demonstrate the idea that discreteness in either the time or LCT domains implies periodic replication and phase modulation in the other domain, and vice versa [9]. If both are present in one domain, they will both also be present in the other domain. It is precisely in this case that, there exists an exact relation between these two sets of samples, as given in (2.8) and (2.15).

Proof of Corollary: Substitute α', β', γ' for α, β, γ in (2.5). Then use (2.9) and the DLCT matrix in (2.4) to obtain $\mathbf{C}_{\mathbf{M}'}[m,k] = \sqrt{\delta u \delta u_{\mathbf{M}}}\, C_{\mathbf{M}}(m\delta u_{\mathbf{M}}, k\delta u)$. Substitute this in (2.8) to obtain (2.10).

2.4 Computation of Continuous LCTs

The exact relation between continuous and discrete LCTs provides the underlying foundation for approximately computing the samples of the LCT of a continuous signal by replacing the transform integral with a finite sum. Sampling the continuous input function and the transform kernel will always lead to a finite sum; however, this sum will not be exactly equal to the samples of the continuous output. We may still choose this finite sum as the definition of the discrete version of our transform, but then the relationship between the discrete input and output vectors, and the samples of the continuous input and output remains to be shown. In particular, for the DLCT in (2.4), the relation of $\hat{f}$ and $\hat{f}_{\mathbf{M}}$ with the samples of the original continuous functions is not apparent and our main contribution is to exactly provide this relation ((2.8) and (2.10)).

Let us assume that a large percentage of the total energy of the signal is respectively concentrated in the intervals $[-\Delta u/2, \Delta u/2]$ and $[-\Delta u_{\mathbf{M}}/2, \Delta u_{\mathbf{M}}/2]$ in the time and LCT domains. Then, $\bar{f}(u)_{(\mathbf{M}^{-1},\Delta u)} \approx f(u)$ and $\bar{f}_{\mathbf{M}}(u)_{(\mathbf{M},\Delta u_{\mathbf{M}})} \approx f_{\mathbf{M}}(u)$ in the respective intervals, and from (2.8) and (2.10) the discrete LCT of the samples of the function are the approximate samples of the continuous LCT of that function:

$$f_{\mathbf{M}}(m\,\delta u_{\mathbf{M}}) \approx \delta u \sum_{k=-N/2}^{N/2-1} f(k\,\delta u)\, C_{\mathbf{M}}(m\,\delta u_{\mathbf{M}}, k\,\delta u) \tag{2.17}$$

$$f_{\mathbf{M}}(m\,\delta u_{\mathbf{M}}) \approx \sqrt{\frac{\Delta u}{\Delta u_{\mathbf{M}}}} \sum_{k=-N/2}^{N/2-1} f(k\,\delta u)\mathbf{C}_{\mathbf{M}'}[m,k], \tag{2.18}$$

where δu, $\delta u_{\mathbf{M}}$, and N are as given in (2.9). If both the functions $f(u)$ and $f_{\mathbf{M}}(u)$ could be identically zero outside of the given intervals, the mapping between the samples of these functions would be exact. But, since the extent of a function and its LCT cannot both be finite for $\beta \neq \infty$ [18], there will be overlaps between the periodically replicated and phase modulated functions, and the DLCT will

be an approximation between the samples of the continuous signals. This approximation for the LCT and FRT is similar to that for the ordinary FT. The functions (2.6) and (2.7) reveal the precise nature of overlap and aliasing that occurs, which is somewhat different than the ordinary Fourier case due to the phase terms appearing in the periodic replication. As with the DFT, the approximation improves with increasing N since this decreases the overlap between the replicas.

As is well-known, if the time-domain vector is periodic or periodically extended, the DFT summation can run over any interval of length N; furthermore, the output vector is periodic with period N. Likewise, if the time-domain vector is chirp-periodic or chirp-periodically extended (as in (2.6)), then the DLCT summation can run over any interval of length N; furthermore, the output vector is chirp-periodic (as in (2.7)).

Both the DLCT in (2.4) and the interval-independent DLCT whose matrix is given in (2.5) can be computed by performing a chirp multiplication, a fast Fourier transform (FFT) and a second chirp multiplication, which takes $2N + (N/2)\log N$ time, where $N = \Delta u \Delta u_{\mathbf{M}} |\beta|$ [9, 4]. It is interesting to compare this approach to computing LCTs with the algorithms given in [17, 19, 5]. All of these produce output vectors which are good approximations to the samples of the continuous transform, limited only by the fundamental fact that a signal cannot have finite extent in more than one domain; since the sampling interval is ensured to satisfy the Nyquist criterion, the output samples can be used to reconstruct good approximations of the continuous output. On the other hand, while the algorithms in [17, 19] also take $\sim N \log N$ time, most of them involve more than one FFT and therefore a larger factor in front, in addition to being less transparent. However, this does not automatically mean that these earlier algorithms are slower since the number of samples N in these works are not directly comparable to that in this letter, as discussed below.

2.5 Generalization of the Time-Bandwidth Product

The conventional time-bandwidth product $\Delta u \Delta \mu$ is the minimum number of samples to identify a signal out of all signals whose energies are confined to time and frequency intervals of length Δu and $\Delta \mu$. Likewise, the product $\Delta u \Delta u_{\mathbf{M}} |\beta|$ is the minimum number of samples to identify a signal out of all signals whose energies are confined to time and LCT intervals of length Δu and $\Delta u_{\mathbf{M}}$. We refer to the product $\Delta u \Delta u_{\mathbf{M}} |\beta|$ as the *time-canonical width product*. More generally, the term *bicanonical width product* will be used to refer to the product $\Delta u_{\mathbf{M}_1} \Delta u_{\mathbf{M}_2} |\beta_{1,2}|$, where $\Delta u_{\mathbf{M}_1}$ and $\Delta u_{\mathbf{M}_2}$ are the extents of the signal in two arbitrary LCT domains and $\beta_{1,2}$ is the parameter of the LCT between these domains. The minimum number of samples needed to uniquely identify a signal is also referred to as the number of degrees of freedom.

The time-bandwidth product is a notion derived from simultaneously specifying the time and frequency extents of signals. Although this product is commonly seen as an intrinsic property, it is in fact a notion that is specific to the FT and the frequency domain. However, it is always possible to specify the extent of a signal in other FRT or LCT domains. The set of signals thus specified will constitute a different family of signals with a different number of degrees of freedom than that defined through specifying the extent in the ordinary frequency domain. Indeed, there is no reason to think that families of signals encountered in practice will necessarily uniformly fall into a rectangular region in the ordinary time-frequency space. For instance, in applications where the underlying physics involves LCT type integrals as is the case with propagation problems, specification of Δu and $\Delta u_{\mathbf{M}}$ may provide a much better fit to the set of signals we are dealing with.

While having a finite extent in one LCT domain is not sufficient to ensure that a family of signals has a finite number of degrees of freedom, specifying two LCT domains in which the signal is approximately confined to finite intervals allows us to approximately represent the family of signals with a finite number of degrees of freedom. The family of signals thus defined depends both on the chosen LCT domains and the extent of the signals in those domains.

To approximately compute LCTs, we assume that the signal is approximately confined to Δu and $\Delta u_{\mathbf{M}}$ in the time and LCT domains. In contrast, in [17, 19] it is assumed that the signal is confined to a rectangle or ellipse orthogonal to the ordinary time-frequency axes in the time-frequency plane, regardless of the parameters of the FRT or LCT to be computed. As noted before, it is not possible to directly compare the present algorithm for computing LCTs to those in [19] since different families of signals are assumed. Therefore, which algorithm is better will depend strongly on what assumptions are best suited to the family of signals we are dealing with. However, if we restrict our attention to [17] which deals with the special case of FRTs, a comparison becomes possible. There the signal is assumed to have negligible energy outside a circle of diameter Δu in the time-frequency plane. This implies that the signal will be approximately confined to Δu in both the time and FRT domains [20], so that the results of this letter can be applied. The value of $N = \Delta u^2 |\csc(a\pi/2)|$ in our complexity expressions is smaller than $N = 2\Delta u^2$ appearing in [17] for $0.5 \leq |a| \leq 1.5$, but the real advantage lies in the fact that the numerical factor in front of $N \log N$ will be considerably smaller than in this widely-used method.

It is interesting to note that the relations between the parameters given in (2.9) are consistent with sampling theorems for the FRT [21, 22, 15, 9, 23, 24] and LCT [12, 13, 14, 25], as well as the definition of the bicanonical width product. In (2.9), $\delta u^{-1} = |\beta| \Delta u_{\mathbf{M}}$ is the minimum rate for sampling the time-domain representation of a signal that has finite extent $\Delta u_{\mathbf{M}}$ in the LCT domain in

question. If we sample the time-domain signal at this rate, the total number of samples over the extent Δu is given by $N = \Delta u/\delta u = \Delta u \Delta u_{\mathbf{M}} |\beta|$, which is the same as the number of samples N given in (2.9), and nothing but the bicanonical width product. Alternatively, $\delta u_{\mathbf{M}}^{-1} = |\beta| \Delta u$ in (2.9) is the minimum rate for sampling the LCT-domain representation of a signal that has finite extent Δu in the time domain. If we sample the LCT-domain signal at this rate, the total number of samples over the extent $\Delta u_{\mathbf{M}}$ is once again given by $N = \Delta u_{\mathbf{M}}/\delta u_{\mathbf{M}} = \Delta u \Delta u_{\mathbf{M}} |\beta|$. Thus we have accomplished to formulate such that the number of samples in both domains are equal to each other regardless of the LCT parameters, and this number of samples is the minimum possible for both domains, for the given extents. This approach is in contrast to some earlier works where the starting assumption is knowledge of the extent of the signal in the ordinary time and frequency domains and the number of samples is determined from the ordinary Nyquist sampling theorem [19, 26], whereas in our formulation it is knowledge of the extents in two LCT domains and the number of samples is determined from the LCT sampling theorem. We also note that the relations in (2.9) reduce to the well-known results for the Fourier transform when $\beta = 1$.

As a final remark, we note that the relation between the extents of the signals and the number of samples expressed as $\Delta u \Delta u_{\mathbf{M}} = N/|\beta|$ is in agreement with the uncertainty relation for LCTs. Since $N \geq 1$ we can write $\Delta u \Delta u_{\mathbf{M}} \geq 1/|\beta|$ which is precisely the uncertainty relation for LCTs [2].

Chapter 3

THE BICANONICAL WIDTH PRODUCT: A GENERALIZATION OF THE TIME-BANDWIDTH PRODUCT

3.1 Introduction

In this chapter, we will first discuss the bicanonical width product in more detail and then give its relationship to the time-frequency plane. The conventional time-bandwidth product is of fundamental importance in many areas of signal processing and information optics because of its interpretation as the number of degrees of freedom [2, 27, 28, 29, 30, 31, 32, 33, 34, 35, 36, 37]. For a family of signals, whose members are approximately confined to an interval of length Δu in the time domain and to an interval of length $\Delta\mu$ in the frequency domain, the

time-bandwidth product N is defined as [2]

$$N \equiv \Delta u \Delta \mu, \tag{3.1}$$

which is always greater than or equal to unity because of the uncertainty relation.

The conventional time-bandwidth product is the minimum number of samples to uniquely identify a signal out of all possible signals whose energies are approximately confined to time and frequency intervals of length Δu and $\Delta \mu$. This argument is based on Nyquist's sampling theorem. The Nyquist rate for sampling the time-domain representation of a signal that has finite extent $\Delta \mu$ in the frequency domain is $\delta u^{-1} = \Delta \mu$. If we sample the time-domain signal at this rate, the total number of samples over the extent Δu is given by $\Delta u / \delta u = \Delta u \Delta \mu$, which is simply the time-bandwidth product N. Alternatively, $\delta \mu^{-1} = \Delta u$ is the Nyquist rate for sampling the frequency-domain representation of a signal that has finite extent Δu in the time domain. If we sample the frequency-domain signal at this rate, the total number of samples over the extent $\Delta \mu$ is given by $\Delta \mu / \delta \mu = \Delta u \Delta \mu$, which is once again the time-bandwidth product N. The time-bandwidth product of the set of time- and band-limited signals can be interpreted as the number of degrees of freedom of the set of signals.

The time-bandwidth product is a notion derived from simultaneously specifying the time and frequency extents of signals. Although this product is commonly seen as an intrinsic property, it is in fact a notion that is specific to the FT and the frequency domain. However, it is always possible to specify the extent of a signal in other FRT or LCT domains. The set of signals thus specified will constitute a different family of signals with a different number of degrees of freedom than that defined through specifying the extent in the ordinary frequency domain. Obviously while having a finite extent in one LCT domain will not be sufficient to ensure that a family of signals has a finite number of degrees of freedom, specifying two LCT domains in which the signal is approximately confined to finite intervals will allow us to approximately represent the family

of signals with a finite number of degrees of freedom. The number of degrees of freedom thus defined will certainly depend on both the chosen LCT domains and the extent of the signals in those domains.

We now define the time-canonical width product, which gives the number of degrees of freedom of signals which are confined to finite intervals in the time and LCT domains. Let us assume that for a family of signals, a large percentage of the total energy of its members is approximately confined to the intervals of length Δu and $\Delta u_{\mathbf{M}}$ in the time and LCT domains, respectively. Then, the *time-canonical width product* is defined as [7]

$$N \equiv \Delta u \Delta u_{\mathbf{M}} |\beta|, \tag{3.2}$$

which is always greater than or equal to unity because of the uncertainty relation for LCTs. Here, β is the parameter of the LCT domain in question. We emphasize that the time-canonical width product constitutes a generalization of the time-bandwidth product. More generally, the term *bicanonical width product* will be used to refer to the product [7]

$$N = \Delta u_{\mathbf{M}_1} \Delta u_{\mathbf{M}_2} |\beta_{1,2}|, \tag{3.3}$$

where $\Delta u_{\mathbf{M}_1}$ and $\Delta u_{\mathbf{M}_2}$ are the extents of the signal in two arbitrary LCT domains and $\beta_{1,2}$ is the parameter of the LCT between these domains.

The time-canonical width product is the minimum number of samples to uniquely identify a signal out of all possible signals whose energies are approximately confined to time and LCT intervals of length Δu and $\Delta u_{\mathbf{M}}$. Our argument is based on the LCT sampling theorem [12, 13, 14], which will be reviewed in Section 3.2. The minimum rate for sampling the time-domain representation of a signal that has finite extent $\Delta u_{\mathbf{M}}$ in the LCT domain with parameter $\mathbf{M}$ is $\delta u^{-1} = |\beta| \Delta u_{\mathbf{M}}$. If we sample the time-domain signal at this rate, the total number of samples over the extent Δu is given by $\Delta u / \delta u = \Delta u \Delta u_{\mathbf{M}} |\beta|$, which is the same as the time-canonical width product. Alternatively, $\delta u_{\mathbf{M}}^{-1} = |\beta| \Delta u$

is the minimum rate for sampling the LCT-domain representation of a signal that has finite extent Δu in the time domain. If we sample the LCT-domain signal at this rate, the total number of samples over the extent $\Delta u_{\mathbf{M}}$ is given by $\Delta u_{\mathbf{M}}/\delta u_{\mathbf{M}} = \Delta u \Delta u_{\mathbf{M}} |\beta|$, which is once again the time-canonical width product. The derivation above can be easily generalized for the bicanonical width product in (3.3). The bicanonical width product of the set of LCT-limited signals in two domains can be interpreted as the number of degrees of freedom of the set of signals.

Indeed, there is no reason to think that families of signals encountered in practice will necessarily uniformly fall into a rectangular region in the ordinary time-frequency plane. As is well-known, when the family of signals does not have a rectangular support, the actual number of degrees of freedom will be less than the time-bandwidth product. That is, we can represent these signals with a number of samples less than the time-bandwidth product. In this case, the bicanonical width product may provide a better approximate to the actual number of degrees of freedom, which will allow us to represent these signals with a less number of samples. For instance, in applications where the underlying physics involves LCT type integrals as is the case with wave propagation problems, specification of Δu and $\Delta u_{\mathbf{M}}$ may provide a much better fit to the set of signals we are dealing with.

In chapter 2, we have presented the exact relation between the continuous LCT and the discrete LCT, which provides the underlying foundation for approximately computing the samples of the LCT of a continuous signal with the DLCT. As we have seen, provided N is chosen to be at least equal to the bicanonical width product of the set of signals we are dealing with, the DLCT which can be efficiently computed on a digital computer by taking $N \log N$ time can be used to obtain a good approximation to the continuous LCT, limited only by the fundamental fact that a signal cannot have finite extent in more than one

domain. The approximation improves with increasing N. In that chapter, we have also showed that chirp-periodicity (or equivalently, finite extent) in either of the time or LCT domains implies discreteness in the other domain and vice versa. If both chirp-periodicity and discreteness are present in either domain, then they will both also be present in the other domain as well, implying a finite number of degrees of freedom (which is given by the bicanonical width product). This is the real basis of the definition of the DLCT, which has been first defined in [4].

3.2 Linear Canonical Transforms

In this section, we will review LCTs for self-completeness. LCTs are a three-parameter family of linear integral transforms which includes the Fourier and fractional Fourier transforms, coordinate scaling, and chirp multiplication and convolution operations as its special cases. LCTs can model a broad class of optical systems involving thin lenses, sections of free space in Fresnel approximation, sections of quadratic graded-index media, and arbitrary combinations of any number of these, also referred to as quadratic-phase systems.

The LCT of $f(u)$ with parameter matrix $\mathbf{M}$ is defined as [8]

$$f_{\mathbf{M}}(u) \equiv (\mathcal{C}_{\mathbf{M}} f)(u) \equiv \int_{-\infty}^{\infty} C_{\mathbf{M}}(u, u') f(u')\, du', \tag{3.4}$$

$$C_{\mathbf{M}}(u, u') \equiv \sqrt{\frac{1}{B}}\, e^{-i\pi/4} \exp\left[i\pi\left(\frac{D}{B}u^2 - 2\frac{1}{B}uu' + \frac{A}{B}u'^2\right)\right],$$

where $\mathcal{C}_{\mathbf{M}}$ is the unitary LCT operator, A, B, C, D are the elements of the matrix $\mathbf{M}$, and $AD - BC = 1$.

The unit-determinant matrix $\mathbf{M}$ whose elements are A, B, C, D are equivalent to the three real parameters α, β, γ and either set of parameters can be obtained

from the other [8]:

$$\mathbf{M} = \begin{bmatrix} A & B \\ C & D \end{bmatrix} = \begin{bmatrix} \gamma/\beta & 1/\beta \\ -\beta + \alpha\gamma/\beta & \alpha/\beta \end{bmatrix} \tag{3.5}$$

The transform matrix $\mathbf{M}$ is useful in the analysis of optical systems because if several systems are cascaded the overall system matrix can be found by multiplication of the corresponding matrices of each cascaded system.

The ath-order fractional Fourier transform (FRT) of a function $f(u)$, denoted by $f_a(u)$, is most commonly defined as [2]

$$f_a(u) \equiv (\mathcal{F}^a f)(u) \equiv \int_{-\infty}^{\infty} K_a(u,u') f(u')\, du', \tag{3.6}$$

$$K_a(u,u') \equiv A_\phi \exp\left[i\pi\left(\cot\phi u^2 - 2\csc\phi uu' + \cot\phi u'^2\right)\right],$$

$$A_\phi = \sqrt{1 - i\cot\phi}, \qquad \phi = a\pi/2$$

when $a \neq 2j$ and $K_a(u,u') = \delta(u-u')$ when $a = 4j$ and $K_a(u,u') = \delta(u+u')$ when $a = 4j \pm 2$, where j is an integer.

Dimensionless variables and parameters are employed throughout this chapter for simplicity and purity and to avoid the problems associated with assigning units to oblique axes in the time-frequency plane. We will assume that a dimensional normalization has been performed on the signals we work with and that the coordinates appearing in the definition of the fractional Fourier transform, linear canonical transform, Wigner distribution, etc., are all dimensionless quantities.

The FRT is also a special case of the LCT with matrix

$$\mathbf{F}^a = \begin{bmatrix} \cos(a\pi/2) & \sin(a\pi/2) \\ -\sin(a\pi/2) & \cos(a\pi/2) \end{bmatrix}, \tag{3.7}$$

differing only by the factor $e^{-ia\pi/4}$:

$$\mathcal{C}_{\mathbf{F}^a} f(u) = e^{-ia\pi/4} \mathcal{F}^a f(u). \tag{3.8}$$

Arbitrary LCTs can be decomposed into cascade combinations of the FRT, scaling, and chirp multiplication operations [19]:

$$\mathbf{M}=\begin{bmatrix} A & B \\ C & D \end{bmatrix}=\begin{bmatrix} 1 & 0 \\ -q & 1 \end{bmatrix}\begin{bmatrix} M & 0 \\ 0 & \frac{1}{M} \end{bmatrix}\begin{bmatrix} \cos\phi & \sin\phi \\ -\sin\phi & \cos\phi \end{bmatrix} \tag{3.9}$$

Here, q is the chirp multiplication parameter, $M > 0$ is the scaling factor and $\phi = a\pi/2$, where a is the order of the FRT. For the matrices of the chirp multiplication and scaling operations, the reader may refer to section 5.1 in chapter 5. The decomposition can be written more explicitly in terms of the LCT and FRT domain representations of the signal in the form

$$f_{\mathbf{M}}(u) = \exp\left[-i\pi q u^2\right]\sqrt{\frac{1}{M}} f_a\left(\frac{u}{M}\right). \tag{3.10}$$

This decomposition was inspired by the optical interpretation in [1] and is also a special case of the widely known Iwasawa decomposition [38, 39, 40]. As we will see, the three parameters a, M, q are sufficient to satisfy the above equality for arbitrary ABCD matrices. If we solve for a, M, q in (3.9), we will obtain the decomposition parameters in terms of the matrix entries A, B, C, D as follows:

$$a = \begin{cases} \frac{2}{\pi}\text{arctan}\left(\frac{\mathrm{B}}{\mathrm{A}}\right), & \text{if } A \geq 0 \\ \frac{2}{\pi}\text{arctan}\left(\frac{\mathrm{B}}{\mathrm{A}}\right) + 2, & \text{if } A < 0 \end{cases} \tag{3.11}$$

$$M = \sqrt{A^2 + B^2}, \tag{3.12}$$

$$q = \begin{cases} -\frac{C}{A} - \frac{B/A}{A^2+B^2}, & \text{if } A \neq 0 \\ -\frac{D}{B}, & \text{if } A = 0 \end{cases} \tag{3.13}$$

The ranges of the arccotangent lie in $(-\pi/2, \pi/2]$.

Lastly, we will review the LCT sampling theorem. Let $f(u)$ be a function which, for a given parameter M, has an LCT with compact support such that $f_{\mathbf{M}}(u)$ is zero outside the interval $[-\Delta u_{\mathbf{M}}/2, \Delta u_{\mathbf{M}}/2]$. Such a function can be reconstructed from its samples taken at intervals $\delta u \leq 1/|\beta|\Delta u_{\mathbf{M}}$. The reconstruction formula, which we will refer to as the LCT interpolation formula, is given by [14]

$$f(u) = \delta u\,|\beta|\,\Delta u_{\mathbf{M}}\, e^{-i\pi\gamma u^2} \sum_{n=-\infty}^{\infty} f(n\,\delta u)\, e^{i\pi\gamma(n\,\delta u)^2} \text{sinc}(\beta\,\Delta \text{u}_{\mathbf{M}}(\text{u} - \text{n}\,\delta\text{u})) \tag{3.14}$$

3.3 The Relation between Fractional Fourier Domains and Linear Canonical Domains

Fractional Fourier domains correspond to oblique axes in the time frequency plane, and thus they are intimately related to time-frequency representations such as the Wigner distribution. The effect of ath-order fractional Fourier transformation on the Wigner distribution of a signal is to rotate the Wigner distribution by an angle $\phi = a\pi/2$ [41, 42, 20]. Mathematically,

$$W_{f_a}(u, \mu) = W_f(u\cos\phi - \mu\sin\phi, u\sin\phi + \mu\cos\phi). \tag{3.15}$$

The Radon transform operator $\mathcal{RDN}_\phi$, which takes the integral projection of the Wigner distribution of $f(u)$ onto an axis making an angle ϕ with the u axis, can be used to restate the previous property in the following manner [2]:

$$\{\mathcal{RDN}_\phi[W_f(u, \mu)]\}(u_a) = |f_a(u_a)|^2, \tag{3.16}$$

where u_a denotes the axis making angle $\phi = a\pi/2$ with the u axis. That is, projection of the Wigner distribution of $f(u)$ onto the u_a axis gives $|f_a(u_a)|^2$, the squared magnitude of the ath order FRT of the function. Hence, the projection axis u_a can be referred to as the ath order fractional Fourier domain (see Fig. 3.1) [41, 42]. The time and frequency domains are merely special cases of the continuum of fractional Fourier domains.

Recently, there has also been increased interest in generalizing the fractional Fourier transform and its properties to linear canonical transforms. From analogy with fractional Fourier domains, the term *LCT domain* has been started to use to refer to the domain where the LCT representation of the signal "lives" [43, 14, 44, 45]. However, although fractional Fourier domains are well-defined in the time-frequency plane [41, 2], it is not yet established where LCT domains exist and what they correspond to in the time-frequency plane. Moreover, LCT domains are characterized by three parameters (one of the four matrix parameters

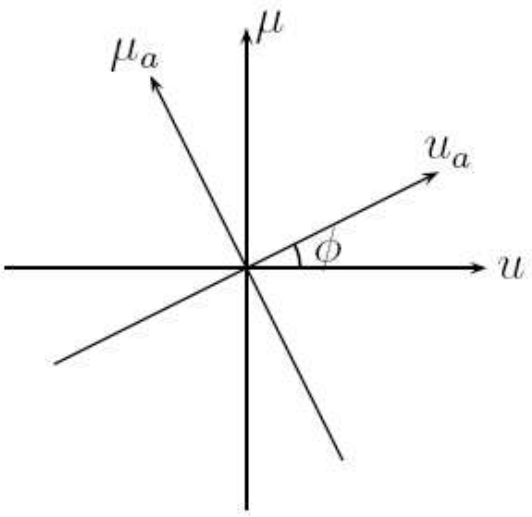

Figure 3.1: The ath order fractional Fourier domain

is redundant because of the unit-determinant condition). Since each parameter can vary independently, LCT domains are a three-parameter space; that is, each LCT domain can be labeled with three parameters, which makes them hard to visualize.

One of the contributions of this work is to figure out where linear canonical domains exist in the ordinary time-frequency plane. We will show that each LCT domain is a scaled FRT domain, and thus any LCT domain can be labeled simply by its associated fractional order a. Therefore, each LCT domain is effectively associated with only one parameter a and this parameter is monotonicly increasing through arbitrary quadratic-phase systems (refer to [1] or chapter 5).

We will now introduce *essentially equivalent domains* by using the Iwasawa decomposition given in (3.10). As we have seen, any arbitrary LCT of a signal can be expressed as chirp multiplied and scaled version of the ath order FRT of the signal, which we repeat here for convenience:

$$f_{\mathbf{M}}(u) = e^{-i\pi q u^2} \sqrt{\frac{1}{M}} f_a\left(\frac{u}{M}\right). \tag{3.17}$$

The parameters of the FRT, scaling, and chirp multiplication are given in terms of the LCT parameters in (3.11), (3.12), and (3.13), respectively. Thus, in order to compute an arbitrary LCT of a signal, we can first take the ath order FRT of the signal. This operation moves the signal to the ath order fractional Fourier domain. Secondly, we scale the transformed signal. Scaling does not effectively move the signal to a different domain, and thus the signal is at a scaled FRT domain after the scaling operation. Finally, we multiply the resulting signal with a chirp to obtain the LCT. Chirp multiplication can be interpreted as a windowing operation in the current domain; thus, it does not change the domain of the signal, just like the scaling operation. Therefore, linear canonical transformed signal lives at a scaled ath order FRT domain. This discussion also reveals that LCT domains are essentially equivalent to scaled fractional Fourier domains, and thus they are not richer than FRT domains. Note that LCTs with the same A/B or equivalently γ parameter, contain the same order of FRT in their decomposition as seen from (3.11) and therefore they are associated with the same FRT domain. We refer to such LCT domains as *essentially equivalent domains*. If a signal has a compact support at a certain LCT domain, then the signal will have also compact support in all essentially equivalent domains of this LCT domain. Similar discussion has been given in [45] in a different context. The condition $A_1/B_1 = A_2/B_2$ for essentially equivalent domains is equivalent to the condition in [45] where the uncertainty relation is not valid.

Let us now consider a set of signals, whose members are approximately confined to the intervals $[-\Delta u_{\mathbf{M}_1}/2, \Delta u_{\mathbf{M}_1}/2]$ and $[-\Delta u_{\mathbf{M}_2}/2, \Delta u_{\mathbf{M}_2}/2]$ in two LCT domains, namely $u_{\mathbf{M}_1}$ and $u_{\mathbf{M}_2}$. Since LCT domains are equivalent to scaled fractional Fourier domains, each interval given in an LCT domain will define a scaled interval in the associated FRT domain. To see this explicitly, we again refer to (3.17), which implies that if $f_{\mathbf{M}}(u)$ is confined to an interval of length $\Delta u_{\mathbf{M}}$, so is $f_a(u/M)$. Then, the extent of $f_a(u)$ is $\Delta u_{\mathbf{M}}/M$, which gives the extent in the

associated ath order FRT domain. Thus, for the set of signals in question, the extent in the a_1th order FRT domain is $\Delta u_{\mathbf{M}_1}/M_1$ and the extent in the a_2th order FRT domain is $\Delta u_{\mathbf{M}_2}/M_2$, where a_1 and a_2 are related to $\mathbf{M}_1$ and $\mathbf{M}_2$ through the equation (3.11). Note that we should take into account the FRT and scaling parameters of the decomposition, but not the chirp multiplication parameter. It is well-known that if the time-, frequency- or FRT-domain representation of a signal is identically zero (negligible) outside a certain interval, so is its Wigner distribution [2]. As a direct consequence of this fact, the Wigner distribution of this set of signals is confined to the corridors of width $\Delta u_{\mathbf{M}_1}/M_1$ and $\Delta u_{\mathbf{M}_2}/M_2$ in the directions orthogonal to u_{a_1} and u_{a_2}, respectively. Thus, the support of the Wigner distribution is a parallelogram defined by these corridors (see Fig. 3.2. In general, if more than two extents are specified in different LCT domains, the time-frequency support will be a centrally symmetrical convex polygon defined by these intervals (Fig. 3.3).

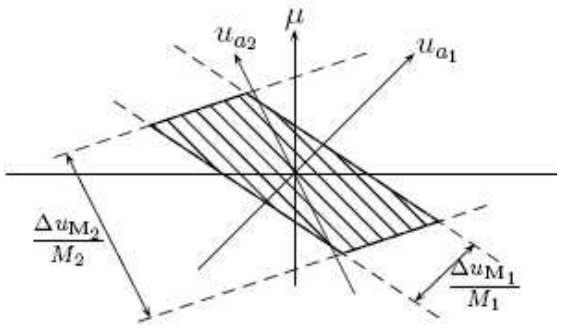

Figure 3.2: Support of the Wigner distribution when two extents are specified

Theorem 1. *The bicanonical width product* $\Delta u_{\mathbf{M}_1}\Delta u_{\mathbf{M}_2}|\beta_{1,2}|$ *is the area of the parallelogram defined by the extents* $\Delta u_{\mathbf{M}_1}$ *and* $\Delta u_{\mathbf{M}_2}$ *in two LCT domains (Fig. 3.2). Equivalently, it is the area of the time-frequency support of the signals, which have finite extents* $\Delta u_{\mathbf{M}_1}$ *and* $\Delta u_{\mathbf{M}_2}$ *in* $u_{\mathbf{M}_1}$ *and* $u_{\mathbf{M}_2}$ *domains, respectively.*

Proof. Let h_1 and h_2 be two heights of a parallelogram and ϕ denote the angle between them. Then, the area of the parallelogram is given by $h_1h_2|\csc\phi|$.

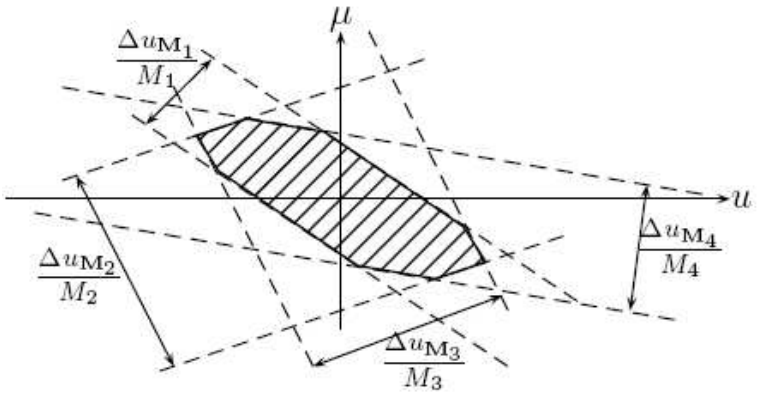

Figure 3.3: Support of the Wigner distribution when more than two extents are specified

For the parallelogram defined by the extents $\Delta u_{\mathbf{M}_1}$ and $\Delta u_{\mathbf{M}_2}$, the heights are $\Delta u_{\mathbf{M}_1}/M_1$ and $\Delta u_{\mathbf{M}_2}/M_2$, which correspond to the widths of the corridors. Then, the area of this parallelogram is

$$\begin{aligned}
\text{Area} &= \frac{\Delta u_{\mathbf{M}_1}}{M_1}\frac{\Delta u_{\mathbf{M}_2}}{M_2}|\csc(\phi_1-\phi_2)| && (3.18)\\
&= \frac{\Delta u_{\mathbf{M}_1}\Delta u_{\mathbf{M}_2}}{M_1M_2|\sin\phi_2\cos\phi_1-\cos\phi_2\sin\phi_1|} && (3.19)\\
&= \frac{\Delta u_{\mathbf{M}_1}\Delta u_{\mathbf{M}_2}}{|A_1B_2-B_1A_2|} && (3.20)\\
&= \Delta u_{\mathbf{M}_1}\Delta u_{\mathbf{M}_2}\frac{|\beta_1\beta_2|}{|\gamma_1-\gamma_2|} && (3.21)\\
&= \Delta u_{\mathbf{M}_1}\Delta u_{\mathbf{M}_2}|\beta_{1,2}| && (3.22)
\end{aligned}$$

□

As is well-known, when two extents are specified in the time and frequency domains, the time-frequency support of the signal is confined to a rectangular region. In this case, the time-bandwidth product equals to the number of degrees of freedom since it gives the area of that rectangular region. We have showed that in the general case when two extents are specified in arbitrary two LCT domains, the time-frequency support of the signal is confined to a parallelogram. In this case, the bicanonical width product equals to the number of degrees of freedom since it gives the area of that parallelogram.

Chapter 4

MINIMAL REPRESENTATION OF SIGNALS: AN APPROACH BEYOND THE TIME-BANDWIDTH PRODUCT

4.1 Introduction

As we have seen in the last chapter, when the extent of the signal is specified in two LCT domains, its time-frequency-frequency support can be represented with a parallelogram. The number of degrees of freedom of the signal is given by the area of the parallelogram, which is equal to the bicanonical width product. We can represent the signal in these two LCT domains with the minimum number of samples, which equals to the number of degrees of freedom of the signal.

In this chapter, we now turn our attention to arbitrary set of signals with arbitrary time-frequency support. Our aim is to find the minimum number of samples to represent these signals based on the LCT sampling criteria and find the LCT domains that we can represent the signal with that minimum number of samples. Since signals limited in two LCT domains have parallelogram shaped Wigner regions, this problem reduces to a simple geometric problem, which aims to find the smallest parallelogram enclosing a given time-frequency support. The problem of finding the smallest enclosing parallelogram with the purpose of representing the signal using LCT interpolation can be considered as the generalization of finding the smallest enclosing rectangle with the purpose of representing the signal using Shannon interpolation. As is well-known, Shannon interpolation restricts us to two orthogonal domains in the time-frequency plane since they must be related to each other through the Fourier transform. However, the LCT interpolation allows us to use any arbitrary two domains in the time-frequency plane since any such domains can be related to each other through the LCT. The reader should refer to (3.14) in chapter 3 for the LCT interpolation formula.

Given an arbitrary time-frequency support, the area of this support gives the number of degrees of freedom of the signal. However, in general, we can not represent the signal with this minimum number of samples by using Shannon or LCT interpolation. Instead, some more sophisticated basis should be used. Nevertheless, if we want to represent the signal using LCT interpolation, the area of the smallest parallelogram enclosing the given region will give the minimum number of samples to represent the signal by using LCT interpolation. This number of samples will be inevitably greater than the number of degrees of freedom of the signal if the given support is not a parallelogram. However, using LCT interpolation to represent the signal is still a better approach than using Shannon interpolation, which is a special case of the LCT interpolation. This is justified by the fact that enclosing a region with a parallelogram (defined by

corridors of arbitrary angle in between) gives more flexibility to us than enclosing it with a rectangle (defined by necessarily orthogonal corridors). Equivalently, the bicanonical width product, which is the area of the smallest enclosing parallelogram will come closer to the number of degrees of freedom of the signal as compared to the time-bandwidth product, which is the area of the smallest enclosing rectangle. Finally, note that the signal can be represented with the number of samples given by the area of the smallest enclosing parallelogram only at the two LCT domains that correspond to two corridors defining the parallelogram. The concept of representing the signal at different LCT domains than the optimal ones will be also discussed later in this chapter.

4.2 Representing Signals in Optimal LCT Domains

The problem of finding the smallest enclosing parallelogram has been discussed in the literature in the context of rational decimation system design [46], sensor selection [47] and pure mathematics [48]. The notion of *minimal enclosing parallelogram (MEP)* has been used to refer to the parallelogram which has the smallest area among all parallelograms that contain the given convex polygonal region. Given a convex polygon C, let denote the MEP of C by P_C and the sides of P_C as e_i for $i = 1, \ldots, 4$. Then, two important properties of the MEP can be given as follows [49, 47]:

Property 1. *For any convex polygon C, there exists a MEP P_C such that either e_1 or e_3 and e_2 or e_4 contain a side of C.*

Property 2. *There exists a line parallel to e_1 and e_3 such that it contains a non-empty intersection of C and P_C on its both sides. Similarly, there exists a line parallel to e_2 and e_4 such that it contains a non-empty intersection of C and P_C on its both sides.*

Given a convex polygon C with n vertices, the MEP of C can be found by using the minimal enclosing parallelogram algorithm of [49], which has a complexity of $O(n)$. This algorithm has also been extended in [46] to find the MEP of an arbitrary polygon, either convex or concave. For this, the convex hull of the input polygon is first computed by using the Graham Scan method [50], which takes $O(n \log n)$ time. Then, the MEP of the convex hull is found by using the minimal enclosing parallelogram algorithm for convex polygons given in [49]. The obtained MEP of the convex hull will be also the MEP of the input polygon. Thus, the technique to compute the MEP of an arbitrary polygonal region is well-known. This technique also applies to non-polygonal regions since any non-polygonal region can be efficiently approximated by a polygonal region.

We now consider an important special case of the MEP problem which is for the case when the given region is a centrally symmetrical convex polygon. Throughout this study, the term *corridor* will be used to refer to a pair of parallel lines that are symmetric with respect to the origin. The region defined by the intersection of arbitrary number of corridors with arbitrary widths and angles will be called *centrally symmetrical convex polygon* [51]. Clearly, a centrally symmetrical convex polygon can be transformed into itself by reflection with respect to the origin. The number of its vertices is even since they exist in opposite pairs which can be connected to each other through the origin. Moreover, any two opposite sides are equal and parallel to each other. When there are only two corridors (equivalently, four sides), a centrally symmetrical convex polygon reduces to a parallelogram.

As we have seen, the time-frequency support is a centrally symmetrical convex polygon if two or more extents are specified in different LCT domains. Then, the problem of finding the minimum number of samples to represent such signals using the LCT interpolation reduces to the problem of finding the smallest paralellogram enclosing the resulting centrally symmetrical convex polygon. The

solution of the MEP gets simpler in this special case based on the following theorem:

Theorem 2. *For any centrally symmetrical convex polygon C, there exists a MEP P_C such that each side of P_C contain a side of C. Equivalently, there exists a P_C defined by two corridors of C.*

Proof: Without loss of generality, from Property 1, let us assume that e_1 contains a side of C, denoted by f. Then, e_3, which is parallel to e_1, must intersect C in at least one point due to Property 2. Since C is centrally symmetric, there is an opposite parallel side for each side of C. This implies that the intersection of e_3 and C will contain the opposite symmetric pair of the side f. Thus, if e_1 contains a side of C, then e_3 necessarily contains its opposite side. Similarly, if e_2 contains a side of C, then e_3 necessarily contains its opposite side. As a result, each side of P_C contains a side of C. Since each parallel sides of C are defined by one corridor, this is equivalent to say that P_C is defined by two corridors of C.

As a result, the MEP of a centrally symmetrical polygon C is the parallelogram which has the smallest area among all parallelograms defined by any two corridors of C. As we have seen before, given any two corridors of width w_1 and w_2, and the angle in between as $\phi_{1,2}$, the area of the parallelogram defined by these corridors is $w_1 w_2 |\csc \phi_{1,2}|$. If we define these corridors in the time-frequency plane by specifying two extents $\Delta u_{\mathbf{M}_1}$ and $\Delta u_{\mathbf{M}_2}$ in the $u_{\mathbf{M}_1}$ and $u_{\mathbf{M}_2}$ LCT domains, the area of the resulting parallelogram is given by the bicanonical width product $\Delta u_{\mathbf{M}_1} \Delta u_{\mathbf{M}_2} |\beta_{1,2}|$. Then, given many extents as $\Delta u_{\mathbf{M}_i}$s in LCT domains, the two extents that minimizes $\Delta u_{\mathbf{M}_i} \Delta u_{\mathbf{M}_j} |\beta_{i,j}|$ among all $i - j$ pairs define the MEP of the centrally symmetrical convex support region.

Now, we want to find upper theoretical limits on the enclosing efficiency of the MEP. Firstly, given a convex polygon C, the area of the MEP of C can be

bounded by [47]

$$\text{Area}(P_C) \leq 2\text{Area}(C) \tag{4.1}$$

This implies the following important result:

> For an arbitrary convex polygonal time-frequency support, the number of samples required to represent the signal by using LCT interpolation is at most two times of the actual number of degrees of freedom of the signal.

In the special case of centrally symmetrical convex polygons, we believe that the enclosing efficiency will be much better. We conjecture that an n-sided centrally symmetrical convex polygon will be enclosed least efficiently when all of its n sides are equal to each other. Then, if this is indeed true, it is clear that the enclosing efficiency will also get worse as $n \to \infty$. The equilateral centrally symmetrical convex polygon converges to an ellipse in the limit $n \to \infty$ and the worst case enclosing efficiency of the MEP will be obtained based on our conjecture by dividing the area of the smallest rectangle enclosing the ellipse to the area of the ellipse:

$$\frac{\text{Area}(P_C)}{\text{Area}(C)} \leq \frac{4ab}{\pi ab} \tag{4.2}$$

where a and b are one-half of the ellipse's major and minor axes, respectively. Thus, for centrally symmetrical convex polygons, we have the following bound for the area of the MEP, under the assumption that our conjecture is true:

$$\text{Area}(P_C) \leq \frac{4}{\pi}\text{Area}(C) \tag{4.3}$$

The mentioned conjecture is based on the following observation. Consider an equilateral centrally symmetrical convex polygon such that there exists at least two MEPs that satisfy the Theorem 2 (see Figure 4.1). Let us denote the corridors of the first MEP as l_1 and l_2 and the corridors of the second MEP as l_3 and l_4. Since each is a MEP of the equilateral polygon, the enclosing efficiency

is same for both of MEPs. Now, consider increasing the width of corridor l_3 upto corners v_1 and v_3 and/or increasing the width of corridor l_4 upto corners v_2 and v_4. After these operations, the polygon defined by all corridors will have sides of different length, but the MEP defined by corridors l_1 and l_2 will remain to be the MEP of the new polygon. Since the area of the new polygon is larger, the enclosing efficiency of the same MEP is better after making the polygon inequilateral. Similarly, if we increase the width of corridors l_1 and l_2 upto corners v_5 and v_7, and v_6 and v_8, the MEP defined by corridors l_3 and l_4 will remain to be the MEP of the region with a higher enclosing efficiency. This illustrates the rationale behind our conjecture, which states that a centrally symmetrical convex polygon will be enclosed worst when all of its sides are of equal length. Unfortunately we do not have a proof of this conjecture at this point.

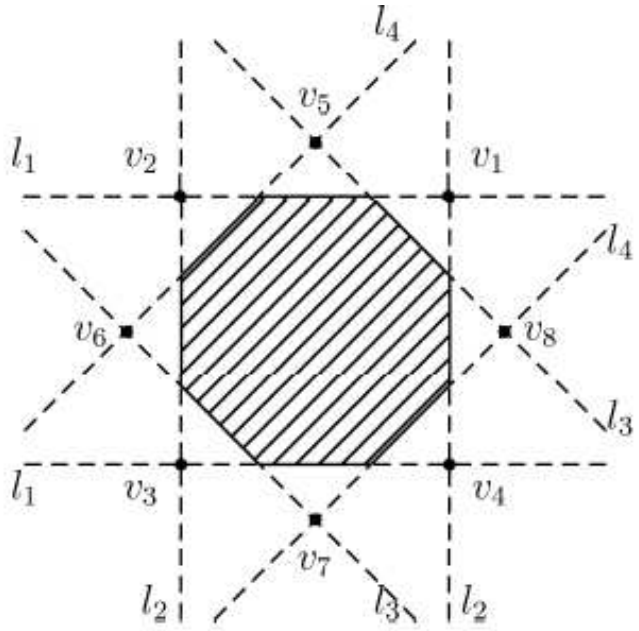

Figure 4.1: Illustration of the conjecture

We will now illustrate with one example the difference between Shannon and LCT interpolation approaches. In the former case, we will find the smallest rectangle enclosing the time-frequency support, while in the latter case we will

find the smallest enclosing parallelogram. In Fig. 4.2, the smallest enclosing parallelogram and rectangle are shown for a given time-frequency support, which is indicated by the colored region. When we compare the area of the smallest parallelogram with the area of the smallest rectangle, we can say that for this example the LCT interpolation requires 27 percent less number of samples than Shannon interpolation.

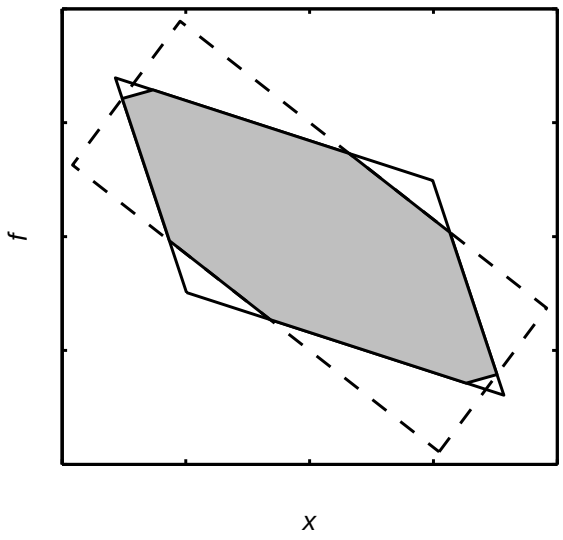

Figure 4.2: The smallest enclosing parallelogram (solid) and rectangle (dashed)

In a different context, the area of the smallest rectangle enclosing the time-frequency support has been referred to as the *generalized time-bandwidth product* [52, 53]. This generalization of the time-bandwidth product has been introduced to obtain a measure for the time-frequency support of the signals that does not change after fractional Fourier transformation operation, or equivalently rotation in the time-frequency plane. That is, this is a rotation invariant measure of compactness. The optimal short-time Fourier transform (STFT) kernel has been derived that has the minimum generalized time-bandwidth product, or equivalently that provides the most compact representation based on this product. This analysis, which has dealt with the support of a signal, lead to signal adaptive STFTs. Although the generalized time-bandwidth product has been regarded as

a better measure for the time-frequency support of signals in these works, it has been also emphasized in [53] that "further research is required in obtaining other forms of generalized time-bandwidth products that are invariant under a more general area preserving time-frequency operations: the symplectic transforms [54]".

The bicanonical width product addresses this issue and it provides a measure that is invariant under linear canonical transformation operation. That is, the bicanonical width product is a linear distortion invariant measure of compactness. Moreover, the area of the smallest parallelogram enclosing the time-frequency support is a better measure than the area of the smallest enclosing rectangle since the former does not necessarily require to fit to the support with two orthogonal corridors with respect to each other. In this thesis work we mostly concentrate on a family of signals instead of one signal, but similar discussions will also hold for the support of a signal. Finding the optimal STFT kernel which minimizes the bicanonical width product of the signal is also left as a subject for future study.

It has also been suggested that instead of taking uniform samples in one of the optimal LCT domains with the minimum number of samples, it may be better to take these samples in the middle of both of these two optimal domains based on the fact that in practice the SNR is usually better near the center of a signal and we can represent the signal better by concentrating on sample values at the center in both domains (Orhan Arikan, private communication).

4.3 Representing Signals in a Specific LCT Domain

In this section, we turn our attention to the problem of finding the minimum number of samples to represent the signal in a specific LCT domain by using the LCT interpolation, when an arbitrary time-frequency support is given. As we have noted before, the signal can be represented with the minimum number of samples given by the area of the MEP only at the two LCT domains that correspond to two corridors defining the MEP. Indeed, we need more samples to represent the signal in the other LCT domains. This is a consequence of the fact that when we want to sample the signal in an LCT domain that is different than the optimal two LCT domains, we lose our flexibility to fit an arbitrary parallelogram to the support region. Instead of fitting to the region with the intersection of arbitrary two corridors, now we can only change one corridor since the other corridor will be defined with respect to the sampling domain. This will cause us to find a larger enclosing parallelogram than the MEP; therefore, we will need more samples to represent the signal in other LCT domains.

The problem of finding the minimum number of samples to represent the signal in a specific LCT domain by using the LCT interpolation reduces to the problem of finding the minimum area parallelogram enclosing a given time-frequency support when one corridor of the parallelogram is fixed. This is the generalization of the problem of finding the minimum number of samples to represent the signal in the time domain by using Shannon interpolation, which requires to find the smallest enclosing rectangle orthogonal to the time-frequency axes. For a convex polygon, the MEP algorithm in [49] can be easily adapted to the problem of finding the MEP when one of its corridors is fixed.

For the special case of centrally symmetrical convex polygons, the solution of the problem again gets simpler. In analogy with the previous approach, the MEP

of a centrally symmetrical convex polygon C with the constraint of having a fixed corridor is the parallelogram which has the smallest area among all parallelograms defined by a corridor of C in addition to the fixed corridor. Given many extents $\Delta u_{\mathbf{M}_i}$s in LCT domains, let us denote the domain that we want to represent the signal as $u_{\mathbf{M}_k}$. The extent of the signal in this domain, denoted by $\Delta u_{\mathbf{M}_k}$, can be obtained from the time-frequency support of the signal or from equation (5.46) in chapter 5. Then, the extent $\Delta u_{\mathbf{M}_i}$ that minimizes the area $\Delta u_{\mathbf{M}_k} \Delta u_{\mathbf{M}_i} |\beta_{ki}|$ with respect to the parameter i define the MEP with the specified constraint. The area of this MEP gives the minimum number of samples to represent the signal in the $u_{\mathbf{M}_k}$ domain by using the LCT interpolation. If we look to the problem from the context of pure geometry, the problem can be solved by minimizing $w_k w_i |\csc \phi_{k,i}|$ with respect to the parameter i, where w_i denote the width of the ith corridor defining the centrally symmetrical convex polygon, w_k denote the width of the fixed corridor and $\phi_{k,i}$ denote the angle between these corridors.

Obviously, the area of the MEP when one of its corridors is fixed will generally be larger than the area of the MEP found without any constraint. That is, when we use the LCT interpolation, the minimum number of samples to represent the signal in a specific LCT domain will be generally larger than the minimum number of samples to represent the signal optimally. Therefore, as noted before, we must take more samples due to the restriction in one corridor. We now want to find an upper bound for this increase in the number of samples. Let MEP_c denote the MEP when one of its corridors is fixed. It is intuitive that the maximum difference will occur when the MEP without any constraint encloses the given region fully, i.e. when the region is a parallelogram, so that MEP_c must enclose this MEP, not a smaller region inside the MEP. We will find the upper bound in the context of time-frequency plane both for simplicity and relevancy, though it can also be easily found in the context of pure geometry. Let us denote the domain that we want to represent the signal as u and consider a parallelogram-shaped time-frequency support defined by two extents $\Delta u_{\mathbf{M}_1}$ and $\Delta u_{\mathbf{M}_2}$, where

the time axis corresponds to the u domain. Then, the extent in the u domain is given by

$$\Delta u = \frac{|\beta_1|\Delta u_{\mathbf{M}_1} + |\beta_2|\Delta u_{\mathbf{M}_2}}{|\gamma_1 - \gamma_2|}, \tag{4.4}$$

which can be obtained via equation (5.43) in chapter 5. The area of the MEP found without any constraint is simply the area of the time-frequency support, which is given by

$$N_{MEP} = \Delta u_{\mathbf{M}_1} \Delta u_{\mathbf{M}_2} |\beta_{1,2}|. \tag{4.5}$$

On the other hand, for the MEP with fixed corridor, one corridor will necessarily come from the extent Δu, and the other corridor will be defined by either $\Delta u_{\mathbf{M}_1}$ or $\Delta u_{\mathbf{M}_2}$, whichever gives a smaller area. Then, the area of MEP_c is given by

$$\begin{aligned} N_{MEP_c} &= \min\{\Delta u \Delta u_{\mathbf{M}_1} |\beta_1|, \Delta u \Delta u_{\mathbf{M}_2} |\beta_2|\} \\ &= \min\left\{ \frac{|\beta_1|^2 \Delta u_{\mathbf{M}_1}^2 + |\beta_1\beta_2| \Delta u_{\mathbf{M}_1} \Delta u_{\mathbf{M}_2}}{|\gamma_1 - \gamma_2|}, \frac{|\beta_2|^2 \Delta u_{\mathbf{M}_2}^2 + |\beta_1\beta_2| \Delta u_{\mathbf{M}_1} \Delta u_{\mathbf{M}_2}}{|\gamma_1 - \gamma_2|} \right\} \end{aligned} \tag{4.6}$$

If $|\beta_1|\Delta u_{\mathbf{M}_1} \leq |\beta_2|\Delta u_{\mathbf{M}_2}$, the first term will be the minimum. Otherwise, the second term will be the minimum. Consider the case when $|\beta_1|\Delta u_{\mathbf{M}_1} \leq |\beta_2|\Delta u_{\mathbf{M}_2}$. Then, the ratio of the area of MEPs with and without any constraint is as follows:

$$\frac{N_{MEP}}{N_{MEP_c}} = \frac{\Delta u_{\mathbf{M}_1} |\beta_1|}{\Delta u_{\mathbf{M}_2} |\beta_2|} + 1 \leq 2 \tag{4.7}$$

since $|\beta_1|\Delta u_{\mathbf{M}_1} \leq |\beta_2|\Delta u_{\mathbf{M}_2}$. Also for the case when $|\beta_1|\Delta u_{\mathbf{M}_1} \geq |\beta_2|\Delta u_{\mathbf{M}_2}$, the same result will be obtained. Note that the ratio is worst when any chosen corridor does not create any difference on the area of the parallelogram defined. The above result implies the following important conclusion for LCT interpolation:

> For an arbitrary polygonal time-frequency support, the minimum number of samples to represent the signal in a specific LCT domain is at most twice the minimum number of samples to represent the signal in any of two optimal LCT domains.

In order to find the minimum number of samples to represent the signal in a specific domain, the most common approach is to use Shannon interpolation,

which requires to fit an enclosing rectangle orthogonal to that specific domain in the time-frequency plane. In the general case where the time-frequency support is not such a rectangle, some of the samples taken with this criterion will be redundant. Instead, LCT interpolation can be used which will also require to fix one corridor, but allow to choose the other corridor arbitrarily. This will be equivalent to the problem of finding the minimum area parallelogram enclosing the given time-frequency support when one corridor of the parallelogram is fixed. The area of this enclosing parallelogram gives the minimum number of samples to use with LCT interpolation. Thus, we can reconstruct a signal by employing LCT interpolation, which will require less number of samples than Shannon interpolation in the general case. The efficiency ratio between LCT and Shannon interpolation is unbounded when a specific domain is specified for the representation of the signal. We can see this easily by considering a very thin oblique strip in the time-frequency plane, which is defined by two corridors of nearly equal, but different angles. Assume that the signal will be represented in a domain different than the oblique axis of the strip. Then, while we can enclose this by a parallelogram of fixed corridor very tightly, a rectangle orthogonal to the specified domain will enclose this very inefficiently; thus in this case, the difference between the area of the smallest enclosing parallelogram and rectangle will be very large.

We can do better than this if we can compute the LCT of the analog signal prior to sampling. This continuous LCT computation can be performed by using chirp modulators for time-domain signals and by using lenses for two dimensional space-domain signals. With these, we can move the signal to one of the two LCT domains, where it can be optimally represented. In this domain, we can represent the equivalent information with less number of samples, which is at most two times of the number of degrees of freedom for convex support regions. If necessary, we can return back to the original domain with $N \log N$ DLCT computation [7] after sampling the signal in the optimal LCT domain.

We will now illustrate the difference between Shannon and LCT interpolation approaches when the signal will be represented in a specific domain. In the former case, we will find the smallest enclosing rectangle orthogonal to the specified domain, while in the latter case we will find the smallest enclosing parallelogram orthogonal to the specified domain, or equivalently when one of its corridors is fixed to the this domain. In Fig. 4.3, the smallest enclosing parallelogram and rectangle are shown when the signal will be represented in the time domain. The shaded region indicates the given time-frequency support. When we compare the area of the parallelogram with the area of the rectangle, we can say for this example that the LCT interpolation requires 35 percent less number of samples than Shannon interpolation.

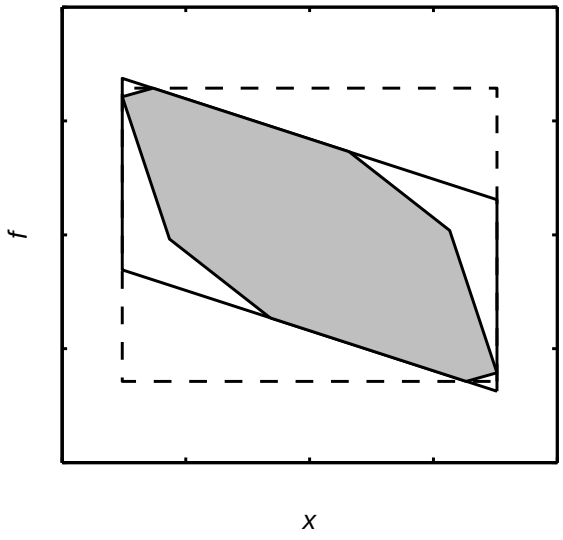

Figure 4.3: The smallest enclosing parallelogram (solid) and rectangle (dashed) when one of their corridors is fixed to the time domain

Chapter 5

ANALYZING OPTICAL SYSTEMS WITH APPLICATIONS TO EXTENT TRACING

In this chapter, we will first extend the results of chapter 3 for dimensionless variables and parameters to dimensional variables and parameters. Then, we will apply these results to analyze quadratic-phase optical systems. We will present the number of degrees of freedom of the system and the largest space-frequency region that can pass through an arbitrary quadratic-phase system without any information loss. We will develop a method to investigate how the extent of an arbitrary input signal changes as it passes through an optical system. Based on this method, we will also provide formulas to directly trace the extent from the given extents of the input signal. These extents will be used to simulate the optical system with discrete-time systems with the same degree of accuracy compared to continuous systems. We will also investigate the redundant and effective apertures in a given system.

5.1 Linear Canonical Transforms

LCTs are a three-parameter family of linear integral transforms which includes the Fourier and fractional Fourier transforms, coordinate scaling, and chirp multiplication and convolution operations as its special cases. LCTs can model a broad class of optical systems involving thin lenses, sections of free space in Fresnel approximation, sections of quadratic graded-index media, and arbitrary combinations of any number of these, also referred to as quadratic-phase systems.

The LCT of $f(x)$ with parameter matrix $\mathbf{M}$ is defined as [8][1]

$$f_{\mathbf{M}}(x) \equiv (\mathcal{C}_{\mathbf{M}} f)(x) \equiv \int_{-\infty}^{\infty} C_{\mathbf{M}}(x, x') f(x')\, dx', \tag{5.1}$$

$$C_{\mathbf{M}}(x, x') \equiv \sqrt{\frac{1}{B}}\, e^{-i\pi/4} \exp\left[i\pi\left(\frac{D}{B}x^2 - 2\frac{1}{B}xx' + \frac{A}{B}x'^2\right)\right],$$

where $\mathcal{C}_{\mathbf{M}}$ is the unitary LCT operator, A, B, C, D are the elements of the matrix $\mathbf{M}$, and $AD - BC = 1$. The unit-determinant matrix $\mathbf{M}$ whose elements are A, B, C, D are equivalent to the three real parameters α, β, γ and either set of parameters can be obtained from the other [8]:

$$\mathbf{M} = \begin{bmatrix} A & B \\ C & D \end{bmatrix} = \begin{bmatrix} \gamma/\beta & 1/\beta \\ -\beta + \alpha\gamma/\beta & \alpha/\beta \end{bmatrix} \tag{5.2}$$

The ath-order fractional Fourier transform (FRT) of a function $f(x)$, denoted by $f_a(x)$, is most commonly defined as [2]

$$f_a(x) \equiv (\mathcal{F}^a f)(x) \equiv \int_{-\infty}^{\infty} K_a(x, x') f(x')\, dx', \tag{5.3}$$

$$K_a(x, x') \equiv \frac{A_\phi}{s} \exp\left[i\pi\left(\frac{\cot\phi}{s^2}x^2 - 2\frac{\csc\phi}{s^2}xx' + \frac{\cot\phi}{s^2}x'^2\right)\right],$$

$$A_\phi = \sqrt{1 - i\cot\phi}, \qquad \phi = a\pi/2$$

when $a \neq 2j$ and $K_a(x, x') = \delta(x - x')$ when $a = 4j$ and $K_a(x, x') = \delta(x + x')$ when $a = 4j \pm 2$, where j is an integer. The scale parameter s has been introduced

[1]The parameters and functions in this chapter correspond to the dimensional parameters and physical functions in [2], which are distinguished from the dimensionless forms with carets.

because the choice of scale has an effect on the fractional order observed at a dimensional plane in an optical system. The above FRT definition reduces to the regular FRT definition with dimensionless arguments when we define the dimensionless variables $u = x/s$ and $u' = x'/s$, or simply when we set $s = 1$.

The FRT is also a special case of the LCT with matrix

$$\mathbf{F}^a = \begin{bmatrix} \cos(a\pi/2) & (s^2)\sin(a\pi/2) \\ -(1/s^2)\sin(a\pi/2) & \cos(a\pi/2) \end{bmatrix}, \tag{5.4}$$

differing only by the factor $e^{-ia\pi/4}$:

$$\mathcal{C}_{\mathbf{F}^a} f(x) = e^{-ia\pi/4} \mathcal{F}^a f(x). \tag{5.5}$$

The transform matrix $\mathbf{M}$ is useful in the analysis of optical systems because if several systems are cascaded the overall system matrix can be found by multiplication of the corresponding matrices of each cascaded system.

Now, we will give the effect of some simple optical components and their transformation matrices. If we denote the wavelength of light in the medium of propagation by λ, a thin lens of focal length f multiplies the wave with $\exp[-i\pi x^2/\lambda f]$, which mathematically corresponds to chirp multiplication. The corresponding LCT matrix is given by

$$\mathbf{Q}^{1/\lambda f} = \begin{bmatrix} 1 & 0 \\ -1/\lambda f & 1 \end{bmatrix}. \tag{5.6}$$

Propagation through a section of free space of length d in the Fresnel approximation is equivalent to convolution with $e^{i2\pi d/\lambda} e^{-i\pi/4} \sqrt{1/\lambda d}\, \exp[i\pi x^2/\lambda d]$, which mathematically corresponds to chirp convolution. The corresponding LCT matrix is given by

$$\mathbf{R}^{\lambda d} = \begin{bmatrix} 1 & \lambda d \\ 0 & 1 \end{bmatrix}. \tag{5.7}$$

The scaling operation with $M > 0$ maps a function $f(x)$ into $1/Mf(x/M)$ and its corresponding transformation matrix is

$$\mathbf{M}_M = \begin{bmatrix} M & 0 \\ 0 & 1/M \end{bmatrix}. \tag{5.8}$$

It is unfortunate that we use $\mathbf{M}$ to denote a generic transformation matrix and that we use M to denote the scaling parameter, but they can be distinguished from context.

The LCT matrix of a quadratic graded-index medium of length d exhibiting a refractive index profile $n^2(x) = n_0^2[1 - (x/\chi)^2]$ is given by

$$\mathbf{F}^{d/d_0} = \begin{bmatrix} \cos[(d/d_0)\pi/2] & (\lambda\chi)\sin[(d/d_0)\pi/2] \\ -(\lambda\chi)^{-1}\sin[(d/d_0)\pi/2] & \cos[(d/d_0)\pi/2] \end{bmatrix}, \tag{5.9}$$

where $d_0 = \chi\pi/2$. This is essentially a fractional Fourier transform relation with order d/d_0 and $s = \sqrt{\lambda\chi}$.

Arbitrary LCTs can be decomposed into cascade combinations of the FRT, scaling, and chirp multiplication operations [19]:

$$\mathbf{M} = \begin{bmatrix} A & B \\ C & D \end{bmatrix} = \begin{bmatrix} 1 & 0 \\ -q/s^2 & 1 \end{bmatrix} \begin{bmatrix} M & 0 \\ 0 & \frac{1}{M} \end{bmatrix} \begin{bmatrix} \cos\phi & \sin\phi s^2 \\ -\sin\phi/s^2 & \cos\phi \end{bmatrix} \tag{5.10}$$

Here, q is the chirp multiplication parameter, $M > 0$ is the scaling factor and $\phi = a\pi/2$, where a is the order of the FRT. The decomposition can be written more explicitly in terms of the LCT and FRT domain representations of the signal in the form

$$f_{\mathbf{M}}(x) = \exp\left[-i\pi\frac{q}{s^2}x^2\right]\sqrt{\frac{1}{M}}f_a\left(\frac{x}{M}\right) \tag{5.11}$$

This decomposition was inspired by the optical interpretation in [1] and is also a special case of the widely known Iwasawa decomposition [38, 39, 40]. As we will see, the three parameters a, M, q are sufficient to satisfy the above equality for arbitrary ABCD matrices. If we solve for a, M, q in (5.10), we will obtain the

decomposition parameters in terms of the matrix entries A, B, C, D as follows:

$$a = \begin{cases} \frac{2}{\pi}\text{arctan}\left(\frac{1}{s^2}\frac{B}{A}\right), & \text{if } A \geq 0 \\ \frac{2}{\pi}\text{arctan}\left(\frac{1}{s^2}\frac{B}{A}\right) + 2, & \text{if } A < 0 \end{cases} \tag{5.12}$$

$$M = \sqrt{A^2 + (B/s^2)^2}, \tag{5.13}$$

$$q = \begin{cases} -s^2\frac{C}{A} - \frac{1}{s^2}\frac{B/A}{A^2+(B/s^2)^2}, & \text{if } A \neq 0 \\ -s^2\frac{D}{B}, & \text{if } A = 0 \end{cases} \tag{5.14}$$

The ranges of the arccotangent lie in $(-\pi/2, \pi/2]$.

We now review the effect of a linear canonical transform on the Wigner distribution (WD) of a signal. Roughly speaking, the WD, $W_f(x, f)$, is a phase-space distribution that gives the distribution of signal energy over space and frequency; its definition in terms of $f(x)$ may be found elsewhere [55, 2]. The WD of $f_{\mathbf{M}}(x)$ is related to the WD of $f(x)$ by a linear distortion:

$$W_{f_{\mathbf{M}}}(Ax + Bf, Cx + Df) = W_f(x, f). \tag{5.15}$$

The Jacobian of this coordinate transformation is equal to the determinant of the matrix $\mathbf{M}$, which is unity. Therefore, this coordinate transformation does not change the support area of the Wigner distribution. The support area of the Wigner distribution can be interpreted as the number of degrees of freedom of the signal.

Let us also review the effect of multiplication on the Wigner distribution. If $g(x) = f(x)h(x)$, then

$$W_g(x, f) = \int W_f(x, f')W_h(x, f - f')df'. \tag{5.16}$$

Thus, if two functions are multiplied in the x domain, their Wigner distributions are convolved along the f direction.

5.2 The Relation between Fractional Fourier Domains and Linear Canonical Domains

Fractional Fourier domains correspond to oblique axes in the space frequency plane, and thus they are intimately related to space-frequency representations such as the Wigner distribution. The effect of ath-order fractional Fourier transformation on the Wigner distribution of a signal is to rotate the Wigner distribution by an angle $\phi = a\pi/2$ [41, 42, 20]. Mathematically,

$$W_{f_a}(x, f) = W_f(x\cos\phi - fs^2\sin\phi,\ xs^{-2}\sin\phi + f\cos\phi). \tag{5.17}$$

The squared magnitude of the ath order FRT of a function $f(x)$ is given by

$$|f_a(x)|^2 = \int W_{f_a}(x, f)df. \tag{5.18}$$

To avoid the problems associated with assigning units to oblique axes in the dimensional space-frequency plane, let u_a denote the axis making angle $\phi = a\pi/2$ with the horizontal axis in the dimensionless space-frequency plane (Fig. 5.1). Then, the above equation is equivalent to say that the projection of the Wigner distribution of a function onto the u_a axis gives the squared magnitude of the ath order FRT of the function with dimensionless parameters. Hence, the projection axis u_a can be referred to as the ath order fractional Fourier domain [41, 42]. The space and frequency domains are merely special cases of the continuum of fractional Fourier domains.

Recently, there has also been increased interest in generalizing the fractional Fourier transform and its properties to linear canonical transforms. From analogy with fractional Fourier domains, the term *LCT domain* has been used to refer to the domain where the LCT representation of the signal "lives" [43, 14, 44, 45]. However, although fractional Fourier domains are well-defined in the space-frequency plane [41, 2], it is not yet established where LCT domains exist and what they correspond to in the space-frequency plane. Moreover, LCT domains

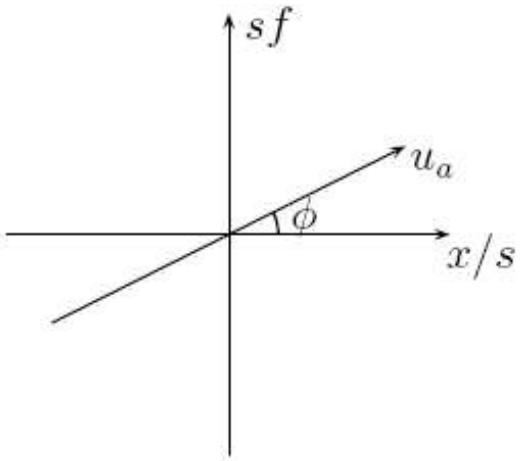

Figure 5.1: The ath order fractional Fourier domain

are characterized by three parameters (one of the four matrix parameters is redundant because of the unit-determinant condition). Since each parameter can vary independently, LCT domains are a three-parameter space; that is, each LCT domain can be labeled with three parameters, which makes them hard to visualize.

One of the contributions of this work is to figure out where linear canonical domains exist in the ordinary space-frequency plane. We will show that each LCT domain is a scaled FRT domain, and thus any LCT domain can be labeled simply by its associated fractional order a. Therefore, each LCT domain is effectively associated with only one parameter a and as we will see, this parameter is monotonically increasing through arbitrary quadratic-phase systems.

We will now introduce *essentially equivalent domains* by using the Iwasawa decomposition given in (5.11). As we have seen, any arbitrary LCT of a signal can be expressed as chirp multiplied and scaled version of the ath order FRT of the signal, which we repeat here for convenience:

$$f_{\mathbf{M}}(x) = \exp\left[-i\pi\frac{q}{s^2}x^2\right]\sqrt{\frac{1}{M}}f_a\left(\frac{x}{M}\right). \tag{5.19}$$

The parameters of the FRT, scaling, and chirp multiplication are given in terms of the LCT parameters in (5.12), (5.13), and (5.14), respectively. We note that all of the variables in (5.19) are dimensional. However, in order to avoid the problems associated with assigning units to oblique axes in phase-space, before refering to FRT domains, we need to define the dimensionless form of $f_a(x)$. The dimensionless form $\bar{f}_a(u)$ and the dimensional form $f_a(x)$ are related to each other through the relation $\bar{f}_a(u) = f_a(su)$. In order to compute an arbitrary LCT of a signal based on (5.19), we can first take the ath order FRT of the signal. This operation moves the signal to the ath order fractional Fourier domain. Secondly, we scale the transformed signal. Scaling does not effectively move the signal to a different domain, and thus the signal is at a scaled FRT domain after the scaling operation. Finally, we multiply the resulting signal with a chirp to obtain the LCT. Chirp multiplication can be interpreted as a windowing operation in the current domain; thus, it does not change the domain of the signal, just like the scaling operation. Therefore, linear canonical transformed signals live at a scaled ath order FRT domain. This discussion also reveals that LCT domains are essentially equivalent to scaled fractional Fourier domains, and thus they are not richer than FRT domains. Note that LCTs with the same A/B or equivalently γ parameter, contain the same order of FRT in their decomposition as seen from (5.12) and therefore they are associated with the same FRT domain. We refer to such LCT domains as *essentially equivalent domains*. The condition $A_1/B_1 = A_2/B_2$ for essentially equivalent domains is equivalent to the condition in [45] where the uncertainty relation is not valid.

As the signal passes through an arbitrary quadratic-phase system, it will continuously visit LCT domains of different parameters. Since LCT domains are equivalent to scaled FRT domains, there exists a FRT order associated with each domain. The order a begins from 0 at the input of the system, and then monotonically increases as a function of distance. The reason is that the FRT order does not change after a lens system and it increases as a function of distance

in a section of free-space or quadratic graded-index media [1]. (To see this, use (5.12) together with equations (5.6), (5.7), (5.9).) Since an arbitrary quadratic-phase system consists of an arbitrary concatenation of thin lenses, sections of free-space and quadratic graded-index media, passing through such a system corresponds to passing through scaled FRT domains of monotonically increasing order.

Let us now consider a set of signals, whose members are approximately confined to the intervals $[-\Delta u_{\mathbf{M}_1}/2, \Delta u_{\mathbf{M}_1}/2]$ and $[-\Delta u_{\mathbf{M}_2}/2, \Delta u_{\mathbf{M}_2}/2]$ in two LCT domains, namely $u_{\mathbf{M}_1}$ and $u_{\mathbf{M}_2}$. Since LCT domains are equivalent to scaled fractional Fourier domains, each interval given in an LCT domain will define a scaled interval in the associated FRT domain. To see this explicitly, we again refer to (5.19), which implies that if $f_{\mathbf{M}}(x)$ is confined to an interval of length $\Delta u_{\mathbf{M}}$, so is $f_a(x/M)$. Then, the extent of $f_a(x)$ is $\Delta u_{\mathbf{M}}/M$ and the extent of its dimensionless form $\bar{f}_a(u)$ is $\Delta u_{\mathbf{M}}/Ms$, which gives the extent in the associated ath order FRT domain in the dimensionless space-frequency plane. Thus, for the set of signals in question, the extent in the a_1th order FRT domain is $\Delta u_{\mathbf{M}_1}/M_1 s$ and the extent in the a_2th order FRT domain is $\Delta u_{\mathbf{M}_2}/M_2 s$, where a_1 and a_2 are related to $\mathbf{M}_1$ and $\mathbf{M}_2$ through equation 5.12. Note that we should take into account the FRT and scaling parameters of the decomposition, but not the chirp multiplication parameter. It is well-known that if the space-, frequency- or FRT-domain representation of a signal is identically zero (negligible) outside a certain interval, so is its Wigner distribution [2]. As a direct consequence of this fact, the Wigner distribution of this set of signals is confined to the corridors of width $\Delta u_{\mathbf{M}_1}/M_1 s$ and $\Delta u_{\mathbf{M}_2}/M_2 s$ in the directions orthogonal to u_{a_1} and u_{a_2}, respectively. Thus, the support of the Wigner distribution is a parallelogram defined by these corridors (see Fig. 5.2). In general, if more than two extents are specified in different LCT domains, the space-frequency support will be a centrally symmetrical convex polygon defined by these intervals (Fig. 5.3).

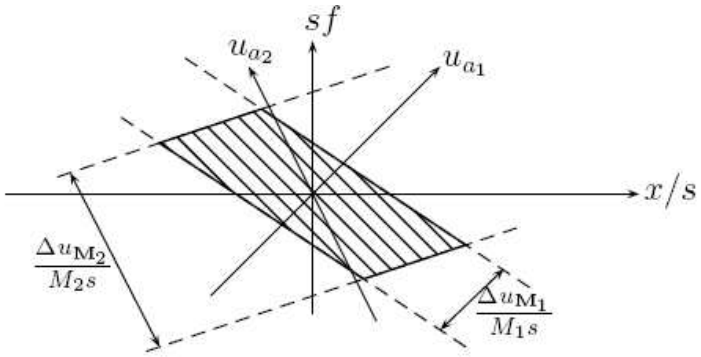

Figure 5.2: Support of the Wigner distribution when two extents are specified

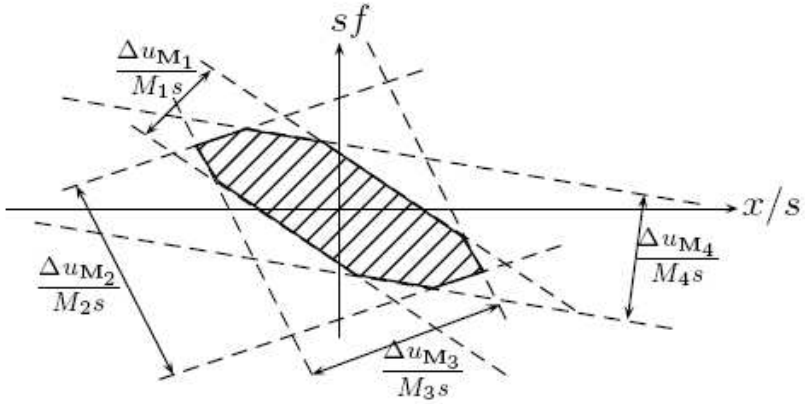

Figure 5.3: Support of the Wigner distribution when more than two extents are specified

Theorem 3. *The bicanonical width product* $\Delta u_{\mathbf{M}_1} \Delta u_{\mathbf{M}_2} |\beta_{1,2}|$ *is the area of the parallelogram defined by the extents* $\Delta u_{\mathbf{M}_1}$ *and* $\Delta u_{\mathbf{M}_2}$ *in two LCT domains (Fig. 5.2). Equivalently, it is the area of the space-frequency support of the signals, which have finite extents* $\Delta u_{\mathbf{M}_1}$ *and* $\Delta u_{\mathbf{M}_2}$ *in* $u_{\mathbf{M}_1}$ *and* $u_{\mathbf{M}_2}$ *domains, respectively.*

Proof. Let h_1 and h_2 be two heights of a parallelogram and ϕ denote the angle between them. Then, the area of the parallelogram is given by $h_1 h_2 |\csc \phi|$. For the parallelogram defined by the extents $\Delta u_{\mathbf{M}_1}$ and $\Delta u_{\mathbf{M}_2}$, the heights are $\Delta u_{\mathbf{M}_1}/M_1 s$ and $\Delta u_{\mathbf{M}_2}/M_2 s$, which correspond to the widths of the corridors.

Then, the area of this parallelogram is

$$\begin{aligned}
\text{Area} &= \frac{\Delta u_{\mathbf{M}_1}}{M_1 s}\frac{\Delta u_{\mathbf{M}_2}}{M_2 s}|\csc(\phi_1-\phi_2)| && (5.20)\\
&= \frac{\Delta u_{\mathbf{M}_1}\Delta u_{\mathbf{M}_2}}{M_1 M_2 s^2|\sin\phi_2\cos\phi_1-\cos\phi_2\sin\phi_1|} && (5.21)\\
&= \frac{\Delta u_{\mathbf{M}_1}\Delta u_{\mathbf{M}_2}}{|A_1B_2-B_1A_2|} && (5.22)\\
&= \Delta u_{\mathbf{M}_1}\Delta u_{\mathbf{M}_2}\frac{|\beta_1\beta_2|}{|\gamma_1-\gamma_2|} && (5.23)\\
&= \Delta u_{\mathbf{M}_1}\Delta u_{\mathbf{M}_2}|\beta_{1,2}| && (5.24)
\end{aligned}$$

□

As is well-known, when two extents are specified in the space and frequency domains, the space-frequency support of the signal is confined to a rectangular region. In this case, the space-bandwidth product equals to the number of degrees of freedom since it gives the area of that rectangular region. We have showed that in the general case when two extents are specified in arbitrary two LCT domains, the space-frequency support of the signal is confined to a parallelogram. In this case, the bicanonical width product equals to the number of degrees of freedom since it gives the area of that parallelogram.

5.3 Phase-Space Window of Optical Systems

We now investigate the largest space-frequency region that can pass through the system without any information loss, which we refer to as the *phase-space window* of the system. The area of the phase-space window will give the number of degrees of freedom of the system. In this section, we develop a method that allows us to find the phase-space window in terms of the system parameters for an arbitrary quadratic phase system with arbitrary number of apertures.

We will first establish the notation that will be used throughout this chapter. Let us consider a quadratic-phase system, which consists of arbitrary number

of lenses, sections of free space and quadratic graded-index media as well as apertures. For simplicity we restrict ourselves to a single transverse dimension. The input plane is defined as $z = 0$. The output plane is variable ranging from $z = 0$ to $z = z_f$, where z_f is the length of the optical system. Each z plane corresponds to an LCT domain. Let $\mathbf{M}(z)$ denote the matrix of the system lying between 0 and z (excluding the apertures), which can be readily calculated using the matrices for lenses, sections of free space and quadratic graded index media, and the concatenation property. The elements of $\mathbf{M}(z)$ will be denoted by $A(z)$, $B(z)$, $C(z)$, and $D(z)$. Since LCT domains are equivalent to scaled FRT domains, let $a(z)$, $M(z)$, $q(z)$ represent the fractional transform order, the scaling factor and chirp multiplication parameter of the FRT description of the system occupying the interval $[0, z]$, which can be determined from $A(z)$, $B(z)$, $C(z)$, and $D(z)$ by using the Iwasawa decomposition. As we have seen before, the order $a(z)$ begins from 0 at the input of the system, and then monotonically increases as a function of distance. We further let L denote the total number of apertures in the system. Then, z_j and Δ_j will denote respectively the position and size of a particular rectangular aperture j in the system. The matrix $\mathbf{M}(z_j, z_k)$ will be used to denote the matrix of the system between jth and kth apertures and $\beta_{j,k}$ will be used to denote its β parameter. $\mathbf{M}(z_j)$ will denote the matrix of the system up to the jth aperture. We will denote its matrix coefficients by A_j, B_j, C_j, D_j, its decomposition parameters by a_j, M_j, q_j and its β parameter by β_j, which is equivalent to $\beta_{0,j}$ by definition. Note that $\mathbf{M}(z_j)$ is also equivalent to $\mathbf{M}(0, z_j)$ by definition. z_j^- and z_j^+ will be used to denote the distance of the planes immediately to the left and immediately to the right of the jth aperture.

We can now investigate the phase-space window of an arbitrary optical system. For a lossless transfer through the system, the extent of the signal just before each aperture must be not larger than the size of the aperture. That is, the following condition must be satisfied for $j = 1, 2, \ldots, L$:

$$\Delta u_{\mathbf{M}_j} \leq \Delta_j, \tag{5.25}$$

where $\Delta u_{\mathbf{M}_j}$ denotes the extent of the signal in the $u_{\mathbf{M}_j}$ domain, which corresponds to the domain at $z = z_j$ plane. For the same reasons discussed in Section 5.2, the above condition is equivalent to

$$\Delta u_{a_j} \leq \Delta_j / M_j s, \tag{5.26}$$

where Δu_{a_j} denotes the extent of the signal in the a_jth order FRT domain. Thus, for every $j \in [1, L]$, the signal must be confined to the interval of length $\Delta_j / M_j s$ in the a_jth order FRT domain. This condition defines a corridor of width $\Delta_j / M_j s$ in the direction orthogonal to u_{a_j} in the space-frequency plane. By intersecting the corridors defined by each aperture, the bounded region in the space-frequency plane can be obtained as a centrally symmetrical convex polygon. (see Figure 5.3 by replacing $\Delta u_{\mathbf{M}_j} / M_j s \rightarrow \Delta_j / M_j s$ for each $j \in [1, 4]$). The resulting centrally symmetrical convex polygon defined by normalized aperture sizes is the *phase-space window* of the system. The area of the phase-space window is the number of degrees of freedom of the system; that is, at most that many number of degrees of freedom can pass through the system.

A concrete example will be useful. Fig. 5.4 shows a system consisting of several apertures and lenses, whose focal lengths have been indicated in meters right above them. The fractional transform order a, the scale parameter M, and the chirp multiplication parameter q of the system are plotted as functions of z in Fig. 5.5. The phase-space window of this system is shown in Fig. 5.6. This region is defined by the 2nd, 4th and 8th apertures in the system. Other apertures does not affect the phase-space window of the system.

We can represent the degrees of freedom of the system both as a region and as a number. Let us denote the phase-space window of the system as R_{sys} and the phase-space region of the input signal as R_{sig}. Let us also denote the area of these regions as A_{sys} and A_{sig}, respectively. For an arbitrary input signal, in order to pass through the system without any information loss, it is necessary that A_{sig} be smaller than A_{sys}. However, this is not sufficient. Even if the area

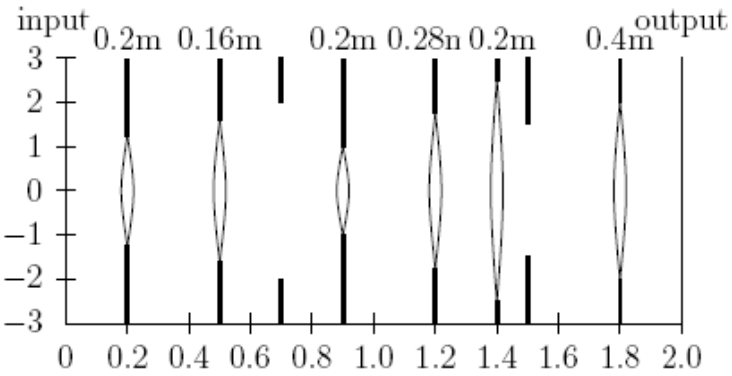

Figure 5.4: Optical system

is smaller, if R_{sig} does not lie completely inside R_{sys}, information loss will take place. A similar discussion has been previously given in [28].

If R_{sys} does not enclose R_{sig} completely, then approximately the intersection of the two regions R_{sig} and R_{sys} will pass through the system. This approximation is valid if after each limiting aperture we can neglect the broadening of the region along the orthogonal domain. To see this, let us first assume that the broadening effects are negligible. Then, given an arbitrary phase-space region R_{sig} at the input, one can obtain the phase-space region at the output by tracing the region throughout the system and simply cutting some parts of it whenever a limiting aperture is reached. With this approach, the obtained phase-space region at the output will be simply the propagated version of the input region given by the intersection of the regions R_{sig} and R_{sys}. Therefore, when a signal with greater number of degrees of freedom is input into a system with smaller number of degrees of freedom, an uninvertible information loss will take place. The amount of lost information will be the area of the non-overlapping regions between R_{sig} and R_{sys}.

However, this simple and intuitive result may lose its validity when we take into account the broadening effects. We will now clarify that the broadening effects are truly negligible for real physical signals and systems, which makes

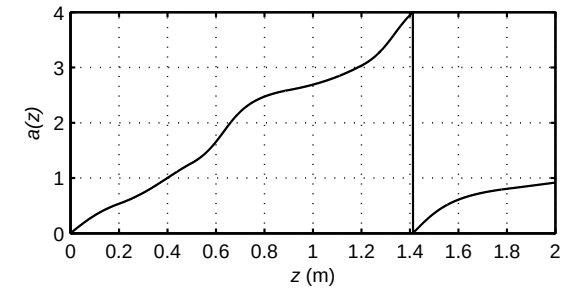

(a)

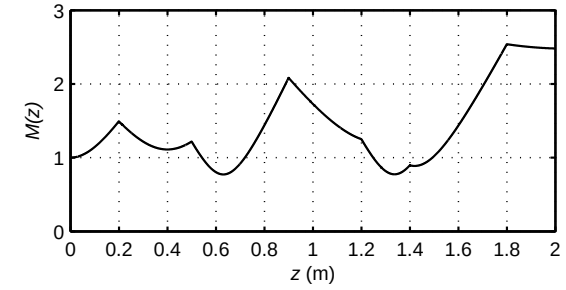

(b)

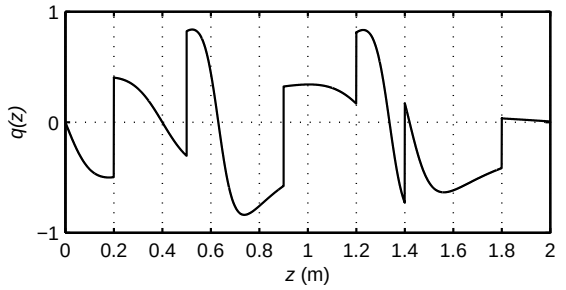

(c)

Figure 5.5: Evolution of $a(z)$, $M(z)$, $q(z)$ as functions of z: $\lambda = 0.5$ μm and $s = 0.3$ mm [1, 2]

the above simple result always valid for our purposes. For simplicity, let us work with rectangular regions in phase-space, and thus take the time-bandwidth product as the measure of number of degrees of freedom. Let us denote the time-bandwidth product of the signal as $\Delta u \Delta \mu = N$, where $N \geq 1$. For an arbitrary window, we can in general approximate the product of its spatial extent Δu_g and spectral extent $\Delta \mu_g$ as unity, equivalently $\Delta u_g \Delta \mu_g \approx 1$. Assume that the window allows only κ portion of the signal to pass, that is $\Delta u_g = \kappa \Delta u$ where $\kappa < 1$. Then, after the window, the new extent in the space domain will be

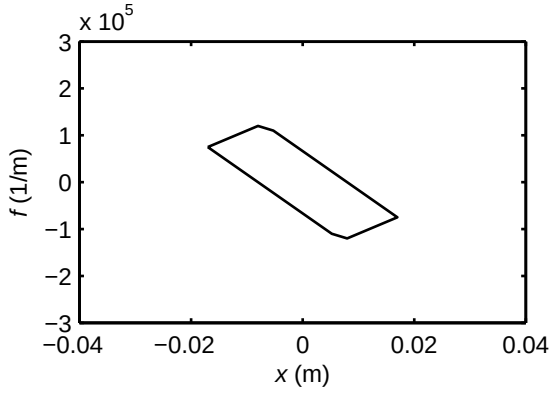

Figure 5.6: The phase-space window of the system

given by $\Delta u' = \kappa \Delta u$. Moreover, since multiplication in space domain implies convolution in the frequency domain, the new extent in the frequency domain will be approximately the sum of the spectral extents of the signal and the window. The spectral extent of the signal is $\Delta\mu = N/\Delta u$ and the spectral extent of the window is $\Delta\mu_g \approx 1/\Delta u_g = 1/\kappa\Delta u = \Delta\mu/\kappa N$. Then, the new extent in the frequency domain is $\Delta\mu' \approx \Delta\mu + \Delta\mu/\kappa N = \Delta\mu(1 + 1/\kappa N)$. Therefore, the time-bandwidth product of the signal after the windowing operation is $\Delta u' \Delta\mu' \approx \Delta u \Delta\mu(\kappa + 1/N)$. Here, the first term corresponds to the decreased region area due to windowing and the second term corresponds to the additional area of the region that comes from the broadening effect. However, if $\kappa \gg 1/N$, or equivalently $N \gg 1/\kappa$, then we can neglect the term $1/N$ as compared to κ. This means that in this case the area coming from the broadening effect is negligible. Thus, we can neglect the broadening effect if $N \gg 1/\kappa$. This condition is true for most real physical signals and systems. For a physical signal that contains any reasonable information, such as an image, the number of degrees of freedom will be much larger than unity and also much larger than $1/\kappa$, as long as κ is not very close to 0, or equivalently the aperture does not nearly fully limit the signal. For instance, consider a window that allows only 0.1 portion of the signal to pass. Even in this case, $N \gg 10$ will be sufficient and most information bearing signals will satisfy this condition easily.

5.4 Wigner-based Extent Tracing

In this section, we investigate how the extent of an arbitrary input signal changes as it passes through an optical system. For this, we will track the Wigner distribution of the signal throughout the system. This investigation will also cover the lossy transfer case which arises when the input signal has a larger phase-space region than the phase-space window of the system. Our main purpose is to use these extents to find the minimum number of samples to represent the physical signal at an arbitrary plane and to simulate the optical system with discrete-time systems. These concepts will be investigated in Section 5.8.

In order to track the Wigner distribution throughout the system, we will assume polygonal regions in phase-space. However, the proposed method will also apply to non-polygonal regions since any non-polygonal region can be efficiently approximated by a polygonal region. In [5] four-sided polygonal phase-space regions have been assumed in order to develop an automated method for tracking the space-bandwidth product. We will develop an automated method for tracking the extent of the signal through the system by making use of the terminology and approach presented in [5].

Let us assume that we are given a polygonal phase-space region of a signal. The matrix that contains the coordinates of the corners of the polygonal region will be denoted by the corner matrix $\mathbf{S}$. For instance, for a polygon with n corners (x_1, f_1), (x_2, f_2), ..., (x_n, f_n), the corner matrix $\mathbf{S}$ is given by [5]

$$\mathbf{S} = \begin{bmatrix} \mathbf{S}_x \\ \mathbf{S}_f \end{bmatrix} = \begin{bmatrix} x_1 & x_2 & \dots & x_n \\ f_1 & f_2 & \dots & f_n \end{bmatrix} \tag{5.27}$$

where $\mathbf{S}_x$ and $\mathbf{S}_f$ are 1xn row vectors which respectively contain the x and f coordinates of the corners. The extent in the space domain is simply the maximum distance between any two of the x coordinates, which is given by

$$\Delta x = \max\{\mathbf{S}_x\} - \min\{\mathbf{S}_x\} \tag{5.28}$$

where max and min operators find respectively the maximum and minimum element in a vector.

Any arbitrary quadratic-phase system is mathematically equivalent to the combination of many LCT blocks and multiplication with rectangular functions. While an LCT block models a section of the quadratic-phase system, multiplication with a rectangular function models the rectangular apertures between the sections of quadratic-phase systems. In order to track the corner matrix $\mathbf{S}$ through the system, we need to find the effect of an LCT block and the effect of a rectangular window on $\mathbf{S}$.

The effect of a linear canonical transform on the Wigner distribution is a linear distortion given by (5.15). Then, the effect of an LCT block on the corner matrix $\mathbf{S}$ is as follows [5]

$$\begin{aligned} \mathbf{S}' &= \mathbf{MS} = \begin{bmatrix} A & B \\ C & D \end{bmatrix} \begin{bmatrix} x_1 & x_2 & \dots & x_n \\ f_1 & f_2 & \dots & f_n \end{bmatrix} \\ &= \begin{bmatrix} Ax_1 + Bf_1 & Ax_2 + Bf_2 & \dots & Ax_n + Bf_n \\ Cx_1 + Df_1 & Cx_2 + Df_2 & \dots & Cx_n + Df_n \end{bmatrix} \end{aligned} \tag{5.29}$$

where $\mathbf{S}$ and $\mathbf{S}'$ are the corner matrices before and after the LCT block, respectively. As seen, although the number of corners remains to be the same after an LCT block, the position of each corner may change due to the change in the shape of the phase-space region.

Secondly, we will investigate the effect of a rectangular windowing on the Wigner distribution and the corner matrix $\mathbf{S}$. Let Δ_j denote the width of the window. Firstly, if the extent of the signal before windowing is already smaller than Δ_j, then clearly the windowing operation will not affect the signal, an thus its phase-space region and corner matrix $\mathbf{S}$. However, if the extent is larger than Δ_j, then the phase-space region will change. Because windowing involves multiplication with a rectangle function, it implies convolution of the Wigner distribution of the signal with the Wigner distribution of the rectangle function

along the f direction (see equation (5.16)). The Wigner distribution of the function rect(x/Δ_{j}) is given by [2]

$$W_{\mathrm{rect}}(x,f) = 2\Delta_j \left[1 - \frac{2|x|}{\Delta_j}\right] \mathrm{rect}\left\{\frac{\mathrm{x}}{\Delta_{\mathrm{j}}}\right\} \mathrm{sinc}\left\{2\Delta_{\mathrm{j}}\left[1 - \frac{2|\mathrm{x}|}{\Delta_{\mathrm{j}}}\right]\mathrm{f}\right\} \qquad (5.30)$$

Observe that the Wigner distribution is nonzero only along the corridor defined by the rectangle function. This will cause compaction of the Wigner distribution to a corridor of width Δ_j which is orthogonal to the x axis. Moreover, convolving the Wigner distribution of the signal with $W_{\mathrm{rect}}(x,f)$ along the f direction will result in broadening of the Wigner distribution in the f direction that is comparable with the extent of $W_{\mathrm{rect}}(x,f)$ in the f direction. This extent is approximately $1/\Delta_j$ independent of x, and thus the spread in the f direction after windowing will be $\sim 1/\Delta_j$ [20]. This result is crude and tricky since it can be problematic when the extent of the signal distribution in the f direction becomes comparable with $1/\Delta_j$ (see the discussion in the appendix). However, for practical physical signals and windows, we will not encounter this problematic case. This approximation will be also valid throughout this work since in our case the extent of the signal in the f direction is much larger than $1/\Delta_j$.

With the understanding of the effect of rectangular windowing on the Wigner distribution, we can now find the effect of this operation on the corner matrix $\mathbf{S}$. Firsly, compaction of the Wigner distribution to a corridor of width Δ_j which is orthogonal to the x axis will define new corners for the Wigner distribution while removing some previously existing ones. After intersecting this corridor with the polygon defined by current $\mathbf{S}$, we can recognize the intersection points as the new additional corners. We should also remove the corners that are outside this corridor. By taking into account these changes, the corner matrix $\mathbf{S}$ will be modified appropriately. Lastly, the broadening effect in the f direction should be reflected to the vertical coordinate of each corner. The intersection points above at the two sides of the corridor and all the corners in between will have increased vertical coordinates by an amount $1/2\Delta_j$. Similarly, the intersection

points below at the two side of the corridor and all the corners in between will have decreased vertical coordinates by an amount $1/2\Delta_j$.

Now, we can investigate how the extent of an input signal changes through an optical system when its phase-space region is specified. Given a polygonal phase-space region, we can define the initial corner matrix. Even if the given region is not a polygon, but an arbitrarily shaped region, then it is always possible to efficiently approximate it by a polygonal region and define the initial corner matrix accordingly. Then, we can track the corner matrix, and thus the extent of the signal through the system.

Instead of specifying the initial phase-space region of the signal, it is possible to specify its extents in two different LCT domains, say $\Delta u_{\mathbf{M}_1}$ and $\Delta u_{\mathbf{M}_2}$. Then, we know from the discussion in Section 5.2 that the initial phase-space region will be a centrally symmetrical convex parallelogram as shown in Fig. 5.2. However, we need to find the corners of this parallelogram in order to apply the above procedure. Since it is most appropriate to define the corridors in dimensionless domains, we will first find the corners of the shape in the dimensionless Wigner domain and then express these corners in the dimensional Wigner domain. The corridors defined by the extent $\Delta u_{\mathbf{M}_1}$ are given by the lines

$$\mu = -\cot\phi_1 u \pm \frac{\Delta u_{\mathbf{M}_1}}{2sM_1 \sin\phi_1} \tag{5.31}$$

Similarly, the corridors defined by the extent $\Delta u_{\mathbf{M}_2}$ are given by the lines

$$\mu = -\cot\phi_2 u \pm \frac{\Delta u_{\mathbf{M}_2}}{2sM_2 \sin\phi_2} \tag{5.32}$$

From the intersection of the lines in (5.31) and (5.32), the corners of the parallelogram in the dimensionless Wigner domain can be obtained as

$$\bar{\mathbf{S}} = \begin{bmatrix} u_1 & u_2 & -u_1 & -u_2 \\ \mu_1 & \mu_2 & -\mu_1 & -\mu_2 \end{bmatrix} \tag{5.33}$$

where

$$u_1 = \frac{1}{\cot\phi_1 - \cot\phi_2}\left(\frac{\Delta u_{\mathbf{M}_1}}{2sM_1\sin\phi_1} + \frac{\Delta u_{\mathbf{M}_2}}{2sM_2\sin\phi_2}\right) \tag{5.34}$$

$$u_2 = \frac{1}{\cot\phi_1 - \cot\phi_2}\left(\frac{\Delta u_{\mathbf{M}_1}}{2sM_1\sin\phi_1} - \frac{\Delta u_{\mathbf{M}_2}}{2sM_2\sin\phi_2}\right) \tag{5.35}$$

$$\mu_1 = \frac{1}{\cot\phi_1 - \cot\phi_2}\left(-\cot\phi_1\frac{\Delta u_{\mathbf{M}_2}}{2sM_2\sin\phi_2} - \cot\phi_2\frac{\Delta u_{\mathbf{M}_1}}{2sM_1\sin\phi_1}\right) \tag{5.36}$$

$$\mu_2 = \frac{1}{\cot\phi_1 - \cot\phi_2}\left(\cot\phi_1\frac{\Delta u_{\mathbf{M}_2}}{2sM_2\sin\phi_2} - \cot\phi_2\frac{\Delta u_{\mathbf{M}_1}}{2sM_1\sin\phi_1}\right) \tag{5.37}$$

Since we can pass to the dimensional Wigner domain from the dimensionless one by scaling the u axis by s and scaling the μ axis by $1/s$, the dimensional form of the above $\mathbf{S}$ matrix can be obtained as

$$\mathbf{S} = \begin{bmatrix} x_1 & x_2 & -x_1 & -x_2 \\ f_1 & f_2 & -f_1 & -f_2 \end{bmatrix} \tag{5.38}$$

where $x_1 = su_1$, $x_2 = su_2$, $f_1 = \mu_1/s$, and $f_2 = \mu_2/s$.

We now apply this procedure for the system in Fig. 5.4. When two extents are specified in two FRT domains, Fig. 5.7 shows the evolution of the extent $E(z)$ as a function of z. The reader can study the evolution of the Wigner distribution in conjunction with the graphs in Fig. 5.8. The simulations are repeated by specifying a much larger initial phase-space region and the results are shown in Fig. 5.9. Observe that even if we start with a very large or infinite support in the phase-space, the signal gets adapted to the system latest after passing the second aperture provided that the first two apertures do not lie in nearly essentially equivalent domains. Then, other apertures cut the region slightly compared to the first two apertures. This is due to the fact that the phase-space region has two dimensions, space and frequency; therefore, we can confine it with at least two corridors. One corridor is not sufficient; at least two corridors are required to bound an unbounded region. These two domains need not be space and frequency domains, they can be any LCT/FRT domains as long as they are not nearly parallel to each other (in order to create different corridors). In the

case that when these two domains are nearly parallel to each other, we will need more than two corridors to meaningfully bound the region.

5.5 Direct Extent Tracing Formulas

Based on the Wigner-based extent tracing method, we will now provide formulas to directly trace the extent from the given extents of the input signal. For this, we will first derive the formulas to find the extent of a signal at an arbitrary LCT domain when arbitrary number of extents are specified in arbitrary LCT domains. Formulas allowing us to find an extent from many given extents will be based on the knowledge obtained in the last section. Then, we will use these formulas to track the extent of a signal as it propagates through an optical system when a centrally symmetrical convex polygonal space-frequency region is given at the input, or equivalently the extent of the signal is specified in arbitrary LCT domains. The advantage of these formulas is that the extent at an arbitrary plane in the system can be found without refering to the Wigner domain and thus, we can trace the extent directly without performing the simulations described in the last section.

Remember from Section 5.2 that if two or more extents are specified in different LCT domains, the space-frequency support will be a centrally symmetrical convex polygon defined by these extents (see Fig. 5.3). First let us concentrate on the case when only two extents are specified. Let $\Delta u_{\mathbf{M}_1}$ and $\Delta u_{\mathbf{M}_2}$ denote the specified extents in the $u_{\mathbf{M}_1}$ and $u_{\mathbf{M}_2}$ domains, respectively. In this case, the support will be a parallelogram, whose corners in the (dimensional) Wigner domain is given in (5.38). Let $u_{\mathbf{M}_3}$ be the domain where we want to find the extent. In order to find $\Delta u_{\mathbf{M}_3}$, we should first take into account the effect of LCT on the Wigner support. We can compute the new corner matrix after the

LCT as

$$\begin{aligned}\mathbf{S}' &= \mathbf{M}_3\mathbf{S} = \begin{bmatrix} A_3 & B_3 \\ C_3 & D_3 \end{bmatrix} \begin{bmatrix} x_1 & x_2 & -x_1 & -x_2 \\ f_1 & f_2 & -f_1 & -f_2 \end{bmatrix} \\ &= \begin{bmatrix} A_3x_1 + B_3f_1 & A_3x_2 + B_3f_2 & -A_3x_1 - B_3f_1 & -A_3x_2 - B_3f_2 \\ C_3x_1 + D_3f_1 & C_3x_2 + D_3f_2 & -C_3x_1 - D_3f_1 & -C_3x_2 - D_3f_2 \end{bmatrix}\end{aligned} \tag{5.39}$$

The corners here defines the support of the Wigner distribution of the transformed signal. Therefore, the horizontal axis x corresponds to the $u_{\mathbf{M}_3}$ domain and the vertical axis f corresponds to the frequency domain with respect to the $u_{\mathbf{M}_3}$ domain. Then, the maximum distance between any two of the x coordinates is the extent of the signal in the $u_{\mathbf{M}_3}$ domain:

$$\Delta u_{\mathbf{M}_3} = \max\{\mathbf{S}'_x\} - \min\{\mathbf{S}'_x\}. \tag{5.40}$$

After considering all possible results of the above equation, $\Delta u_{\mathbf{M}_3}$ can be expressed more explicitly as follows:

$$\Delta u_{\mathbf{M}_3} = |A_3x_1| + |B_3f_1| \tag{5.41}$$

$$= \left(\left| \frac{A_3 - B_3\frac{\cot\phi_2}{s^2}}{M_1 \sin\phi_1} \right| \Delta u_{\mathbf{M}_1} + \left| \frac{A_3 - B_3\frac{\cot\phi_1}{s^2}}{M_2 \sin\phi_2} \right| \Delta u_{\mathbf{M}_2} \right) \frac{1}{|\cot\phi_1 - \cot\phi_2|} \tag{5.42}$$

$$= \left(\left| \frac{A_3 - B_3A_2/B_2}{B_1} \right| \Delta u_{\mathbf{M}_1} + \left| \frac{A_3 - B_3A_1/B_1}{B_2} \right| \Delta u_{\mathbf{M}_2} \right) \frac{1}{|A_1/B_1 - A_2/B_2|} \tag{5.43}$$

$$= \left| \frac{(\gamma_3 - \gamma_2)\beta_1}{(\gamma_2 - \gamma_1)\beta_3} \right| \Delta u_{\mathbf{M}_1} + \left| \frac{(\gamma_3 - \gamma_1)\beta_2}{(\gamma_2 - \gamma_1)\beta_3} \right| \Delta u_{\mathbf{M}_2} \tag{5.44}$$

Here, the equations (5.12) and (5.13) is used in (5.42) to obtain (5.43), which gives the extent in terms of the matrix entries A, B, C, D. Moreover, (5.2) is used in (5.43) to obtain (5.44), which gives the extent in terms of the parameters α, β, γ.

Now, we will concentrate on the case when three extents are specified. Let $\Delta u_{\mathbf{M}_1}$, $\Delta u_{\mathbf{M}_2}$, and $\Delta u_{\mathbf{M}_3}$ denote the specified extents in the $u_{\mathbf{M}_1}$, $u_{\mathbf{M}_2}$, and $u_{\mathbf{M}_3}$ domains, respectively. Let $u_{\mathbf{M}_4}$ be the domain where we want to find the extent. Now, we will follow the same procedure as the two extents given case. The three corridors defined by the extents will be given in the similar form with (5.31).

These corridors will intersect at six points, which will give the corners in the **S** matrix. Then, the new corner matrix will be computed after applying the LCT with parameter $\mathbf{M}_4$. After simplifications the extent in the $u_{\mathbf{M}_4}$ domain can be obtained as follows, although the algebra is somewhat involved:

$$\begin{aligned}\Delta u_{\mathbf{M}_4} = \min & \left(\left| \frac{A_4 - B_4 A_2/B_2}{B_1} \right| \Delta u_{\mathbf{M}_1} + \left| \frac{A_4 - B_4 A_1/B_1}{B_2} \right| \Delta u_{\mathbf{M}_2} \right) \frac{1}{|A_2/B_2 - A_1/B_1|}, \\ & \left(\left| \frac{A_4 - B_4 A_3/B_3}{B_1} \right| \Delta u_{\mathbf{M}_1} + \left| \frac{A_4 - B_4 A_1/B_1}{B_3} \right| \Delta u_{\mathbf{M}_3} \right) \frac{1}{|A_3/B_3 - A_1/B_1|}, \\ & \left(\left| \frac{A_4 - B_4 A_3/B_3}{B_2} \right| \Delta u_{\mathbf{M}_2} + \left| \frac{A_4 - B_4 A_2/B_2}{B_3} \right| \Delta u_{\mathbf{M}_3} \right) \frac{1}{|A_3/B_3 - A_2/B_2|} \end{aligned} \quad (5.45)$$

It is now straightforward to generalize equations (5.43) and (5.45) to the case when k extents are specified. Given k extents $\Delta u_{\mathbf{M}_1}$, ..., $\Delta u_{\mathbf{M}_k}$ in the $u_{\mathbf{M}_1}$, ..., $u_{\mathbf{M}_k}$ domains for $k \geq 2$, the extent in the $u_{\mathbf{M}_{k+1}}$ domain is given by

$$\begin{aligned} \Delta u_{\mathbf{M}_{k+1}} &= \min_{\substack{i,j \\ i \neq j \\ 1 \leq i,j \leq k}} \left(\left| \frac{A_{k+1} - B_{k+1} A_j/B_j}{B_i} \right| \Delta u_{\mathbf{M}_i} + \left| \frac{A_{k+1} - B_{k+1} A_i/B_i}{B_j} \right| \Delta u_{\mathbf{M}_j} \right) \\ &\quad \times \frac{1}{|A_j/B_j - A_i/B_i|} \qquad (5.46) \\ &= \min_{\substack{i,j \\ i \neq j \\ 1 \leq i,j \leq k}} \left| \frac{(\gamma_{k+1} - \gamma_j)\beta_i}{(\gamma_j - \gamma_i)\beta_{k+1}} \right| \Delta u_{\mathbf{M}_i} + \left| \frac{(\gamma_{k+1} - \gamma_i)\beta_j}{(\gamma_j - \gamma_i)\beta_{k+1}} \right| \Delta u_{\mathbf{M}_j} \qquad (5.47) \end{aligned}$$

Note that if only one extent $\Delta u_{\mathbf{M}_1}$ is given in the $u_{\mathbf{M}_1}$ domain, the extent in the $u_{\mathbf{M}_2}$ domain will be infinite unless $u_{\mathbf{M}_2}$ is an esentially equivalent domain of $u_{\mathbf{M}_1}$. If $A_1/B_1 = A_2/B_2$, then the scaled extents must be equal to each other since we are essentially in the same domain: $\Delta u_{\mathbf{M}_2}/sM_2 = \Delta u_{\mathbf{M}_1}/sM_1$. Therefore, for the case when one extent is given, $\Delta u_{\mathbf{M}_2} = \Delta u_{\mathbf{M}_1} M_2/M_1$ if $A_1/B_1 = A_2/B_2$, and $\Delta u_{\mathbf{M}_2} = \infty$, otherwise.

We now return to the discussion of tracing the extent through an optical system by using the direct extent tracing formulas. Let us assume that the phase-space region of the input signal is given as a centrally symmetrical convex polygon or equivalently the extent of the signal is specified in arbitrary LCT domains. Then, a careful examination of the method introduced in Section 5.4

reveals that the phase-space region of the signal at an arbitrary plane in the system is always given by the intersection of some corridors. First of all, based on our assumption, the initial phase-space region is defined by the intersection of some corridors. Moreover, each aperture introduces an additional new corridor in the phase-space and as we will see below, if it is limiting it will broaden all of the previously defined corridors with the appropriate trigonometric ratio. Then, the extent at any intermediate plane can be obtained from direct extent tracing formulas by taking into account the extents defining the corridors of the phase-space region at that intermediate plane. We will first give the theorem for the broadening term and prove it before describing the method.

Theorem: Compaction to an interval of extent $\sim \Delta u$ in any domain u necessarily results in a spread in the LCT domain $u_{\mathbf{M}}$ by the amount $\sim 1/|\beta|\Delta u$.

Proof using Convolution Theorem for LCTs: The convolution theorem for LCTs is as follows [14]:

$$\mathcal{C}_{\mathbf{M}}\{f(x)g(x)\} = |\beta|e^{i\pi\alpha x^2}[(e^{-i\pi\alpha x^2} f_{\mathbf{M}}(x)) * G(\beta x)] \tag{5.48}$$

where $G(x)$ is the FT of $g(x)$. Compaction of a signal f in the u domain can be realized by multiplying $f(u)$ with the window $\mathrm{rect}(\frac{\mathrm{u}}{\Delta \mathrm{u}})$ in that domain. By using the above formula, we can express the effect of compaction as follows:

$$\mathcal{C}_{\mathbf{M}}\{f(u)\mathrm{rect}(\frac{\mathrm{u}}{\Delta \mathrm{u}})\} = |\beta|\mathrm{e}^{\mathrm{i}\pi\alpha\mathrm{u}^2}[(\mathrm{e}^{-\mathrm{i}\pi\alpha\mathrm{u}^2}\mathrm{f}_{\mathbf{M}}(\mathrm{x})) * \Delta\mathrm{usinc}(\beta\,\Delta\mathrm{u}\,\mathrm{u})] \tag{5.49}$$

Thus, multiplication with a rectangle function implies convolution of the chirp multiplied version of the LCT of the signal with a sinc function in the LCT domain, followed by final a chirp multiplication. Since we are interested in the extent, we can take the absolute value of both sides of (5.49). Then, the extent in the $u_{\mathbf{M}}$ domain after multiplication with a rectangle in the u domain can be approximated as the extent of the chirp multiplied version of $f_{\mathbf{M}}(u)$ plus the extent of the sinc function. Since the extent of the chirp multiplied version of $f_{\mathbf{M}}(u)$ is equal to the extent of $f_{\mathbf{M}}(u)$, broadening of the distribution of f in the

$u_{\mathbf{M}}$ direction is comparable to the extent of the the sinc function in (5.49). This extent is simply $1/|\beta|\Delta u$.

Of course, this theorem is a consequence of the generalized uncertainty relation for LCTs.

Proof from geometry: This will be the extension of the proof of compaction in FRT domains given in [20]. Compaction to an interval of extent Δu in any domain u necessarily results in a spread $\sim |\sin\phi|/\Delta u$ in any FRT domain u_a (see Fig. 5.10). Consider an LCT domain $u_{\mathbf{M}}$, which is esentially equivalent to the FRT domain u_a. This implies that Iwasawa decomposition of $\mathbf{M}$ contains the FRT order a. Then, by using the relation between the extents of essentially equivalent domains given in section 5.1, the spread in $u_{\mathbf{M}}$ domain can be obtained as $\sim (M|\sin\phi|)/\Delta u$. This is equal to $\sim 1/|\beta|\Delta u$ based on (5.10).

Let P extents $\Delta u_{\mathbf{M}_1},\ldots,\Delta u_{\mathbf{M}_P}$ be specified in the $u_{\mathbf{M}_1},\ldots,u_{\mathbf{M}_P}$ domains for the input signal, where $P \geq 0$. We let β_j^l denote the β parameter between the LCT domains of jth aperture and lth extent, equivalently between the LCT domains with parameter $\mathbf{M}(z_j)$ and $\mathbf{M}_l$. Then, until we arrive at the 1st aperture, i.e. for $z \leq z_1^-$, the extent in the LCT domain with parameter $\mathbf{M}(z)$ can be found from (5.45) given the extents $\Delta u_{\mathbf{M}_1},\ldots,\Delta u_{\mathbf{M}_P}$ in $u_{\mathbf{M}_1},\ldots,u_{\mathbf{M}_P}$. When $z = z_1^+$, if the aperture is not limiting (i.e. if $\Delta_i > E(z_1^-)$), then $E(z_1^+) = E(z_1^-)$. However, if the aperture is limiting, then $E(z_1^+) = \Delta_i$ and all of the previously specified extents will broaden with the appropriate trigonometric ratio. By also including the new corridor defined by the 1st aperture, the corridors in the phase-space will now have the widths $\Delta u_{\mathbf{M}_1}+1/|\beta_1^1|\Delta_1,\ldots,\Delta u_{\mathbf{M}_P}+1/|\beta_1^P|, \Delta_1$ in the $u_{\mathbf{M}_1},\ldots,u_{\mathbf{M}_P}, u_{\mathbf{M}_{z_1}}$ domains. Then, for $z_1^+ < z \leq z_2^-$, the extent in the LCT domain with parameter $\mathbf{M}(z)$ can be found from (5.45) given the extents $\Delta u_{\mathbf{M}_1} + 1/|\beta_1^1|\Delta_1,\ldots,\Delta u_{\mathbf{M}_P} + 1/|\beta_1^P|, \Delta_1$ in $u_{\mathbf{M}_1},\ldots,u_{\mathbf{M}_P}, u_{\mathbf{M}_{z_1}}$. Then, after the second aperture, the extent at this plane will remain the same if the aperture

is not limiting. However, if it is limiting, the extent at this plane will necessarily be the aperture size Δ_2 and new corridors will be defined by the extents $\Delta u_{\mathbf{M}_1} + 1/|\beta_1^1|\Delta_1[E(z_1^-) > \Delta_1] + 1/|\beta_2^1|\Delta_2$,...,$\Delta u_{\mathbf{M}_P} + 1/|\beta_1^P|\Delta_1[E(z_1^-) > \Delta_1] + 1/|\beta_2^P|\Delta_2$,$\Delta_1 + 1/|\beta_{1,2}|\Delta_2$,$\Delta_2$ in $u_{\mathbf{M}_1}$,...,$u_{\mathbf{M}_P}$, $u_{\mathbf{M}_{z_1}}$, $u_{\mathbf{M}_{z_2}}$. The brackets $[-]$ denotes the Iverson brackets. If x is true, $[x] = 1$ and otherwise, $[x] = 0$. We can repeat this approach until we reach the end of the system.

Finally, the phase-space region at the output will be defined by the extents

$$\begin{aligned}
&\left(\Delta u_{\mathbf{M}_1} + \frac{1}{|\beta_1^1|\Delta_1}[E(z_1^-) > \Delta_1] + \ldots + \frac{1}{|\beta_L^1|\Delta_L}[E(z_L^-) > \Delta_L]\right), \ldots, \\
&\left(\Delta u_{\mathbf{M}_P} + \frac{1}{|\beta_1^P|\Delta_1}[E(z_1^-) > \Delta_1] + \ldots + \frac{1}{|\beta_L^P|\Delta_L}[E(z_L^-) > \Delta_L]\right), \\
&\left(\Delta_1 + \frac{1}{|\beta_{1,2}|\Delta_2}[E(z_2^-) > \Delta_2] + \ldots + \frac{1}{|\beta_{1,L}|\Delta_L}[E(z_L^-) > \Delta_L]\right), \\
&\left(\Delta_2 + \frac{1}{|\beta_{2,3}|\Delta_3}[E(z_3^-) > \Delta_3] + \ldots + \frac{1}{|\beta_{1,L}|\Delta_L}[E(z_L^-) > \Delta_L]\right), \ldots, \Delta_L
\end{aligned} \tag{5.50}$$

in the following domains:

$$u_{\mathbf{M}_1}, \ldots, u_{\mathbf{M}_P}, u_{\mathbf{M}_{z_1}}, u_{\mathbf{M}_{z_2}}, \ldots, u_{\mathbf{M}_{z_L}} \tag{5.51}$$

5.6 Redundant Apertures

We have seen that for a given family of signals if the extent of the signal at the plane just before an aperture is smaller than the size of the aperture ,i.e. $E(z_i^-) < \Delta_i$, then this aperture will not be limiting, or equivalently will be redundant. Thus, upto this point, we talked about redundant apertures *for a given family of signals*. In this section, our aim is to find the apertures in a system that are redundant *for any given family of signals*. We will refer to these apertures as *absolutely redundant* apertures. Removing the absolutely redundant apertures from the system (or replacing them with apertures of infinite size) will not create any difference in the behaviour of the system. Equivalently, the

system with removed apertures is fully equivalent to the original system with all apertures in addition to providing a simpler analysis.

> If an aperture is redundant when the input signal has infinite space-frequency support, then this aperture is *absolutely redundant*, equivalent to say it is redundant for any given family of signals.

This result can be verified as follows: If the input signal has infinite support, then the first aperture will introduce the first corridor to the region. The second aperture will introduce the second corridor and will also enlarge the first corridor with the appropriate trigonometric ratio. Therefore, just after the ith aperture, the phase-space region will be confined to the corridors defined by the extents $(\Delta_1 + 1/|\beta_{1,2}|\Delta_2 + \ldots + 1/|\beta_{1,i}|\Delta_i)$, $(\Delta_2 + 1/|\beta_{2,3}|\Delta_3 + \ldots + 1/|\beta_{2,i}|\Delta_i)$, ..., Δ_i in the $u_{\mathbf{M}_{z_1}}$, $u_{\mathbf{M}_{z_2}}$, ..., $u_{\mathbf{M}_{z_i}}$ domains. Now, consider the case when an arbitrary family of signals is given at the input with its extents specified as $\Delta u_{\mathbf{M}_1}$,...,$\Delta u_{\mathbf{M}_P}$ in the domains $u_{\mathbf{M}_1}$,...,$u_{\mathbf{M}_P}$. For this set of signals, just after the ith aperture, the phase-space region will be confined to the corridors defined by the extents $(\Delta u_{\mathbf{M}_1} + 1/|\beta_1^1|\Delta_1 + \ldots + 1/|\beta_i^1|\Delta_i)$, ..., $(\Delta u_{\mathbf{M}_P} + 1/|\beta_1^P|\Delta_1 + \ldots + 1/|\beta_i^P|\Delta_i)$ in the domains $u_{\mathbf{M}_1}$,..., $u_{\mathbf{M}_P}$ in addition to the corridors of the region of the infinite-support signal. Since the phase-space region of the arbitrary family of signals contains additional corridors that comes from the initial region at any plane in the system, it lies inside the phase-space region of infinite-support signals. As a result, the phase-space region at any plane in the system will be the largest when the input signal has infinite support. Therefore, if an aperture does not cut the region of the infinite-support signals, it can not also cut the region of any other family of signals, which lies inside this. This implies that redundant apertures for the infinite-support signals are also redundant for any family of signals. Note that the first two aperture of the system can never be absolutely redundant as long as they are not at essentially equivalent domains since they always limit the region of an infinite-support input signal. We also note that

for a given family of signals, there may be redundant apertures other than the absolutely redundant apertures. In our example system, the 3th, 5th, 6th, and 7th apertures are absolutely redundant.

We have also seen in Section 5.3 that the phase-space window of the system is defined by some of the apertures, but not all. Since the absolutely redundant apertures can be removed from the system without introducing any change in the behaviour of the system, the following statement is always true:

> The absolutely redundant apertures can not define the phase-space window of the system.

In our example system, the phase-space window is defined by the 2th, 4th, and 8th apertures, which are not absolutely redundant.

5.7 Effective Apertures

In this section, we are interested in a pure geometrical problem which aims to find the smallest centrally symmetrical convex polygon enclosing a given centrally symmetrical convex polygon with more number of sides. The general case of this problem for convex polygons has been previously discussed in [56, 57, 58].

Consider a given n-sided centrally symmetrical convex polygon defined by $n/2$ corridors. Our aim is to approximate this polygon with a k-sided centrally symmetrical convex polygon defined by $k/2$ corridors, where $k \in \{4, 6, \ldots, n-2\}$. Then, we define the error in approximating the polygon as the ratio of the area of the non-overlapping regions between the original and approximated polygons to the area of the original polygon. The approximation will be considerably good even when we approximate with 4 sides, or equivalently with 2 corridors. We have previously conjectured that the approximation error will be the largest

when an n-sided symmetrical convex polygon becomes an ellipse in the limiting case of $n \to \infty$. In this limiting case, if we fit a rectangular to the ellipse, which corresponds to approximating with 2 corridors, the normalized error is given by

$$\text{error} = \frac{4ab - \pi ab}{4ab} = \frac{4 - \pi}{4} \approx 0.21 \tag{5.52}$$

where a and b are one-half of the ellipse's major and minor axes, respectively. Thus, assuming our conjecture is true, the worst case error is 21%, which occurs when the polygon converges to an ellipse in the limit $n \to \infty$ and when we approximate the ellipse with only 2 corridors. Provided that our conjecture is true, even when we approximate with 2 corridors, the approximation will be considerably good.

We have proved before that the corridors of the minimum area enclosing parallelogram are from the corridors of the original polygon. In the general case, the smallest enclosing symmetrical polygon with fewer number of sides will be defined by the corridors of the original symmetrical polygon, which has been proved in [56].

Let the original polygon be constructed with n corridors and k be the number of corridors we want to keep in the approximate polygon. We conjecture that the smallest enclosing polygon with $k+1$ corridors contains all the corridors of the smallest enclosing polygon with k corridors. That is, the smallest enclosing polygon with $k+1$ number of corridors can be constructed by adding one additional corridor to the corridors of that with k corridors.

The above geometrical observations allow two meaningful interpretations in the context of apertured optical systems. First, we can model the phase-space window of a system with fewer number of apertures than the number of non-redundant apertures to a good degree of approximation. Second, the state of the signal at any arbitrary plane can be approximated with fewer number of corridors (upto minimum of two corridors) to represent its phase-space region. That is,

we can select fewer number of apertures than the number of non-redundant apertures to approximately represent all of the apertures in the system. Now, we will discuss these interpretations more deeply based on our example system.

Fig. 5.11 presents the phase-space window of our system and the smallest parallelogram enclosing it. As we have seen in Section 5.6, this window is defined by three apertures, which are the 2nd, 4th, and 8th apertures in the system. The smallest enclosing paralelogram defined by two apertures is obtained from the previous three apertures as the 2nd and 4th ones. Observe that the error in approximating the phase-space window with this closest fitting parallelogram is considerably small.

The smallest enclosing paralelogram will have the smallest area among those defined by other pairs of apertures. The way to find these apertures from the present apertures is to find the apertures that define the parallelogram with the smallest area. As we have seen in the Section 5.2, the area of the parallelogram defined by two corridors of width $\Delta u_{\mathbf{M}_1}/M_1 s$ and $\Delta u_{\mathbf{M}_2}/M_2 s$ in two LCT domains is given by the bicanonical width product $\Delta u_{\mathbf{M}_1} \Delta u_{\mathbf{M}_2} |\beta_{i,j}|$. Also remember that each aperture defines a corridor of width Δ_i / M_{z_i} in $u_{\mathbf{M}_i}$ domain. Then, the apertures that minimizes $\Delta_i \Delta_j |\beta_{i,j}|$ are the apertures that define the smallest enclosing parallelogram. We refer to these apertures as the most *effective apertures*.

As we have seen in Section 5.6, there are four absolutely redundant apertures in the system we considered. The non-redundant apertures in the absolute sense are the 1st, 2nd, 4th, and 8th apertures in the system. After removing the absolutely redundant apertures, both the system and the state of the signal at any arbitrary plane will remain the same. Now, we want to investigate the effect of decreasing the number of apertures beyond the number of non-redundant apertures on the state of the signal. Fig. 5.12a shows the extent of the signal after one of the non-redundant apertures is removed from the system. The legend

shows the remaining apertures in the system. Fig. 5.12b presents the extent of the signal after two non-redundant apertures are removed from the system. For comparison, the extent of the signal when all of the non-redundant apertures are present in the system is also given in each figure. Observe that although some apertures are not absolutely redundant, removing some of them from the system may not change the behaviour of the system much after some point. When we choose the apertures to be removed correctly, similar extent will be obtained at the output, as compared to the exact extent.

Fig. 5.12c shows the extent of the signal when the phase-space region of the signal at the output is approximated optimally with 2 apertures and 3 apertures. The removed apertures are chosen such that they causes minimal error in the phase-space region at the output. Observe that when we leave only the 2nd and 4th apertures in the system, this has a very similar behaviour both at the output and at the region after these two apertures, as compared to the system with all apertures.

5.8 Simulating Optical Systems

The fact that all physical systems support only a finite number of degrees of freedom means that their effect on signals can be simulated with discrete-time systems with the same degree of accuracy compared to continuous systems. Further insight on these matters may be obtained from chapter 2, which discusses how the DLCT provides an approximation to the continuous LCT. It has been presented in that chapter that provided N is chosen to be at least equal to the bicanonical width product of the set of signals we are dealing with, the DLCT which can be efficiently computed on a digital computer by taking $N \log N$ time can be used to obtain a good approximation to the continuous LCT. The approximation improves with increasing N.

Now, we will discuss how we can simulate an apertured optical system by using the DLCT mentioned in [7] and defined in [4]. As discussed before, such an optical system is equivalent to the combination of many LCT blocks and rectangular windows. We will make sure that at every stage, the number of samples is sufficient for recovery of the continuous signal in the LCT sampling sense with careful attention to representational efficiency. Special care is taken to choose the minimum number of samples to represent the signal at intermediate stages so that the method is as efficient as possible.

Let the phase-space region and N samples of the input signal is given, where N is sufficient to recontruct its continuous version. In order to simulate each LCT block, we examine the phase-space region after the LCT computation, and then we determine the extent of the output signal from this region. Then, the number of samples required to represent the signal is the bicanonical width product $\Delta u \Delta u_{\mathbf{M}} |\beta|$, where β is the parameter of the LCT to be computed, Δu and $\Delta u_{\mathbf{M}}$ are the extent of the signal before and after the LCT, respectively. Let denote the number of samples before the LCT block as N_i and the number of samples required after the LCT block as N_o. If $N_o = kN_i$, we must upsample the signal before the LCT block by a factor of k when $k > 1$ and downsample by a factor of k when $k < 1$. Then, we can compute the DLCT with the parameter of the LCT block. The samples obtained will be good approximations of the true samples of the transformed signal. Whenever we reach to a aperture, we can multiply the samples of the intermediate result with the samples of the rectangle function, which will be equivalent to removing some of the samples from the tail ends. The number of samples at the output of the window will be always sufficient to recontruct the continuous signal since this number of samples will give the area of the parallelogram with corridors defined at the same domains as compared to the one before the window and therefore will cover all the phase-space region after the window (In fact, fewer number of samples may also be sufficient to represent the signal after the aperture when the high frequency components are confined to the

removed regions, but here we do not need to downsample because resampling will be needed for the next LCT block computation anyway.) Then, we will repeat the described process for the next LCT block and window until we reach to the end of the system. Thus, by carefully following the evolution of the space-frequency support region through each LCT block, we can obtain the output samples, which are good approximations of the samples of the continuous output function and the continuous output function (that is, they can be recovered via interpolation of these samples). Note that although downsampling operations are not necessary for the algorithm to work properly, they are performed since representational efficiency is our ultimate goal. In practice, one can choose not to perform downsampling operations during the actual computation.

Finally, we discuss the relation for down and upsampling operations. The issue of sampling rate conversion has been explored in many works including [44, 24, 59]. Let us consider a function f, whose extents are given in the u and $u_{\mathbf{M}_1}$ domains as Δu and $\Delta u_{\mathbf{M}_1}$. Then, the function is recoverable from its samples when the sampling interval δu equals to $1/|\beta_1|\Delta u_{\mathbf{M}_1}$:

$$f(u) = e^{-i\pi\gamma_1 u^2} \sum_{n=-N_1/2}^{N_1/2-1} f(n\delta u) e^{i\pi\gamma_1 \delta u^2 n^2} \mathrm{sinc}(\frac{\mathrm{u}}{\delta \mathrm{u}} - \mathrm{n}), \tag{5.53}$$

where $N_1 = \Delta u \Delta u_{\mathbf{M}_1} |\beta_1|$. If we want to resample the function such that it has N_2 number of samples, then the new samples $\hat{f}$ can be obtained as follows:

$$\hat{f}(k\hat{\delta u}) = e^{-i\pi\gamma_1 \hat{\delta u}^2 k^2} \sum_{n=-N_1/2}^{N_1/2-1} f(n\delta u) e^{i\pi\gamma_1 \delta u^2 n^2} \mathrm{sinc}(\mathrm{k}\frac{\hat{\delta \mathrm{u}}}{\delta \mathrm{u}} - \mathrm{n}) \tag{5.54}$$

for $k \in [-N_2/2, N_2/2 - 1]$, where $\hat{\delta u} = \delta u N_1/N_2$. Note that this requires the additional knowledge of γ_1.

5.9 Future Work

The convolution theorem for LCTs is given as [14]

$$\mathcal{C}_{\mathbf{M}}\{f(x)g(x)\} = |\beta|e^{i\pi\alpha x^2}[(e^{-i\pi\alpha x^2} f_{\mathbf{M}}(x)) * G(\beta x)] \tag{5.55}$$

where $G(x)$ is the FT of $g(x)$. The dual of this theorem can be obtained as follows:

$$\mathcal{C}_{\mathbf{M}}\{f(x)g(x)\} = |\alpha|e^{i\pi\alpha x^2} * [(e^{-i\pi\alpha x^2} * f_{\mathbf{M}}(x))g(\frac{\alpha}{\beta}x)] \tag{5.56}$$

The derivation of the above result is straightforward, which takes as a starting point $\mathcal{F}\{\mathcal{F}^{-1}\mathcal{C}_{\mathbf{M}}\{f(x)g(x)\}\}$, apply the convolution theorem in (5.55) for the operator $\mathcal{F}^{-1}\mathcal{C}_{\mathbf{M}}$ and then the convolution property of the Fourier transform for the operator $\mathcal{F}$. When one of the functions is a rectangle function, the convolution relations reduce to the following equations:

$$\begin{aligned}
\mathcal{C}_{\mathbf{M}}\{f(x)\mathrm{rect}(\frac{\mathrm{x}}{\Delta})\} &= |\beta|e^{i\pi\alpha x^2}[(e^{-i\pi\alpha x^2} f_{\mathbf{M}}(x)) * \mathrm{sinc}(\Delta\beta\mathrm{x})] && (5.57)\\
&= |\beta|e^{i\pi\alpha x^2}[(e^{-i\pi\alpha x^2}\mathcal{C}_{\mathbf{M}}\{\mathrm{rect}(\frac{\mathrm{x}}{\Delta})\}) * \mathrm{F}(\beta\mathrm{x})] && (5.58)\\
&= |\alpha|e^{i\pi\alpha x^2} * [(e^{-i\pi\alpha x^2} * f_{\mathbf{M}}(x))\mathrm{rect}(\frac{\alpha}{\beta\Delta}\mathrm{x})] && (5.59)\\
&= |\alpha|e^{i\pi\alpha x^2} * [(e^{-i\pi\alpha x^2} * \mathcal{C}_{\mathbf{M}}\{\mathrm{rect}(\frac{\mathrm{x}}{\Delta})\})\mathrm{f}(\frac{\alpha}{\beta}\mathrm{x})] && (5.60)
\end{aligned}$$

Multiplication with a rectangle function is like windowing in the FRT domains whose orders are close to 0 and in the LCT domains which are essentially equivalent to these FRT domains. But, this windowing operation is a modified one as seen in (5.59). Moreover, this operation is like convolution with a sinc function in the FRT domains whose orders are close to 1 and in the LCT domains which are essentially equivalent to these FRT domains. But, this convolution operation is a modified one as seen in (5.57). Whether it is like a windowing or convolution operation depends on the shape of the Wigner support. To see this, consider the figure in 5.10. If we intersect the region before and after the windowing, which are drawn with dashed and solid lines in the figure, the FRT domain that contains the intersection point is the critical domain for us. If a domain is above

this critical domain, then the effect of the operation is more like a convolution operation and the extent in this domain increases after the operation, which can be approximated as $\Delta u_{\mathbf{M}} + 1/\Delta|\beta|$ by using (5.57). If a domain is below the critical domain, then the effect of the operation is more like a windowing operation and the extent in this domain decreases after the operation, which can be approximated as $M\Delta\cos\phi + \Delta\mu/|\beta|$ by using (5.58).

It may be possible to track the extent by using these formulas. The output can be written explicitly in terms of the input by using only the first of the above equations, which will be insufficient to extract the extent information; however, it seems to be hard to do this by using two of the equations. This problem is left as a subject for future study because of the following reasons. First, we have reached all of our goals by using the Wigner-based extent tracing method and direct extent tracing formulas. Second, this approach will be less acurate than the proposed method. Third, this does not also have a computational advantage. In the Wigner-based method, we only work with corner points, which does not create more computational cost than this. In fact, in the direct extent tracing formulas, the Wigner distribution is totally dispensed with.

5.10 Appendix

In this part, we will investigate the broadening effect of rectangular windowing on the Wigner distribution for three different cases and different values of x. As we have discussed, rectangular windowing results in convolution of the Wigner distribution of the signal with the Wigner distribution of the rectangle function along the f direction. This cause broadening in the f direction and the amount of broadening seems to depend on the value of x. Let us denote the width of the rectangular window by Δx and the extent of the signal in the f direction in the Wigner domain by Δf. We investigate the following cases: $\Delta f \ll 1/\Delta x$,

$\Delta f = 1/\Delta x$, and $\Delta f \gg 1/\Delta x$ when $x = 0$, $x = 0.25\Delta x$, and $x = 0.45\Delta x$. Note that x can take values between $[-\Delta x/2, \Delta x/2]$, in general. The results of the convolution are shown in Fig. 5.13.

When $\Delta f \ll 1/\Delta x$, the extent of the signal in the f direction is very small compared to the main lobe of the sinc function, which is the Fourier transform of the rectangle function. For this reason, after convolution the envelope of the sinc function is preserved. The extent of the convolved function can be defined with respect to this envelope, which is given by $\Delta f + 1/\Delta x$ for all x. For the case $\Delta f \gg 1/\Delta x$, the extent of the signal in the f direction is very large compared to the main lobe of the sinc function. Based on the full width at half maximum (FWHM) criterion, we can define the extent of the convolved function as $\Delta f + 1/\Delta x$ for all x. However, for the case $\Delta f = 1/\Delta x$, the extent of the signal in the f direction is comparable to the main lobe of the sinc function. In this case, it is problematic to define the extent as the sum of the extent of convolved functions, which would be the same for all x, as it can be seen from Fig. 5.13b. Therefore, approximating the spread in the f direction after windowing as $\sim 1/\Delta_j$ is crude and tricky and can be problematic when the extent of the signal distribution in the f direction becomes comparable with $1/\Delta x$.

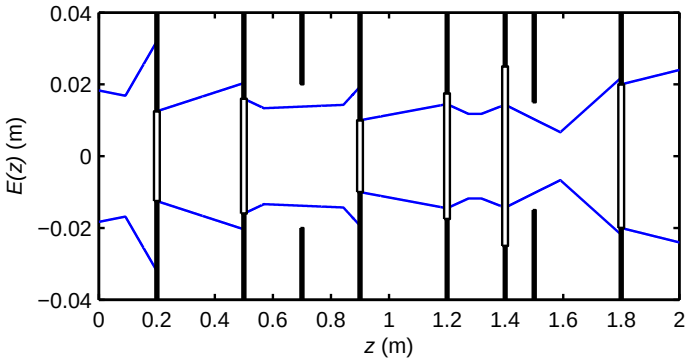

(a) When the apertures are present in the system

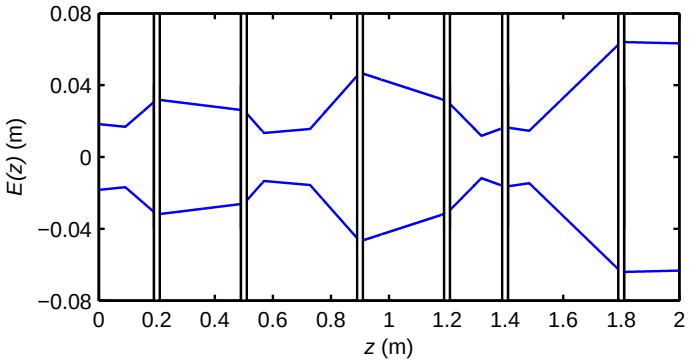

(b) When the apertures are not present in the system

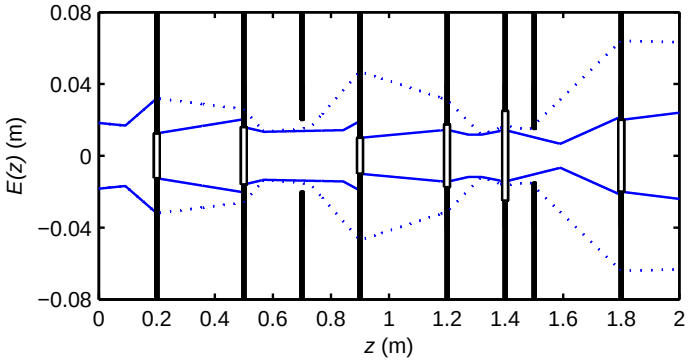

(c) When the apertures are present and are not present in the system

Figure 5.7: $E(z)$ vs z for the system shown in figure 5.4

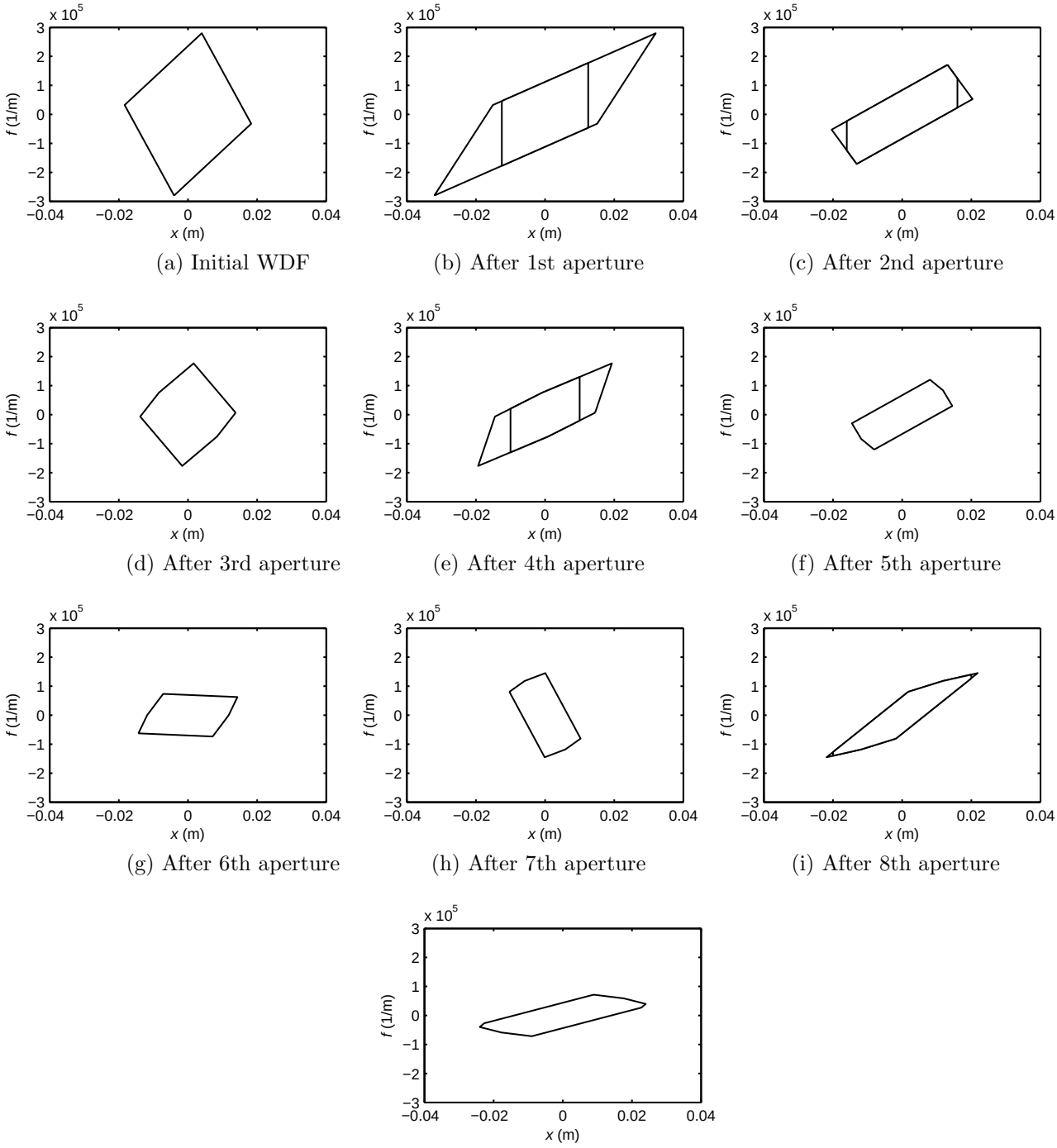

(a) Initial WDF (b) After 1st aperture (c) After 2nd aperture

(d) After 3rd aperture (e) After 4th aperture (f) After 5th aperture

(g) After 6th aperture (h) After 7th aperture (i) After 8th aperture

(j) Final WDF

Figure 5.8: Evolution of Wigner distribution

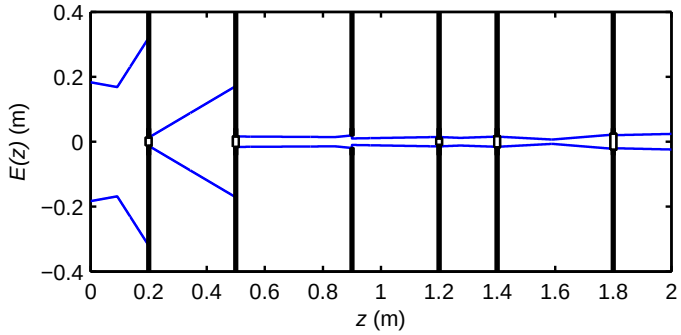

(a) When the apertures are present in the system

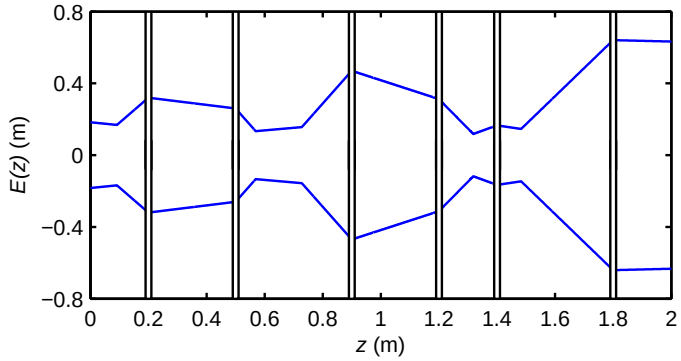

(b) When the apertures are not present in the system

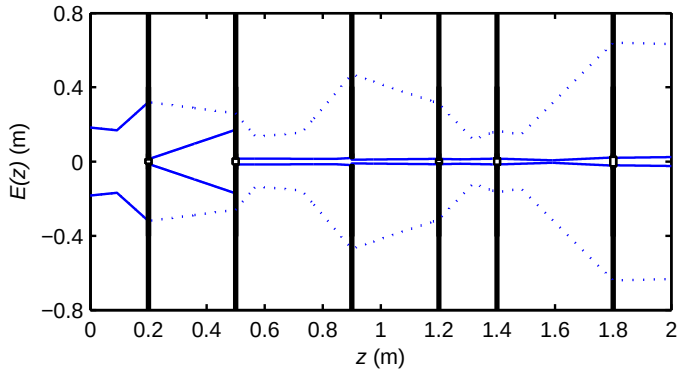

(c) When the apertures are present and are not present in the system

Figure 5.9: $E(z)$ vs z for a larger initial phase-space region

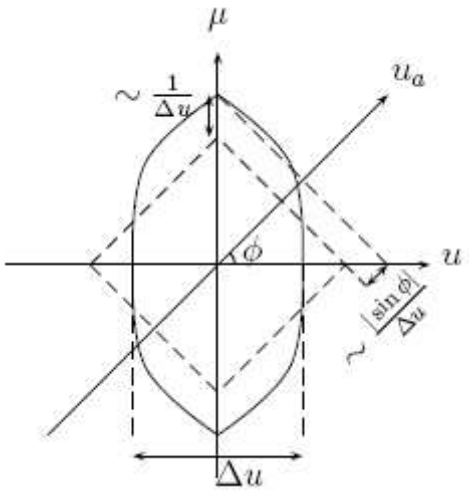

Figure 5.10: Compaction in the ath domain

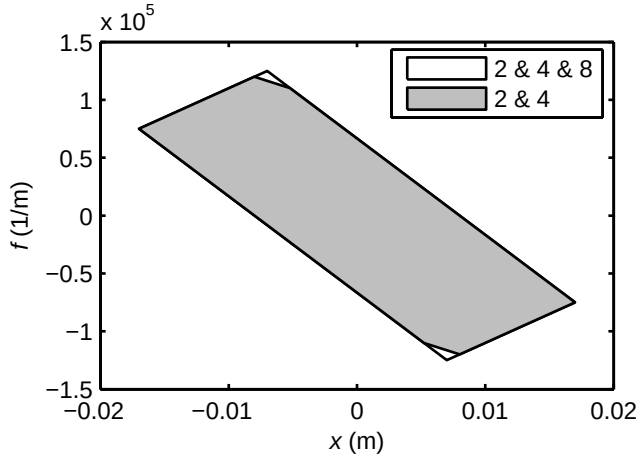

Figure 5.11: The phase-space window of the system and its approximation

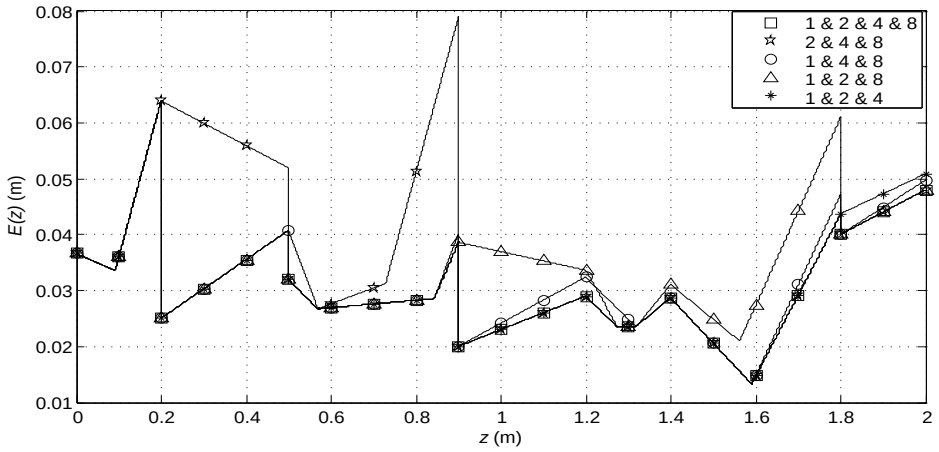

(a) After one non-redundant aperture is removed

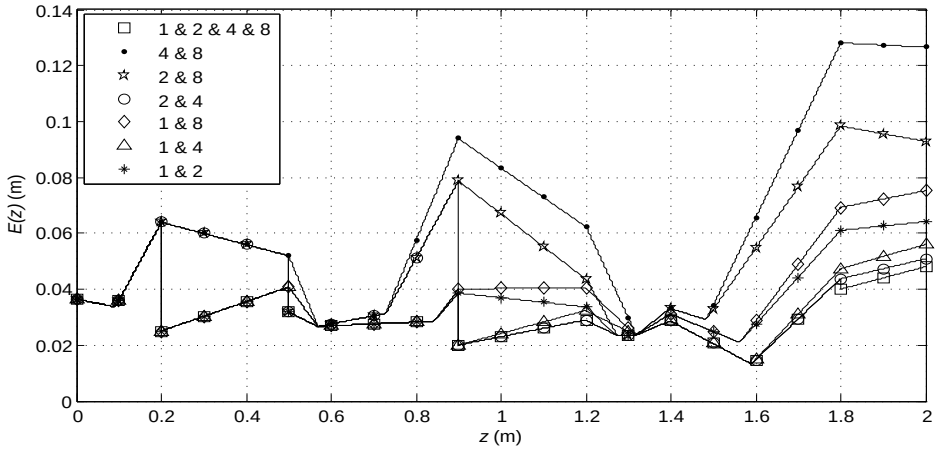

(b) After two non-redundant apertures are removed

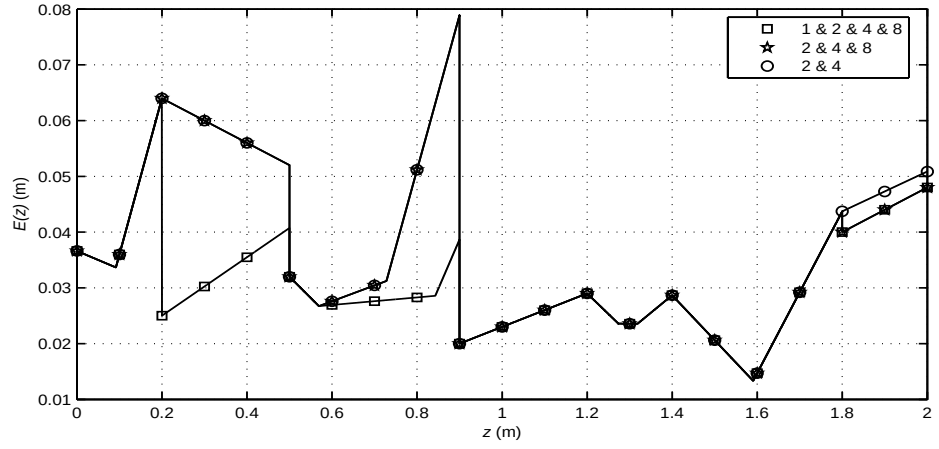

(c) After approximating the phase-space region optimally with 2 and 3 apertures

Figure 5.12: The extent of the signal for different removed apertures

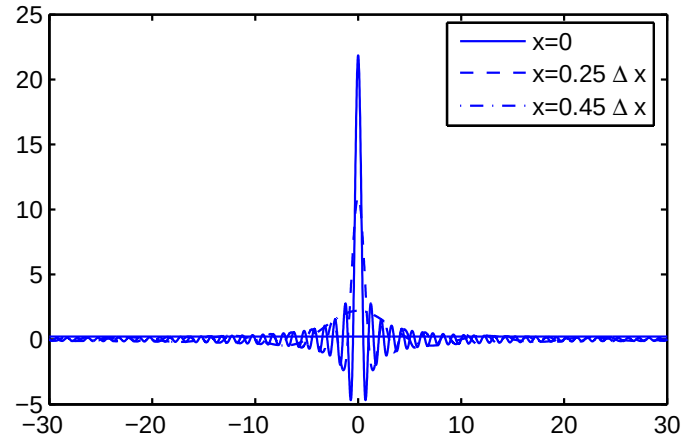

(a) $\Delta f \ll 1/\Delta x$

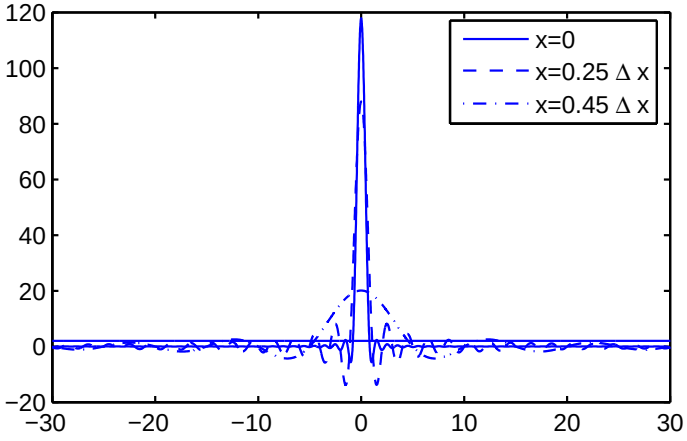

(b) $\Delta f = 1/\Delta x$

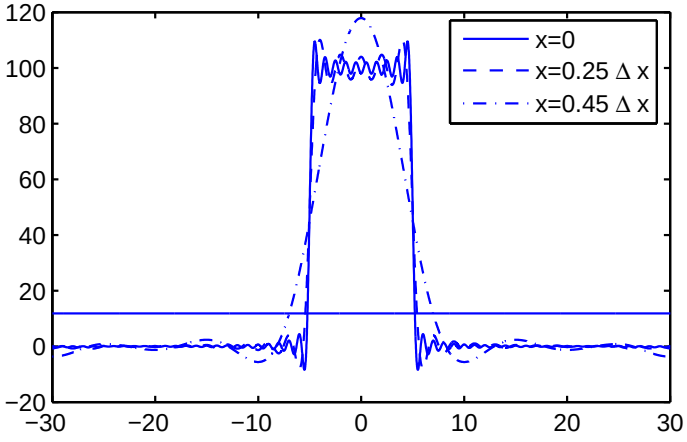

(c) $\Delta f \gg 1/\Delta x$

Figure 5.13: Convolution results for different values of x

Chapter 6

EFFECTIVE POINT SPREAD OF THE FRACTIONAL FOURIER TRANSFORM

In this chapter, we will investigate the effect of one point in the input to the points in the output as a function of the fractional order a when the output is related to its input through a FRT. We will refer to the mostly affected region in the output as the *effectiveness region* of the input point. The width of this region will be also referred to as the *effectiveness width*. We will also look to this problem from the reverse side and investigate how one point in the output is affected from the points in the input. We will refer to the mostly affecting region in the input as the *dependency region* of the output point. The width of this region will be also referred to as the *dependency width*. Moreover, the change in the effective output width as a function of the fractional order a will define an expanding cone from input to output and the change in the dependency width as a function of the fractional order a will define an expanding cone from output to input. Thus, cones are bidirectional. Our aim is to find the dependency and

effectiveness regions and their associated cones both for the continuous-time and the discrete-time systems.

The effectiveness and dependency regions have physical meanings. The effectiveness region of an input point gives the points at the output that we observe a change when we vary that particular input point. Similarly, the dependency region of an output point gives the points in the input that create a change on that particular output point. The points outside the effectiveness and dependency region have negligible effects on the particular point in the reverse plane and we can say that particular point depends only on the points inside these regions.

6.1 Continuous Case

Consider a function whose Wigner distribution is approximately confined to a circle of diameter Δu. This means that a sufficiently large percentage of the signal energy is contained in this circle. That is, the representations of the signal in all fractional Fourier domains are approximately confined to the interval $[-\Delta u/2, \Delta u/2]$, or equivalently the representations of the signal in all fractional Fourier domains are bandlimited to $[-\Delta u/2, \Delta u/2]$. Then, consider a system whose output is related to its input through a FRT. We will use two analytical approaches to derive the effectiveness and dependency regions for the set of continuous-time signals, which satisfy our assumption. The first approach will rely on the functions and the second approach will make use of the instantaneous frequency.

6.1.1 First Approach

Consider a system whose output is related to its input through a FRT. Let $f(u)$ denote the input function and $f_a(u)$ denote the output function, where the relation between $f(u)$ and $f_a(u)$ is given by the ath order FRT. Based on our assumption, the input function is bandlimited to the interval $[-\Delta u/2, \Delta u/2]$. If we denote its Fourier transform by $F(\mu)$, we have

$$F(\mu) = F(\mu) \times \text{rect}(\frac{\mu}{\Delta u}) \tag{6.1}$$

and equivalenly,

$$f(u) = f(u) * \Delta u \,\text{sinc}(\Delta u\, u) \tag{6.2}$$

Since the output function is also bandlimited to the same interval, we can similarly write

$$f_a(u) = f_a(u) * \Delta u \,\text{sinc}(\Delta u\, u) \tag{6.3}$$

We want to find the effective FRT kernel, denoted by $\bar{K}_a^{ef}(u, u')$, when the input and output functions satisfy (6.2) and (6.3), respectively. If we start with the FRT relation and then use (6.2), we obtain

$$\begin{aligned} f_a(u) &= \int K_a(u, u')\, f(u')\, du' && (6.4)\\ &= \int K_a(u, u') \int f(u'')\Delta u \,\text{sinc}(\Delta u(u' - u''))\, du''\, du' && (6.5)\\ &= \int f(u'') \left(\int K_a(u, u')\Delta u \,\text{sinc}(\Delta u(u' - u''))du' \right) du'' && (6.6) \end{aligned}$$

where the expression inside brackets is the effective kernel obtained after using (6.2), or equivalenly the effective kernel for a bandlimited input function. This kernel is the convolution of the original kernel with sinc function along the

direction of u':

$$\begin{aligned} K_a^{ef}(u,u') &= K_a(u,u') * \Delta u \,\mathrm{sinc}(-\Delta u u') && (6.7)\\ &= \int K_a(u,u'')\Delta u \,\mathrm{sinc}(\Delta u(u''-u'))du'' && (6.8)\\ &= F^a(\Delta u \,\mathrm{sinc}(\Delta u(u-u'))) && (6.9)\\ &= e^{i\pi u'^2 \sin\phi\cos\phi} e^{-i2\pi u u' \sin\phi} F^a\{\Delta u \,\mathrm{sinc}(\Delta u\, u)\}(u - u'\cos\phi) && (6.10) \end{aligned}$$

where the final equality follows due to the following property

$$f(u-\xi) \xrightarrow{\mathcal{F}^a} e^{i\pi\xi^2 \sin\phi\cos\phi} e^{-i2\pi u\xi \sin\phi} f_a(u - \xi\cos\phi) \qquad (6.11)$$

We will further take into account bandlimitedness in the output domain by using (6.3):

$$\begin{aligned} f_a(u) &= f_a(u) * \Delta u \,\mathrm{sinc}(\Delta u u) && (6.12)\\ &= \left(\int K_a^{ef}(u,u')\, f(u')\, du'\right) * \Delta u \,\mathrm{sinc}(\Delta u u) && (6.13)\\ &= \int f(u') \left(\int K_a^{ef}(u'',u')\, \Delta u \,\mathrm{sinc}(\Delta u(u-u''))\, du''\right) du' && (6.14) \end{aligned}$$

where the expression inside brackets is the final effective kernel when both the input and output are assumed to be bandlimited. This kernel is the convolution of the previous effective kernel with sinc function along the direction of u:

$$\begin{aligned} \bar{K}_a^{ef}(u,u') &= K_a^{ef}(u,u') * \Delta u \,\mathrm{sinc}(\Delta u u) && (6.15)\\ &= K_a(u,u') * \Delta u \,\mathrm{sinc}(-\Delta u u')) * \Delta u \,\mathrm{sinc}(\Delta u u) && (6.16) \end{aligned}$$

We can write the above result in two more different forms:

$$\begin{aligned} &\bar{K}_a^{ef}(u,u') = e^{-i\pi u'^2 \sin\phi\cos\phi} && (6.17)\\ &\quad \times \left(e^{-i2\pi u'(u-u'\cos\phi)\sin\phi} F^a\{\Delta u \,\mathrm{sinc}(\Delta u\, u)\}(u - u'\cos\phi)\right) * \Delta u \,\mathrm{sinc}(\Delta u u) \end{aligned}$$

$$\begin{aligned} &\bar{K}_a^{ef}(u,u') = e^{-i\pi u^2 \sin\phi\cos\phi} && (6.18)\\ &\quad \times \left(e^{-i2\pi u(u'-u\cos\phi)\sin\phi} F^a\{\Delta u \,\mathrm{sinc}(\Delta u\, u')\}(u' - u\cos\phi)\right) * \Delta u \,\mathrm{sinc}(-\Delta u u') \end{aligned}$$

We can now investigate the effectiveness and dependency regions by using the above effective kernels. Firstly, we will investigate the effect of one point in the input to points in the output. To find the effectiveness region, consider a particular u' value, which corresponds to a particular input point and investigate the extent of the effective kernel with respect to the output parameter u. For this, let us consider the magnitude of the kernel in (6.17) by taking u' as a constant. Since convolution is a translation invariant operation, we can first convolve the unshifted versions of the functions and then shift the result by $u' \cos\phi$. As we will discuss below, the extent after convolution can be approximated as the sum of the extent of the convolved terms. The extent of $e^{-i2\pi u' u \sin\phi} F^a\{\Delta u \operatorname{sinc}(\Delta u\, u)\}(u)$ is equal to the extent of $|F^a\{\Delta u \operatorname{sinc}(\Delta u\, u)\}(u)|$ since we can think in terms of magnitude. This extent can be approximated as $\Delta u |\sin\phi|$ (see the appendix for its crude derivation and supporting simulation results). The extent of $\Delta u \operatorname{sinc}(\Delta u u)$ is $\sim 1/\Delta u$, which can be neglected. Thus, we can conclude that the effectiveness region has width $\sim \Delta u |\sin\phi|$, which is centered at $u = u' \cos\phi$.

As mentioned above, we have approximated the extent after convolution as the sum of the extent of the convolved terms. This approximation is valid in our case since the complex exponential which multiplies the FRT of the sinc before convolution does not oscillates more rapidly compared to the convolved sinc function. To see this, consider the instantaneous frequency of the complex exponential $\exp(-i2\pi u'(u - u' \cos\phi)\sin\phi)$ with respect to the u parameter since we convolve over this variable in (6.17). The instantaneous frequency of the complex exponential is given by $(2\pi)^{-1} 2\pi u' \sin\phi = u' \sin\phi$. Since we have assumed that u' is in the interval $[-\Delta u/2, \Delta u/2]$, the frequency can be at most $\Delta u \sin\phi/2$. (We can find this as $\Delta u \sin^2\phi/2$ if we limit ourselves to the approximate support length of the FRT of the sinc, which is given by $\Delta u \sin\phi$.) Then, the highest oscillation frequency of the complex exponential will be obtained as $\Delta u/2$ when $a = 1$. The highest frequency of the convolved sinc function is also $\Delta u/2$. As

a result, the complex exponential oscillates at most with the same frequency as the sinc function, and thus it will never wash out the convolution integral.

Similarly, we can investigate how one point in the output is affected from the points in the input. To find the dependency width, consider a particular u value, which corresponds to a particular output point and investigate the extent of the effective kernel with respect to the input parameter u'. For this, let us consider the magnitude of the kernel in (6.18) by taking u as a constant. Again, we can first convolve the unshifted versions of the functions and then shift the result by $u\cos\phi$. The extent after convolution can be approximated as the sum of the extent of the convolved terms. The extent of $e^{-i2\pi uu'\sin\phi}F^a\{\Delta u\,\mathrm{sinc}(\Delta u\,u')\}(u')$ is equal to the extent of $|F^a\{\Delta u\,\mathrm{sinc}(\Delta u\,u')\}(u')|$, which is given by $\sim \Delta u|\sin\phi|$. The extent of $\Delta u\,\mathrm{sinc}(\Delta uu')$ is $\sim 1/\Delta u$, which can be again neglected. Thus, we can conclude that the dependency region has width $\sim \Delta u|\sin\phi|$, which is centered at $u' = u\cos\phi$. Note that the dependency and effectiveness widths are the same, given by $\sim \Delta u|\sin\phi|$. We will see that this is also true in the discrete case.

Fig. 6.1 shows the magnitudes of the effective kernel for different transform orders when $\Delta u = 16$ and either u or u' is zero. The vertical axis can be considered as the variable parameter of the kernel, either u or u', whichever is nonzero. The width for three different definitions are plotted in figure 6.2. The solid curve shows the width computed based on the full width at half maximum (FWHM) criterion where the maximum is taken as the average of values in the region, which does not fall below 1. The dashed curve shows the width when FWHM criterion is used by considering the maximum value of the kernel as the maximum. The chain-dotted line represents the width when the threshold is defined as 1 and the width is determined from the length of the region that has higher value than this threshold. For comparison, the approximation $\Delta u|\sin\phi|$ is also plotted with dotted line. Although the definition for the approximate

width is ambiguous, observe that the approximation is satisfactory for all values of the fractional order and for all width definitions. For easier interpretation, the expanding cones from input to output and output to input are also plotted in figures 6.3 and 6.4.

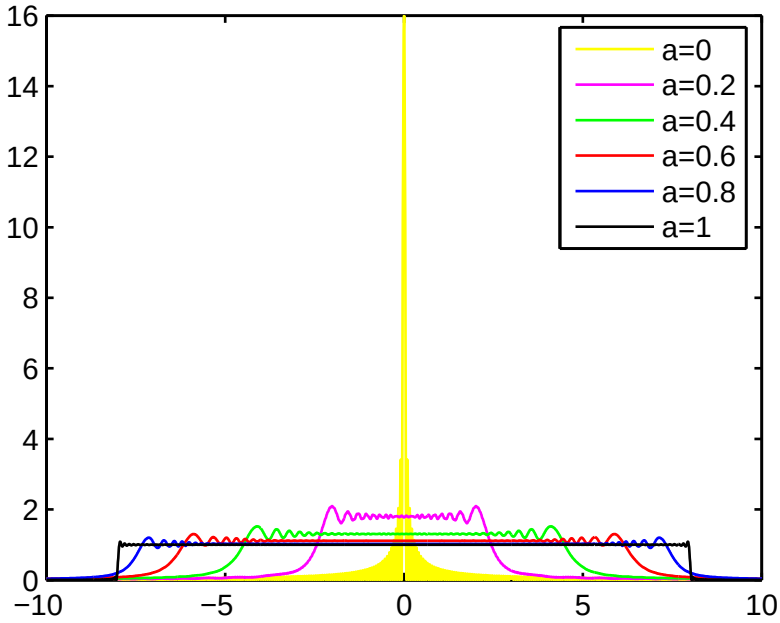

Figure 6.1: Magnitudes of the effective kernel for different transform orders when $\Delta u = 16$

6.1.2 Second Approach

The FRT kernel $K_a(u, u')$ is a complex exponential which exhibits a varying instantaneous frequency both as a function of u and u'. In order to compute the FRT of a function $f(u)$, we need to integrate it after multiplication with the kernel. Let us assume that the input signal $f(u)$ is bandlimited to the interval $[-\Delta u/2, \Delta u/2]$. Then, we can say that if the kernel changes with larger frequency than $\kappa\frac{\Delta u}{2}$ where $\kappa \geq 1$ is a chosen constant, then the contribution of these parts to the integral can be approximated as zero. The reasoning is that the function does not contain higher frequencies than $\Delta u/2$ and if the exponential oscillates

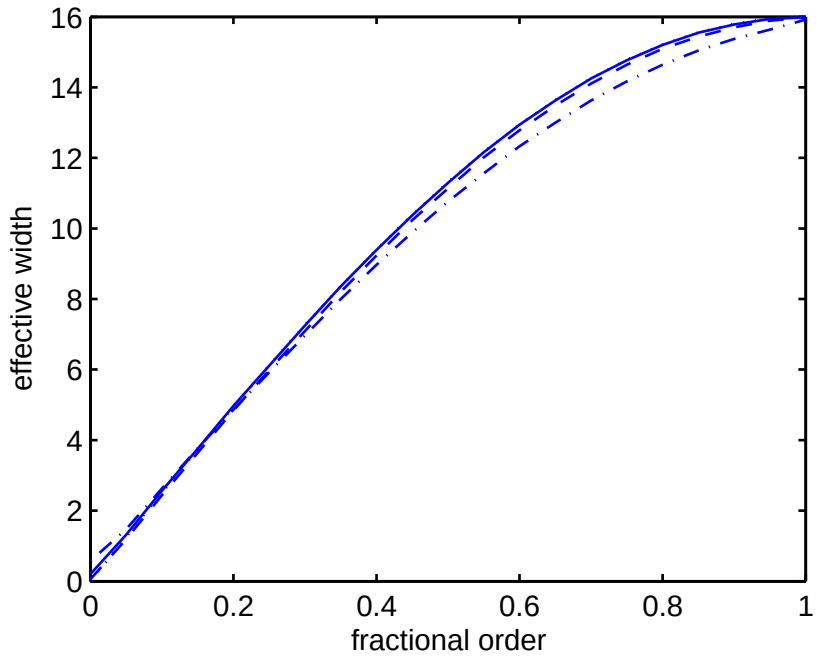

Figure 6.2: Effective width of the kernel based on FWHM (solid) and its approximation (dashed) as a function of the fractional order

faster, it will wash out the integral at these parts. Based on these ideas, for a bandlimited function we will define the effective width of the kernel as the range where the instantaneous frequency is larger than $\kappa\frac{\Delta u}{2}$.

Since we integrate with respect to the u' variable for computation of the FRT, we need to find the instantaneous frequency of the kernel by taking u' as a variable and u as a constant. Then, the instantaneous frequency can be obtained as $(2\pi)^{-1}d(\pi\cot\phi u^2 - 2\pi\csc\phi uu' + \pi\cot\phi u'^2)/du' = -\csc\phi\, u + \cot\phi u'$. By setting this equal to $\pm\kappa\frac{\Delta u}{2}$, we have

$$-\csc\phi\, u + \cot\phi u' = \pm\kappa\frac{\Delta u}{2} \tag{6.19}$$

If we also assume that the output signal is bandlimited to the interval $[-\Delta u/2, \Delta u/2]$, we can find another relation between u and u'. For this, consider the inverse FRT relation between the input and output signal. In order

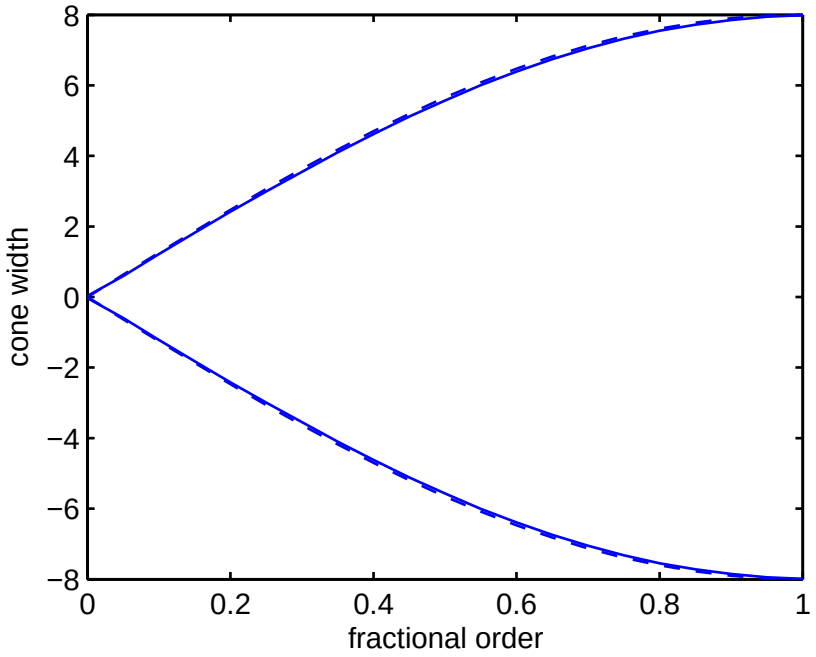

Figure 6.3: Expanding cone from input to output when the width is computed based on FWHM (solid) and when the width is approximated (dashed)

to compute the inverse FRT of $f_a(u)$, we need to integrate it after multiplication with the kernel $K_{-a}(u', u)$. Similarly, we can say that if the kernel changes with larger frequency than $\kappa\frac{\Delta u}{2}$ where $\kappa \geq 1$ is a chosen constant, then the contribution of these parts to the integral can be approximated as zero. Thus, we can define the effective width of the kernel as the range where the instantaneous frequency is larger than $\kappa\frac{\Delta u}{2}$. Since we integrate with respect to the u variable for computation of the inverse FRT, we need to find the instantaneous frequency of the kernel by taking u as a variable and u' as a constant. Note that we always use the variable u for the output variable and u' for the input variable. Then, the instantaneous frequency can be obtained as $(2\pi)^{-1}d(-\pi\cot\phi u'^2 + 2\pi\csc\phi u'u - \pi\cot\phi u^2)/du = \csc\phi\, u' - \cot\phi u$. By setting this equal to $\pm\kappa\frac{\Delta u}{2}$, we have

$$\csc\phi\, u' - \cot\phi u = \pm\kappa\frac{\Delta u}{2} \tag{6.20}$$

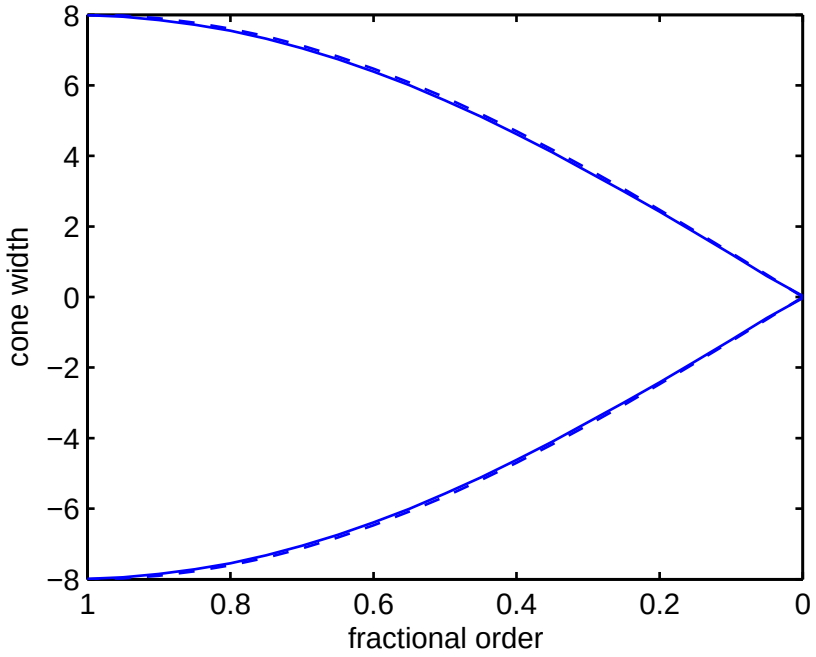

Figure 6.4: Expanding cone from output to input when the width is computed based on FWHM (solid) and when the width is approximated (dashed)

If we solve for u in (6.19), we obtain

$$u = \cos\phi u' \pm \sin\phi\kappa\frac{\Delta u}{2} \tag{6.21}$$

The above equation gives us the range of u values at the output for which the contribution of the input at point u' to the integral is nonnegligible. This defines the mostly affected region in the output from a point in the input, which we refer to as effectiveness region. Here, the first term $\cos\phi u'$ defines the center of the region at the output according to the input point u', which is simply a shift in u. The second term gives us the width of the region as $|\sin\phi|\kappa\Delta u$, which is simply the effectiveness width. Therefore, when we investigate the effect of an input point u' to the output, the kernel is centered at $u = \cos\phi u'$ with a width of $|\sin\phi|\kappa\Delta u$. Note that this result is completely consistent with the result given in Section 6.1.1 if we choose $\kappa = 1$.

If we solve for u' in (6.20), we obtain

$$u' = \cos\phi u \pm \sin\phi\kappa\frac{\Delta u}{2} \tag{6.22}$$

The above range of u' values defines the mostly affecting region in the input for a point in the output, which we refer to as the dependency region. Therefore, the effective kernel is centered at $u' = \cos\phi u$ with a width of $|\sin\phi|\kappa\Delta u$. Note that this result is also consistent with the result given in Section 6.1.1 if we choose $\kappa = 1$. However, if we solve for u' in (6.19) and u in (6.20), we will obtain different range of values for u and u', which are inconsistent with the results of Section 6.1.1. Exploring the reason behind this remains as an open problem, but we suspect that these solutions are not valid under our approximations.

We will also define the height of the effective kernel as the magnitude of the original FRT kernel, which is given by $|A_\phi| = |\sqrt{1 - i\cot\phi}|$. By approximating the effective kernel as a rectangle of width $|\sin\phi|\kappa\Delta u$ and height $|\sqrt{1 - i\cot\phi}|$, we can investigate how the energy changes as a function of the order a:

$$\begin{aligned}
Energy &= Height^2 \times Width && (6.23)\\
&= |\sqrt{1 - i\cot\phi}|^2 |\sin\phi|\kappa\Delta u && (6.24)\\
&= |1 - i\cot\phi| |\sin\phi|\kappa\Delta u && (6.25)\\
&= \sqrt{1 + (\cot\phi)^2}|\sin\phi|\kappa\Delta u && (6.26)\\
&= \kappa\Delta u && (6.27)
\end{aligned}$$

Therefore, the energy is the same for all values of order a.

6.2 Discrete Case

We will now explore the concepts of effectiveness and dependency regions in the discrete case. For this, we will consider the discrete FRT defined in [10]. Let us denote the ath order discrete FRT matrix as $\mathbf{F}^a$. In order to investigate

the contribution of samples in one domain to a sample in the other domain, we investigate the change in the magnitude of the coefficients throughout one row and one column of $\mathbf{F}^a$. Investigating the change throughout one row tells us how much one sample in the output domain (corresponding to that row) is affected from the samples in the input domain. Similarly, investigating the change throughout one column tells us how much one sample in the input domain (corresponding to that column) affect the samples in the output domain. In fact, both row and column investigation will give the same result since $\mathbf{F}^a$ is a symmetric matrix. Therefore, the effect of an input point to the output and the dependency of an output point to the input will be the same. From now on, we will only investigate the dependency region, but the reader should remember that all of the results hold also for the effectiveness region.

Let N denote the number of samples in both domains. Then, the range of input and output samples is $[-N/2, N/2-1]$. We choose $N = 256$ for illustration purposes. Firstly, we investigate the effect of input samples to the 0th output sample. As shown in figure 6.5, the influence or dependency of a point in one domain to the points in the other domain spreads as a increases, similar with the continuous case. (See in figure 6.6 that the width increases with the order a) We will refer to this phenomena as the *spread of information*. For small values of a, there is only local dependency and as a increases, the contribution of other points increases while the contribution of points in the local area sharply decreases, by this way the contribution of all points starts to be equalized as $a \to 1$.

We will now investigate the effect of input samples to an output sample when the output sample is located at different points than the center. As seen in Figure 6.7, the effect at different locations than the center is approximately a shifted version of the effect at the center, which is similar with the result of the continuous case. However, they are not an exact shift as in the continuous case since some distortions also take place, which may be caused due to discrete

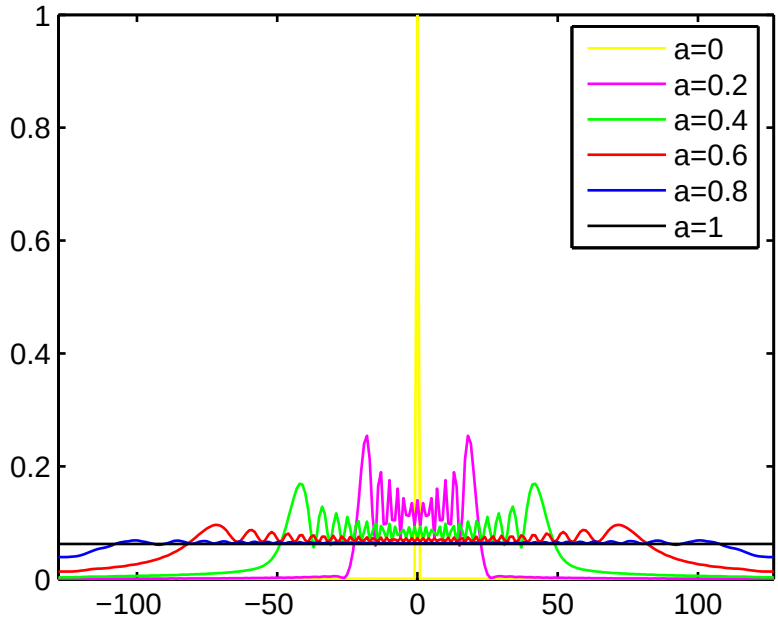

Figure 6.5: The effect on 0th sample for different transform orders

approximation. We also note that the discrete FRT has a periodic nature since its eigenvectors are periodic with period N [2]. Then, the input vector which is decomposed in terms of these eigenvectors is in fact assumed to be periodic with N, and thus the output is also periodic with N. We observe this periodic nature also in the figures of 6.7 since the effect on one end is continuously followed by the effect on the other end. Also note that we can further assume periodicity in the continuous case to match the results of the discrete case in this sense.

Let us compare the results of the discrete case with the results of the continuous case. In the continuous case, we have assumed an input function whose Wigner distribution is approximately confined to a circle of diameter Δu. If we sample such a function, we need to take at least $N = \Delta u^2$ samples. Then, the results of the discrete case obtained with $N = 256$ samples correspond to the case when $\Delta u = 16$ in the continuous case. The continuous and discrete kernels are plotted in Figure 6.8 for comparison. The effective width has been approximated as $\Delta u|\sin\phi|$ in the continuous case and the accordingly defined width corridors

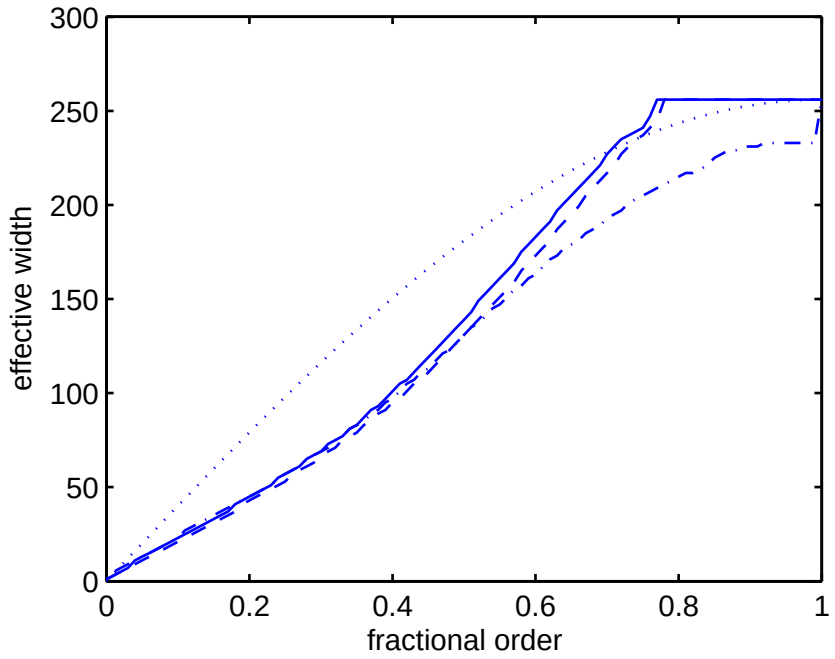

Figure 6.6: Width in the discrete case based on FWHM (solid) and the approximation in the continuous case (dashed)

are also plotted on the continuous kernel. The equivalence of these corridors in the discrete case can be found by taking $\Delta u|\sin\phi|/(1/\sqrt{N}) = N|\sin\phi|$ samples in the dependency region. The corridors defined accordingly are also plotted on the discrete kernel. As seen in Figure 6.8, approximating the dependency region as $N|\sin\phi|$ produce a close approximation in the discrete case, although it is not very tight. We can see this also in Figure 6.6 where the dependency width is computed based on three different width definitions. The solid curve shows the width defined by the FWHM criterion where the maximum is taken as the average of values in the region, which does not fall below 1/16. The dashed curve shows the width when FWHM criterion is used by considering the maximum value of the kernel as the maximum. The chain-dotted line represents the width when the threshold is defined as 1/16 and the width is determined from the length of the region that has higher value than this threshold. For comparison, the approximation $N|\sin\phi|$ is also plotted with dotted line. Although the

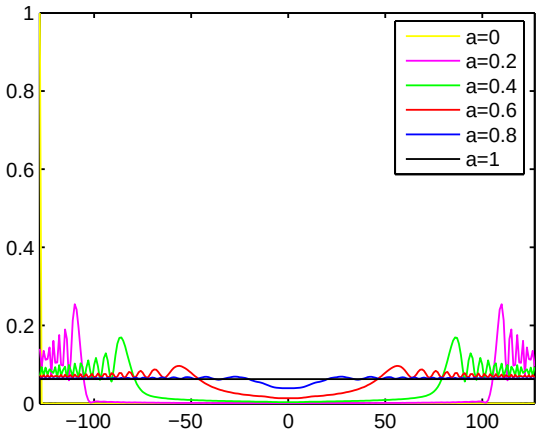

(a) Effect on -128th sample

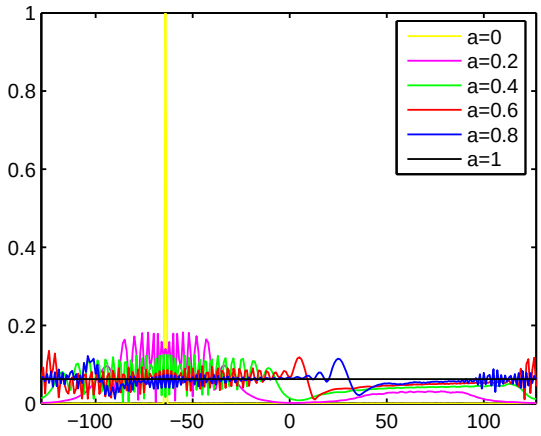

(b) Effect on -64th sample

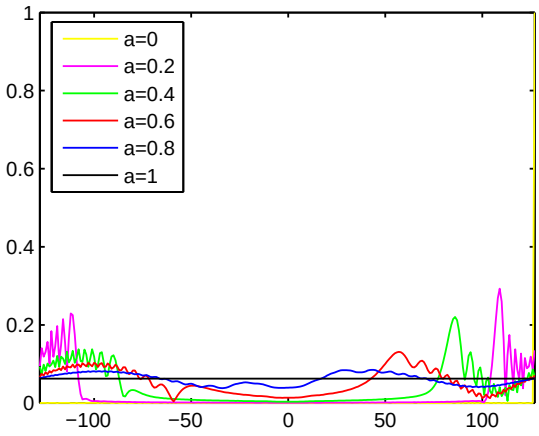

(c) Effect on 127th sample

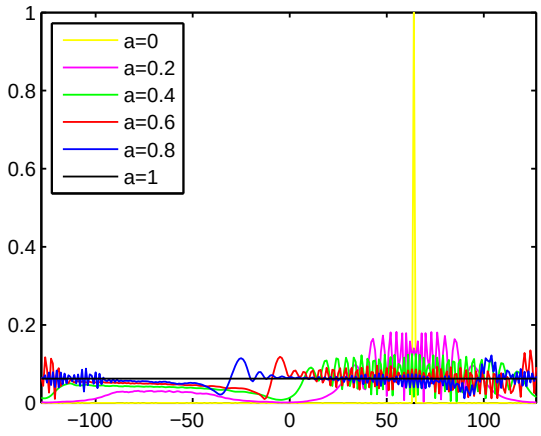

(d) Effect on 64th sample

Figure 6.7: The effect on samples located at different points than the center for different transform orders

definition for the approximate width is ambiguous, observe that all of the three widths are close to the approximate width $N|\sin\phi|$.

Let us also investigate the change in the energy for the discrete case. Let us define the height as the average of the values in the dependency region. Remember that we have defined the dependency region based on three different criterions. For comparison with the continuous case, this is multiplied with Δu and the approximation of the height in the continuous case, given by $|\sqrt{1-i\cot\phi}|$, is also plotted with dashed lines (Figure 6.9). As shown in Figure 6.9, roughly

speaking, the energy is the same for all values of a also in the discrete case, where the errors may be due to our width and height definitions. We also note that for direct comparison with the continuous case, we can normalize the width in the discrete case by $1/\sqrt{N}$, since each sample is taken at intervals of this length. After normalization, the energy will be approximately $\sqrt{N}$ for all values of a, which is equal to Δu, and thus it is also consistent with the continuous case.

6.3 Appendix

In this part, we will figure out the extent of the FRT of sinc and rectangle functions. Let us consider the function $\Delta u \operatorname{sinc}(\Delta u\, u)$. We can assume that the sinc function is confined to the intervals of length $\sim 1/\Delta u$ and Δu in the time and frequency domains, respectively. Roughly speaking, this will define a rectangular region in the time-frequency plane. If we compute ath order FRT of a sinc, this will correspond to a rotation in the time-frequency plane and the width of the transformed function can be found via projection onto the rotated axis. As seen from Fig. 6.10, this width is simply $\sim \Delta u \sin\phi + (1/\Delta u)\cos\phi$. When $\Delta u \gg 1$, this can be further approximated as $\sim \Delta u \sin\phi$.

We will now illustrate that $\Delta u \sin\phi + (1/\Delta u)\cos\phi$ provides a satisfactory approximation to the extent of a transformed sinc function. Fig. 6.11 shows the magnitudes of the fractional Fourier transforms of a sinc function for different orders when $\Delta u = 16$. The extent based on the full width at half maximum (FWHM) criterion and the approximation $\Delta u \sin\phi + (1/\Delta u)\cos\phi$ are plotted in figure 6.12. Observe that the approximation is valid for all values of the fractional order.

With similar arguments, it is possible to approximate the effective width of the ath order FRT of a rectangle function $\operatorname{rect}(u/\Delta u)$ as $\sim (1/\Delta u)\sin\phi + \Delta u \cos\phi$. When $\Delta u \gg 1$, this can be further approximated as $\sim \Delta u \cos\phi$.

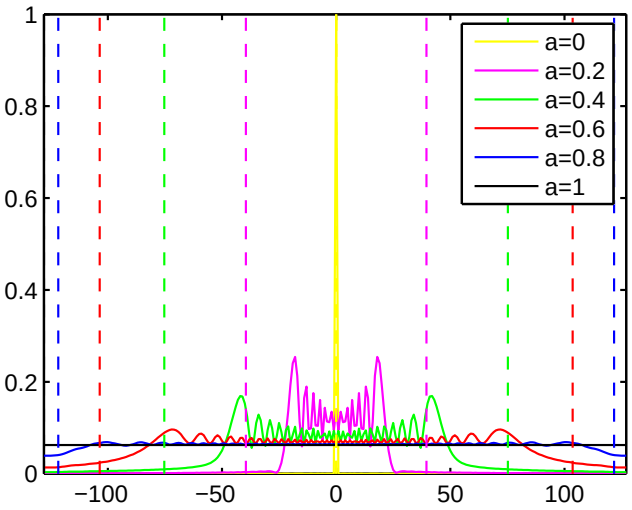

(a) Discrete case

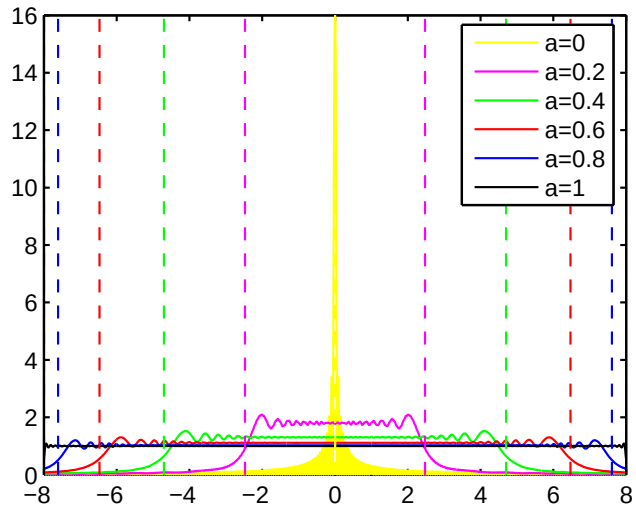

(b) Continuous case

Figure 6.8: The kernel in the discrete and continuous cases for different transform orders

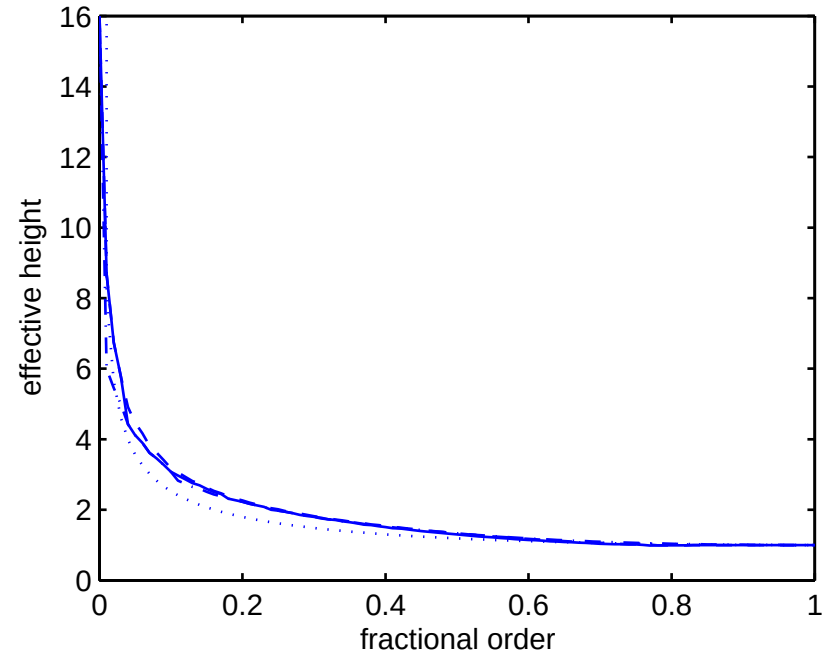

(a) Height

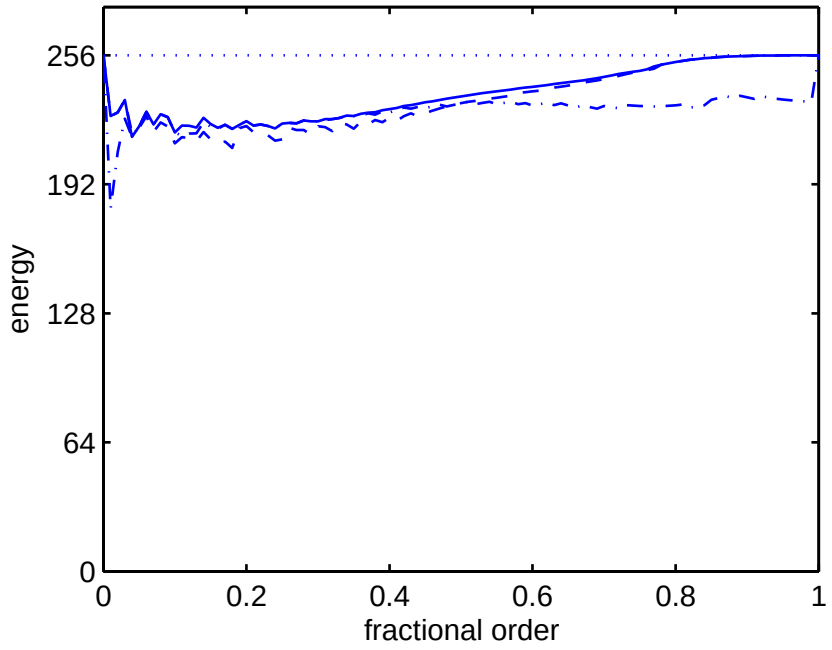

(b) Energy

Figure 6.9: Height and energy in the discrete case (solid) and their approximation in the continuous case (dashed)

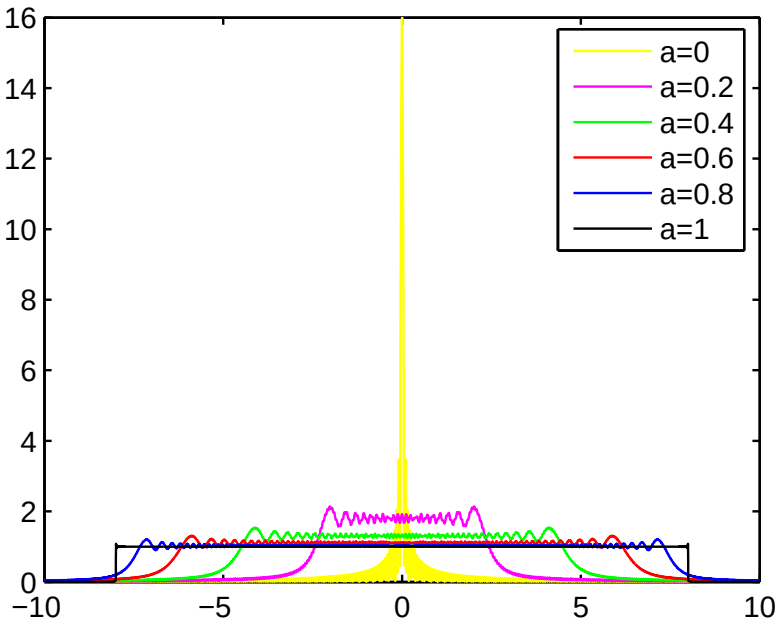

Figure 6.10: FRT of a sinc function

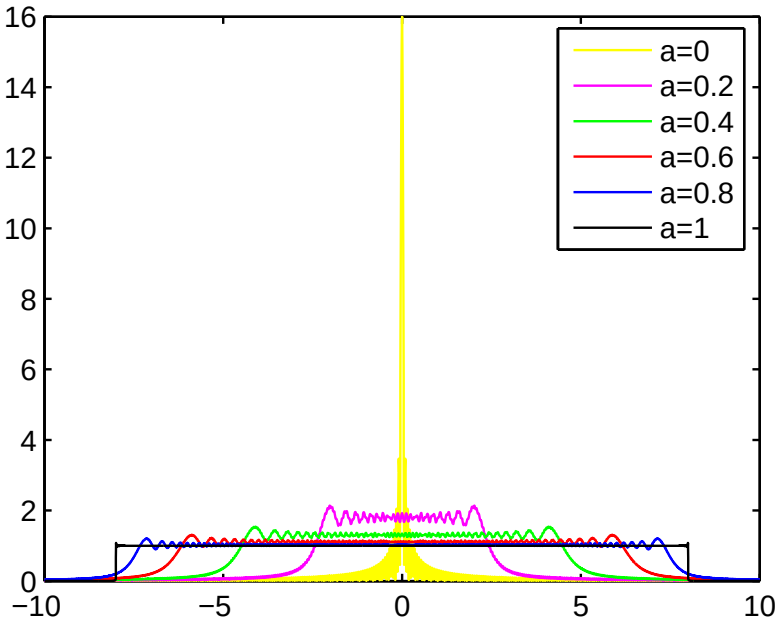

Figure 6.11: Magnitudes of the fractional Fourier transforms of a sinc function with $\Delta u = 16$

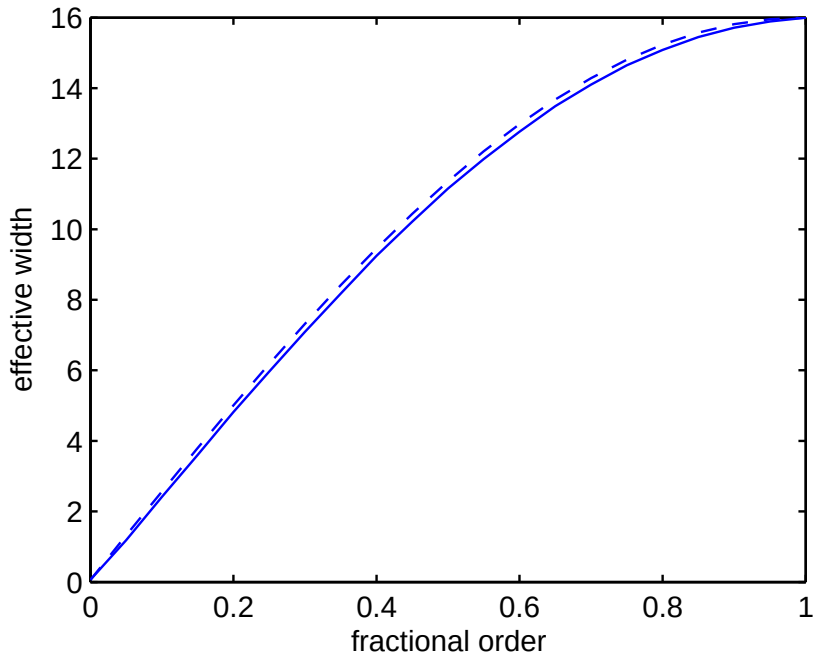

Figure 6.12: Effective width of the FRT of a sinc as a function of the fractional order based on FWHM (solid) and its approximation (dashed)

Chapter 7

LINEAR ALGEBRAIC ANALYSIS OF SIGNAL RECOVERY FROM PARTIAL FRACTIONAL FOURIER DOMAIN INFORMATION

7.1 Introduction

In this chapter, we will turn our attention to a class of signal recovery problems where partial information in two or more fractional Fourier domains are available and the aim is to find the unknown signal values by using known information. These problems have been motivated by the existence of wide applications in optical, acoustical, electromagnetic, and other wave propagation problems [2]. This is because, the propagation of waves can be considered as a process of continual fractional Fourier transformation, where the fractional order monotonically

increases as a function of the distance [60]. As the wave propagates, first the function itself, then its fractional Fourier transforms of increasing order and finally in the far-field its Fourier transform is observed. The measurement planes perpendicular to the axis of propagation correspond to fractional Fourier domains (FRFDs). Thus, the problem considered here corresponds to the problem of recovering waves from their measurements distributed over several planes. We can encounter with these problems in many different situations. For instance, if measurements can not be taken with sufficient spatial resolution, but with a lower one or if it is not possible to take measurements at some parts of the measurement plane, then we can take measurements at more than one plane under these constraints and find all unknown samples at a certain plane by using these measurements [61]. By this way, we can compensate for the information deficiency caused by the measurement constraints.

While some ad hoc algorithms have been applied to these problems, there has not been much theoretical progress. A numerical solution to the problem in pure fractional Fourier domain context has been given in [62], where an iterative algorithm has been developed based on the method of projections onto convex sets. The problem when amplitude measurements are not possible has been addressed in [63], which deals with the problem of recovering a complex signal from the magnitudes of multiple fractional Fourier transforms. A numerical approach to the recovery of the signal from its samples at arbitrarily distributed points has been presented in an optical context in [64]. An information theoretic approach has been discussed in [65].

Our purpose in this work is to develop a novel linear algebraic approach to these problems. We will formulate the problem as a linear system of equations and deal with the sensitivity issues of ill-posed problems. With these, we aim to investigate how much data is needed to recover the signal within some tolerable error and explore the redundancy and information relations between the given

data for different sample distributions and independently from the signal to be recovered.

7.2 Problem Definition

Consider two fractional Fourier domains such that each domain is sampled at N uniform points. Let a_1 and a_2 be the orders of these two domains. Let $\mathbf{f} = [f(-N/2), ..., f(N/2-1)]^T$ and $\mathbf{g} = [g(-N/2), ..., g(N/2-1)]^T$ denote the vectors of length N which represent the samples of the signals f and g in the a_1th and a_2th order FRFDs, respectively. If $a = a_2 - a_1$, the relation between the signals at these domains is given by

$$\mathbf{g} = \mathbf{F^a f}, \tag{7.1}$$

where $\mathbf{F}^a$ denotes the $N \times N$ ath order discrete FRT matrix given in [10]. Here, we approach the problem in a purely discrete context. However, if we consider the vectors as the samples of continuous-time signals, then the above relation will be an approximation and and there will also be a contribution to the error coming from this approximation. As we will see later in (7.7), condition number will also be a measure for this error.

Let m_1 and m_2 denote the number of known samples in the a_1th and a_2th order FRFDs, respectively. If the known indices in both domains form the vectors $\mathbf{k} = [k_1, ..., k_{m_1}]^T$ and $\mathbf{n} = [n_1, ..., n_{m_2}]^T$, then the vectors $f(\mathbf{k}) = [f(k_1), ..., f(k_{m_1})]^T$ and $g(\mathbf{n}) = [g(n_1), ..., g(n_{m_2})]^T$ contain the known signal values of f and g, respectively. Similarly, if the indices in vectors $\bar{\mathbf{k}}$ and $\bar{\mathbf{n}}$ are unknown respectively for f and g, then $f(\bar{\mathbf{k}})$ and $g(\bar{\mathbf{n}})$ represent the unknown signal values.

Let $\mathbf{F^a}(\mathbf{n}, \mathbf{k})$ be an m_2 x m_1 submatrix of $\mathbf{F}^a$ obtained by choosing its n_1th,...,n_{m_2}th rows and k_1th,...,k_{m_1}th columns. By choosing the same rows and

the remaining columns, one can also construct the submatrix $\mathbf{F^a}(\mathbf{n}, \bar{\mathbf{k}})$, which is m_2 x $(N - m_1)$. Then, the relation in (7.1) can be rewritten as follows:

$$g(\mathbf{n}) = \mathbf{F^a}(\mathbf{n}, \bar{\mathbf{k}}) f(\bar{\mathbf{k}}) + \mathbf{F^a}(\mathbf{n}, \mathbf{k}) f(\mathbf{k}). \tag{7.2}$$

Since $f(\bar{\mathbf{k}})$ contains known samples of f, we can move it to the left hand side (LHS). Then, by denoting the known term in the LHS as $\mathbf{g'} = g(\mathbf{n}) - \mathbf{F^a}(\mathbf{n}, \mathbf{k}) f(\mathbf{k})$, the linear system of equations for the solution of the problem can be obtained as

$$\mathbf{g'} = \mathbf{F^a}(\mathbf{n}, \bar{\mathbf{k}}) f(\bar{\mathbf{k}}). \tag{7.3}$$

Thus, in order to find $f(\bar{\mathbf{k}})$ which contains the unknown signal values of f, we need to solve the above system of equations. Similarly, to find $g(\bar{\mathbf{n}})$ which contains the unknown signal values of g, we should solve

$$\mathbf{f'} = \mathbf{F^{-a}}(\mathbf{k}, \bar{\mathbf{n}}) g(\bar{\mathbf{n}}), \tag{7.4}$$

where $\mathbf{f'} = f(\mathbf{k}) - \mathbf{F^{-a}}(\mathbf{k}, \mathbf{n}) g(\mathbf{n})$.

Knowing the signal completely in one domain is equivalent to knowing it in all domains. Thus, when the signal is partially known in two domains, it is enough to find the signal either in the a_1th or a_2th order domain. In this work, we choose to find the signal firstly in the domain with largest number of known samples. We refer to the domain where we want to find the signal as the *reference plane*. That is, if $m_1 > m_2$, the reference plane is chosen as the a_1th order FRFD and otherwise, it is chosen as the a_2th order FRFD.

We could also choose the reference plane as the domain with fewer number of samples or as any other domain that does not contain any known sample. Although the problem solution should be independent of the chosen reference plane theoretically, the condition number will differ by a small amount depending on which one is chosen. However, there is at most one order of difference between these condition numbers and this largest difference is obtained only when the accuracy of the solution is good. Thus, in fact the chosen reference plane will

not create much difference on our numerical results. Moreover, when we choose the domain with largest number of known samples as the reference plane, the condition number is experimentally minimum among other choices of reference plane. Besides giving more accurate solutions, this choice is also more practical since it requires us to solve for a fewer number of unknowns. Because of these advantages, we choose the reference plane as the domain with largest number of known samples.

7.3 Analysis

In this work, our aim is to investigate the redundancy and information relations between the known samples. For this purpose, we will investigate the sensitivity or accuracy of the solution of the problem, which can be obtained by using (7.3) or (7.4). As is well known, if the matrix $\mathbf{F^a}(\mathbf{n}, \bar{\mathbf{k}})$ or $\mathbf{F^{-a}}(\mathbf{k}, \bar{\mathbf{n}})$ is rank deficient, for the unknown signal values there are infinitely many solutions if the known signal values are consistent with each other and there is no solution when both rank deficiency and inconsistency exist. If the matrix has full rank, although the solution is unique, the accuracy of it depends on the conditioning of the problem. This is because, the solution of the problem will be affected from the limited machine precision and measurement errors depending on its conditioning. Throughout this study, we will use the condition number of the system matrix as the measure of conditioning. With this, we will investigate how the condition number of $\mathbf{F^a}(\mathbf{n}, \bar{\mathbf{k}})$ or $\mathbf{F^{-a}}(\mathbf{k}, \bar{\mathbf{n}})$ is affected from the distribution of known samples.

Before continuing to our discussion, we will first provide a basic review of the condition number and its properties. The condition number associated with the linear equation $Ax = b$ gives a bound on how inaccurate the solution x and measures the rate at which the solution x will change with respect to a change

in b or A [66]. Change in b can come from experimental data or from roundoff, and can change the solution completely when we have a large condition number.

The condition number of a nonsingular square matrix $\mathbf{A}$ is defined as [66]

$$\text{cond}(\mathbf{A}) = \|\mathbf{A}\|\|\mathbf{A}^{-1}\| \tag{7.5}$$

with respect to a given matrix norm. For rectangular matrices, pseudoinverse is used instead of inverse in the definition of the condition number. Condition number of a matrix measures its closeness to rank deficiency and thus for square matrices, it is the measure of closeness to singularity.

In this study, condition number in l_2 norm is used, which is given by the ratio of the largest singular value to the smallest [66]:

$$\text{cond}(\mathbf{A}) = \frac{\sigma_{\max}(\mathbf{A})}{\sigma_{\min}(\mathbf{A})} \tag{7.6}$$

Although the value of the condition number depends on the particular norm used, these values can differ by at most a fixed constant because of the equivalence of the underlying vector norms. Thus, they are equally useful as quantitative measures of conditioning [66].

Let $\mathbf{A}$ be an arbitrary $m \times n$ matrix, where $m \geq n$. Then, some of the important properties of the condition number are as follows [66]:

- $\text{cond}(\mathbf{A}) \geq 1$.
- $\text{cond}(\mathbf{A}) = 1$ if $\mathbf{A}$ is unitary.
- $\text{cond}(\mathbf{A}) = \infty$ if $\text{rank}(\mathbf{A}) < n$.
- $\text{cond}(\gamma\mathbf{A}) = \text{cond}(\mathbf{A})$ for any nonzero scalar γ.

Values of condition number close to 1 indicate a well-conditioned matrix and small uncertainty in the solution.

The condition number is an amplification factor that bounds the maximum relative error in the solution due to a given relative error in the input data. For a square matrix, the error bounds are given by [66]:

$$\frac{\|\delta\mathbf{x}\|/\|\mathbf{x}\|}{\|\delta\mathbf{b}\|/\|\mathbf{b}\|} \leq \text{cond}(\mathbf{A}), \qquad \frac{\|\delta\mathbf{x}\|/\|\mathbf{x}+\delta\mathbf{x}\|}{\|\delta\mathbf{A}\|/\|\mathbf{A}\|} \leq \text{cond}(\mathbf{A}) \tag{7.7}$$

We may not be able to rely on the results of computations when an ill-conditioned matrix is used. If the input data is accurate to machine precision, then the relative error in the computed solution can be reasonably bounded by [66]

$$\frac{\|\delta\mathbf{x}\|}{\|\mathbf{x}\|} \lessapprox \text{cond}(\mathbf{A})\epsilon_{\text{mach}} \tag{7.8}$$

The usual rule of thumb is that about $\log_{10}(\text{cond}(\mathbf{A}))$ decimal digits of accuracy is lost in the computed solution relative to the accuracy of the input.

Returning back to our discussion, for the purpose of investigating the redundancy and information relations between the given data, we use condition number as a measure of redundant information in given samples. The reasoning is that since the condition number measures the sensitivity of the solution to perturbations in the input data, large condition numbers are associated with large uncertainties in the solution. It is also intuitive that as the dependency in the given data increases, the uncertainty in the solution will also increase. Thus, conditioning of the problem can be a measure for dependency. If the condition number is high, it can be suggested that there is much dependency between given samples, or equivalently we do not have enough information to recover the signal accurately.

Since the matrix $\mathbf{F}^a$ is unitary and symmetric, we can show that the following equalities are true for the 2-norm condition number:

$$\begin{aligned} \text{cond}_2(\mathbf{F}^{\mathbf{a}}(\mathbf{n},\bar{\mathbf{k}})) &= \text{cond}_2(\mathbf{F}^{\mathbf{a}}(\bar{\mathbf{k}},\mathbf{n})) && (7.9)\\ &= \text{cond}_2(\mathbf{F}^{-\mathbf{a}}(\bar{\mathbf{k}},\mathbf{n})) && (7.10)\\ &= \text{cond}_2(\mathbf{F}^{-\mathbf{a}}(\mathbf{n},\bar{\mathbf{k}})) && (7.11) \end{aligned}$$

The condition numbers above indicate that the accuracy of the solution is the same for the following problems, respectively:

1. The indices in $\mathbf{k}$ are known for the signal f and the indices in $\mathbf{n}$ are known for the signal g.

2. The indices in $\bar{\mathbf{n}}$ are known for the signal f and the indices in $\bar{\mathbf{k}}$ are known for the signal g.

3. The indices in $\bar{\mathbf{k}}$ are known for the signal f and the indices in $\bar{\mathbf{n}}$ are known for the signal g.

4. The indices in $\mathbf{n}$ are known for the signal f and the indices in $\mathbf{k}$ are known for the signal g.

Thus, all of the above problems are equivalent to each other in terms of redundancy. If we consider the first and third ones together, it is clear that the accuracy of the solution is the same when we exchange the knowns and unknowns with each other in both domains. Moreover, if we consider the first and last ones together, changing the sample distributions between two domains does not affect the accuracy of the solution. This supports the symmetrical structure of the problem and shows that as expected, the direction of propagation does not create any difference on the solution.

Equation (7.9) follows from the following derivation. The matrix norm induced by the Euclidean vector norm is the largest singular value of the matrix: $\|\mathbf{A}\|_2 = \sigma_{\max}(\mathbf{A})$ [66]. Since the transpose of a matrix has the same singular values with the original matrix, we have $\|\mathbf{A}\|_2 = \|\mathbf{A}^T\|_2$. Then,

$$\mathrm{cond}_2(\mathbf{A}^T) = \|\mathbf{A}^T\|_2\|(\mathbf{A}^T)^{-1}\|_2 = \|\mathbf{A}^T\|_2\|(\mathbf{A}^{-1})^T\|_2 = \|\mathbf{A}\|_2\|\mathbf{A}^{-1}\|_2 = \mathrm{cond}_2(\mathbf{A}) \tag{7.12}$$

Since $\mathbf{F}^a$ is a symmetric matrix, $\mathbf{F}^a(\mathbf{n}, \bar{\mathbf{k}}) = (\mathbf{F}^a(\bar{\mathbf{k}}, \mathbf{n}))^T$. From the above result, the condition numbers of $\mathbf{F}^a(\mathbf{n}, \bar{\mathbf{k}})$ and $\mathbf{F}^a(\bar{\mathbf{k}}, \mathbf{n})$ are also the same. This completes the proof of (7.9).

The equation (7.11) follows from the fact that $\mathbf{F}^a$ is a unitary matrix, i.e. $(\mathbf{F}^a)^H = \mathbf{F}^{-a}$. Since $\mathbf{F}^a$ is also symmetric, $(\mathbf{F}^a)^* = \mathbf{F}^{-a}$, and thus $(\mathbf{F}^a(\mathbf{n}, \bar{\mathbf{k}}))^* = \mathbf{F}^{-a}(\mathbf{n}, \bar{\mathbf{k}})$. Since the conjugate of a matrix has the same singular values with the original matrix, we have $\text{cond}_2(\mathbf{A}^*) = \text{cond}_2(\mathbf{A})$. Then, $\mathbf{F}^a(\mathbf{n}, \bar{\mathbf{k}})$ and $\mathbf{F}^{-a}(\mathbf{n}, \bar{\mathbf{k}})$ have the same condition number. This completes the proof of (7.11). By combining (7.9) and (7.11), one can also obtain (7.10).

As noted before, instead of choosing the domain with largest number of known samples as the reference plane, one could also choose an empty domain as the reference plane. We will now discuss this case in more detail. Without loss of generality, we can say that 0th order domain does not contain any known sample so that we can choose it as reference. To formulate the problem, let us denote the signal in the reference plane as h. Then, the relation between signals are given by $\mathbf{f} = \mathbf{F}^{\mathbf{a_1}}\mathbf{h}$ and $\mathbf{g} = \mathbf{F}^{\mathbf{a_2}}\mathbf{h}$. If we write these relations only for known samples and combine together, we obtain

$$\begin{bmatrix} f(\mathbf{k}) \\ g(\mathbf{n}) \end{bmatrix} = \begin{bmatrix} \mathbf{F}^{a_1}(\mathbf{k}) \\ \mathbf{F}^{a_2}(\mathbf{n}) \end{bmatrix} \mathbf{h}, \tag{7.13}$$

where $\mathbf{F}^{a_1}(\mathbf{k})$ and $\mathbf{F}^{a_2}(\mathbf{n})$ denote submatrices of $\mathbf{F}^{a_1}$ and $\mathbf{F}^{a_2}$ obtained by choosing k_1th,...,k_{m_1}th rows and n_1th,...,n_{m_2}th rows, respectively. We need to solve the above system of equations in order to find the signal in the reference plane. Although $\mathbf{F}^{a_1}(\mathbf{k})$ and $\mathbf{F}^{a_2}(\mathbf{n})$ have orthogonal rows seperately, their combination may contain non-orthogonal rows since the rows of FRT matrices of order a_1 and a_2 are not necessarily orthogonal to each other.

Based on the above formulation, we will now prove that the chosen reference plane does not create any difference on the accuracy of the solution. For this, we need to prove the following lemma:

Lemma: For any arbitrary matrix $\mathbf{A}$ and unitary matrix $\mathbf{B}$,

$$\text{cond}(\mathbf{AB}) = \text{cond}(\mathbf{A}) \tag{7.14}$$

Proof of Lemma:

$$cond(\mathbf{AB}) = \|\mathbf{AB}\|\|(\mathbf{AB})^{-1}\| = \|\mathbf{AB}\|\|\mathbf{B}^{-1}\mathbf{A}^{-1}\| \tag{7.15}$$

From unitary property of the matrix $\mathbf{B}$, one can obtain

$$\|\mathbf{AB}\| = max_{x\neq 0}\frac{\|\mathbf{AB}x\|}{\|x\|} = max_{y\neq 0}\frac{\|\mathbf{A}y\|}{\|\mathbf{B}^{-1}y\|} = max_{y\neq 0}\frac{\|\mathbf{A}y\|}{\|y\|} = \|\mathbf{A}\| \tag{7.16}$$

where we make the substitution $y = \mathbf{B}x$ and use the fact that since $\mathbf{B}^{-1}$ is unitary, it preserves the length, equivalently $\|\mathbf{B}^{-1}y\| = \|y\|$. Similarly,

$$\|\mathbf{B}^{-1}\mathbf{A}^{-1}\| = max_{x\neq 0}\frac{\|\mathbf{B}^{-1}\mathbf{A}^{-1}x\|}{\|x\|} = max_{x\neq 0}\frac{\|\mathbf{A}^{-1}x\|}{\|x\|} = \|\mathbf{A}^{-1}\| \tag{7.17}$$

If we substitute these two results in (7.15), we can recognize the final result as cond($\mathbf{A}$). This completes the proof of (7.14).

By using this lemma, we can now show that the chosen reference plane does not create any difference on the conditioning of the problem. Let us choose the ath order domain as reference. Then, the accuracy of the solution depends on the condition number of the following matrix:

$$\mathbf{F_1} = \begin{bmatrix} \mathbf{F}^{a_1-a}(\mathbf{k}) \\ \mathbf{F}^{a_2-a}(\mathbf{n}) \end{bmatrix} \tag{7.18}$$

If we choose the $\hat{a}^{th}$ order domain as the reference such that $\hat{a} \neq a$, the accuracy depends on the following matrix:

$$\mathbf{F_2} = \begin{bmatrix} \mathbf{F}^{a_1-\hat{a}}(\mathbf{k}) \\ \mathbf{F}^{a_2-\hat{a}}(\mathbf{n}) \end{bmatrix} \tag{7.19}$$

Since $\mathbf{F}^{a_1-a} * \mathbf{F}^{a-\hat{a}} = \mathbf{F}^{a_1-\hat{a}}$, if we multiply $\mathbf{F_1}$ from right by $\mathbf{F}^{a-\hat{a}}$, we will obtain $\mathbf{F_2}$. That is, $\mathbf{F_2} = \mathbf{F_1}\mathbf{F}^{a-\hat{a}}$. Since $\mathbf{F}^{a-\hat{a}}$ is a unitary matrix, by using the above lemma, we have cond($\mathbf{F_2}$) = cond($\mathbf{F_1}$). Thus, the conditioning of the problem is the same for different reference plane choices.

7.4 Numerical Results

In the numerical results, the fractional order a is varied in the range $[0, 1]$ with equal intervals of length 0.1 and the number of samples N in both domains is chosen as 256. We take m_1 and m_2, which represents the number of known samples in two domains, as powers of 2 up to 128 and then choose their symmetric values with respect to 128 up to 256. In the plots, for different m_1 and m_2 pairs, the change in the logarithm of the condition number (to base 10) is investigated as a function of the order a.

We apply the developed approach to a number of distributions, which will be explained by using figure 7.1. Here, we denote the known samples with dark squares and the unknown samples with empty squares. There are mainly two groups: uniform vs accumulated distributions and complemantary vs overlapping distributions. In the uniform distribution, the known samples are distributed uniformly in both domains. When number of known samples in both domains are equal to each other, the illustration of this distribution is given in figures 7.1a and 7.1b. On the other hand, in the accumulated distribution, the known samples are accumulated at one side in both domains, which is again illustrated in figures 7.1c and 7.1d for the equal number of knowns case. Moreover, known samples in one domain can be chosen as complementary or overlapping with respect to the known samples in the other domain. For the complementary case, the unknown indices in one domain are known in the other domain as illustrated in 7.1a and 7.1c. In contrast, for the overlapping case, the known indices in one domain are known in the other domain, as shown in 7.1b and 7.1d. When the number of known samples is more than N, complementary and overlapping is applied such that respectively maximum possible nonoverlapping and overlapping occurs between known samples in two domains. We look to each four combinations of these groups. The reason for investigation of these distributions is that they provide good examples of the best case and worst case distributions.

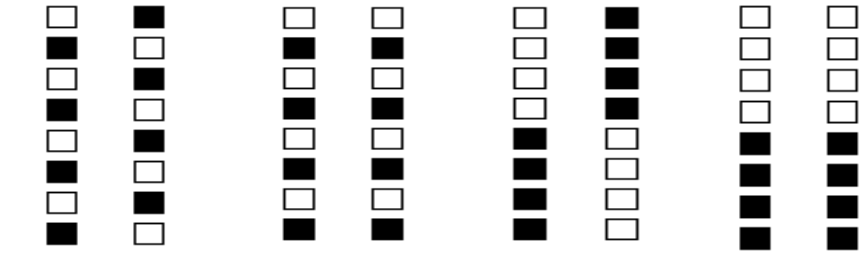

Figure 7.1: Illustration of different distributions

More precisely, if we denote the number of known samples in one domain as m, we use the following rules for the sample distributions:

1. Uniform-overlapping distribution: For both domains,
   (a) For $m \leq N/2$, multiples of N/m are the known points and the remaining ones are unknown.
   (b) For $m > N/2$, the points which satisfy $N/(N-m)-1 \pmod{N/(N-m)}$ are unknown and the remaining ones are the known points.
2. Uniform-complementary distribution: Rules for the a_1th order domain are the same as above. For the a_2th order domain, the rules are reversed as following:
   (a) For $m \leq N/2$, the points which satisfy $N/m-1 \pmod{N/m}$ are the known points and the remaining ones are unknown.
   (b) For $m > N/2$, multiples of $N/(N-m)$ are the unknown points and the remaining ones are known.
3. Accumulated-overlapping distribution: For both domains, the first m samples from below are known and the remaining ones are unknown.
4. Accumulated-complementary distribution: For the a_1th order domain, the first m samples from below are known and the remaining ones are unknown

whereas for the a_2th order domain, the first m samples from above are known and the remaining ones are unknown.

The uniform distribution corresponds to the physical situation when we have a measurement device with insufficient spatial resolution. In order to know the wave with the desired full resolution, we take measurements with the insufficient resolution at two different planes [61]. Moreover, the accumulated distribution corresponds to the case when we can take measurements only in a limited interval at a measurement plane, but with full resolution. In this case, to know the wave completely at one plane, we take measurements in limited intervals at two planes.

As we have seen in chapter 6, the spread of light on a plane perpendicular to the propagation axis increases as a function of distance. That is, the fractional order a, which depends on the distance for free space propagation, increases, a point in one domain affects more points in the other domain. A similar argument also holds for the dependency of the points. These concepts will be used to comment on the numerical results. For interpretations, we will originate cones from the known points in the domain with fewer number of knowns (in order to deal with fewer number of cones). If a cone originated from a known sample contains only known points in the opposite domain, then roughly speaking, this known sample is redundant since it completely depends on already known samples. However, if the cone contains one unknown sample in the opposite domain, then it will be nonredundant since the known samples in the opposite domain can not determine its value by their own. Thus, whether a cone contains an unknown or not is important for our redundancy investigation. More precisely, the optimal case occurs when each cone originating from a known sample contains only one unknown. Since each known sample is affected only by one different unknown in the opposite domain, there is no dependency between these known samples. However, when the cones start to contain some unknowns in common, then this means that each known is affected by these common unknowns. Even worse than

this is when the knowns are close to each other so that the common unknowns inside their cones affect these known samples similarly. Naturally, such similarity will create dependency between known samples. We note that this approach investigates the effect of unknown samples in one domain to known samples in the other domain and the constructed submatrix of the recovery problem also contains these effects.

In the experiments, we investigate for different distributions the change in the condition number as a function of the order a when total number of known samples in two domains is equal to and more than N. In our interpretations, we will use the term *strict redundancy* to refer to the case when the system matrix has linearly dependent columns, or equivalently the matrix is rank-deficient and the term *relative redundancy* to refer to the case when the columns are close to being linearly dependent. When we have linearly dependent rows, the associated known samples will be considered as strictly redundant whereas when the rows are close to being linearly dependent, the associated known samples will be considered as relatively redundant. In the numerical results, we have observed strict redundancy when $a = 0$ and $a = 1$. Since the discrete FRT matrix does not have a closed-form expression for other values of a, we can only speak in terms of relative redundancy in this case. We also note that the results may not be reliable when we are very close to the strict redundancy cases at $a = 0$ and $a = 1$ since chirp functions exhibit unusual behaviours in these limits.

7.4.1 Case where total number of knowns are equal to the number of unknowns

In this part, total number of known samples is equal to N, i.e. $m_1 + m_2 = N$. Figure 7.2, 7.3, 7.5 and 7.4 show condition number vs. a curves for accumulated and uniform distributions when known samples are shared differently between

two domains. The dotted lines in these figures show the condition number curves when we exchange the values of m_1 and m_2 in the corresponding solid line. Although solid and dotted lines are very close to each other, they are not the same for some distributions. The difference occurs because, when N is even, the samples at the edges are $-N/2$ and $N/2-1$, so that there is a slight difference between two versions of a distribution, which touch to the bottom and above edges. For easier comparison, the curves for all distributions when $m_1 = 16$, $m_2 = 240$ are plotted together in figure 7.6.

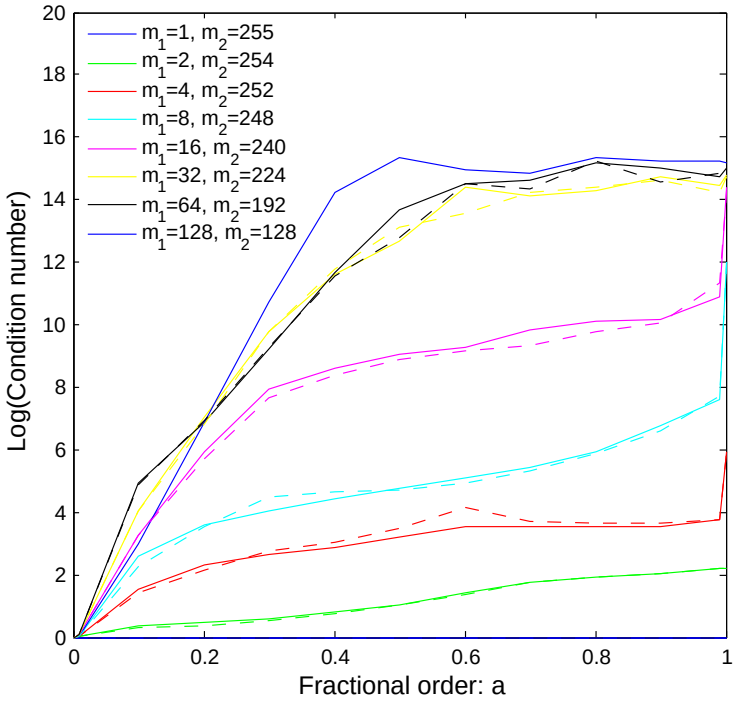

Figure 7.2: Condition number vs a for accumulated-complementary distribution and different pairs of m_1 and m_2 satisfying $m_1 + m_2 = N$ (The legend is also valid for Figure 7.3)

As seen in the figures, as $m_1 \to N/2$, the condition number gets worse for all distributions. That is, as the number of known samples in two domains gets closer to each other, the condition number increases for all distributions. This indicates that distributing known samples equally to each domain causes the largest amount of redundant information in the given data. To understand

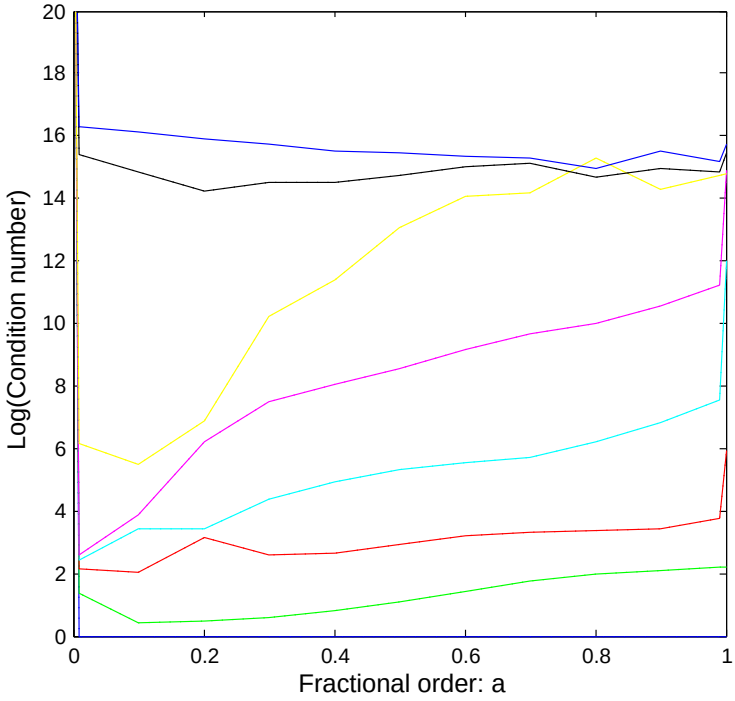

Figure 7.3: Condition number vs a for accumulated-overlapping distribution and different pairs of m_1 and m_2 satisfying $m_1 + m_2 = N$

the reasoning behind this, consider the cones originating from the knowns in the domain with the fewer number of knowns. As $m_1 \rightarrow N/2$, we will have more cones, each with overlapping regions with each other that contain both known and unknown samples. Thus, the relative dependency between these known samples increases as $m_1 \rightarrow N/2$. To see this more easily, let us first consider the domain with maximum number of known samples. Known samples in this domain are completely independent from each other, and thus there is no redundancy between them. Say, we have 240 known samples in one domain and 16 known samples in the other domain. Then, these 240 known samples are strictly non-redundant since they are in the same domain. However, other 16 samples will relatively depend on each other. As $m_1 \rightarrow N/2$, the number of fully non-redundant known samples decreases. Thus, we can consider the maximum number of known samples in one domain as a lower limit for number

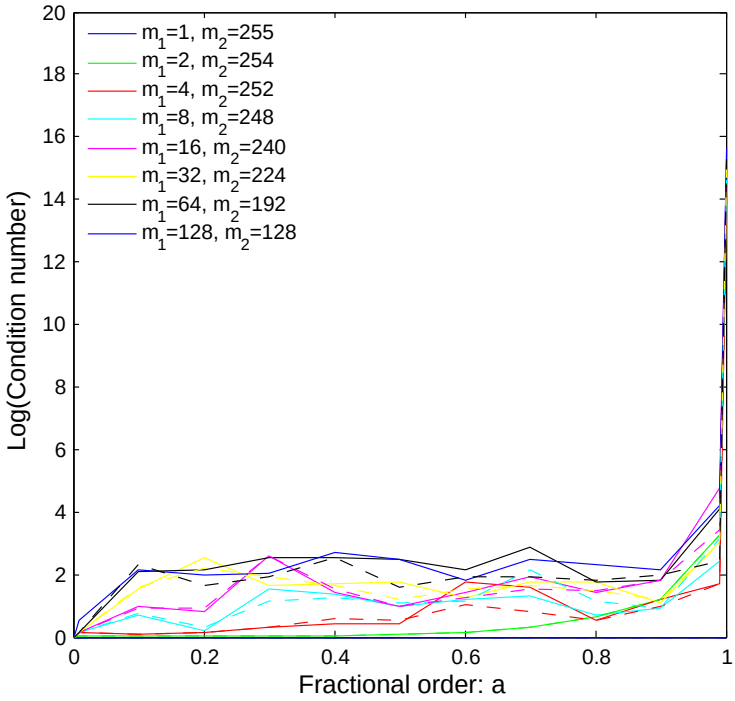

Figure 7.4: Condition number vs a for uniform-complementary distribution and different pairs of m_1 and m_2 satisfying $m_1 + m_2 = N$ (The legend is also valid for Figure 7.4)

of nonredundant samples. As $m_1 \to N/2$, the lower limit decreases and the gap between this limit and N increases, and thus it becomes harder for other relatively dependent known samples to fill this gap.

Observe from the figures that as a increases, the condition number also increases in general for all distributions. This is because, when a is small, there is only local dependency and as a approaches 1, each known point will be dependent with equal weights to the points in the other domain. If we think in terms of the cones, the overlap between cones increases as a increases, and thus the dependency between known samples defining these cones also increases.

Let us first investigate the accumulated-complementary case in detail. At $a = 0$, known points in two domains are fully complementary to each other, and thus there is no redundancy between them. For very small values of a, there is still local dependency and each cone contains only one unknown in the other

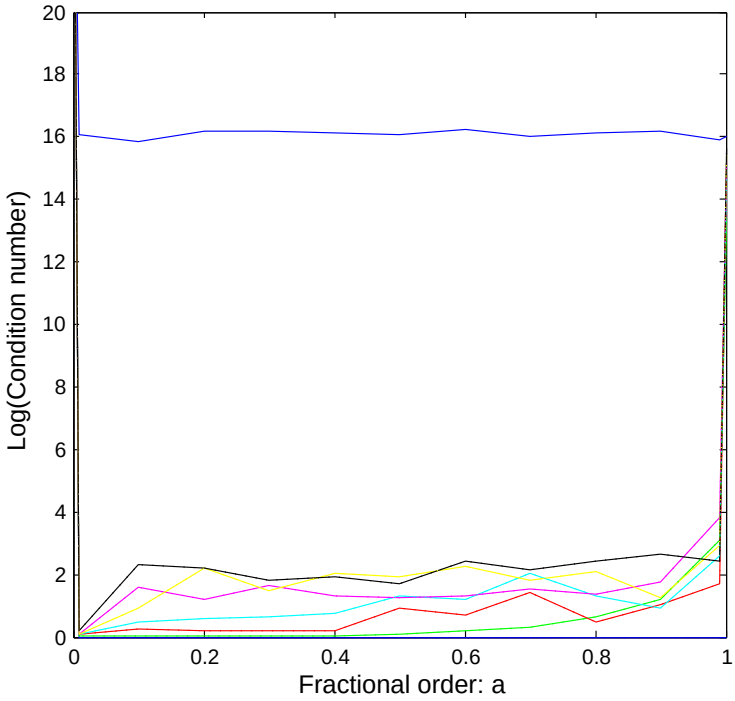

Figure 7.5: Condition number vs a for uniform-overlapping distribution and different pairs of m_1 and m_2 satisfying $m_1 + m_2 = N$

domain, so there is still no redundancy. When a increases sligthly, there will be overlaps between the cones and they will start to contain common unknowns. Thus, relative dependency between known samples will increase. As we increase a further, after some point each cone will start to contain all of the unknowns in the other domain. Since known samples are very close to each other, they will define similar cones, and thus the effect of unknown samples to each known sample will be very similar for all known samples. Since there is similar dependency between each known sample in one domain and unknown samples in the other domain, there will be dependency between known samples in this domain. Until we reach this situation, the condition number will increase sharply since the equations become to be closely linearly dependent to each other. After this point, slight increase in the condition number will be observed since the effect of unknown samples becomes more similar for each known sample as $a \rightarrow 1$. As noted before, there is a limit to how much redundancy can be involved and this limit depends on the maximum number of known samples in one domain, or equivalently closeness

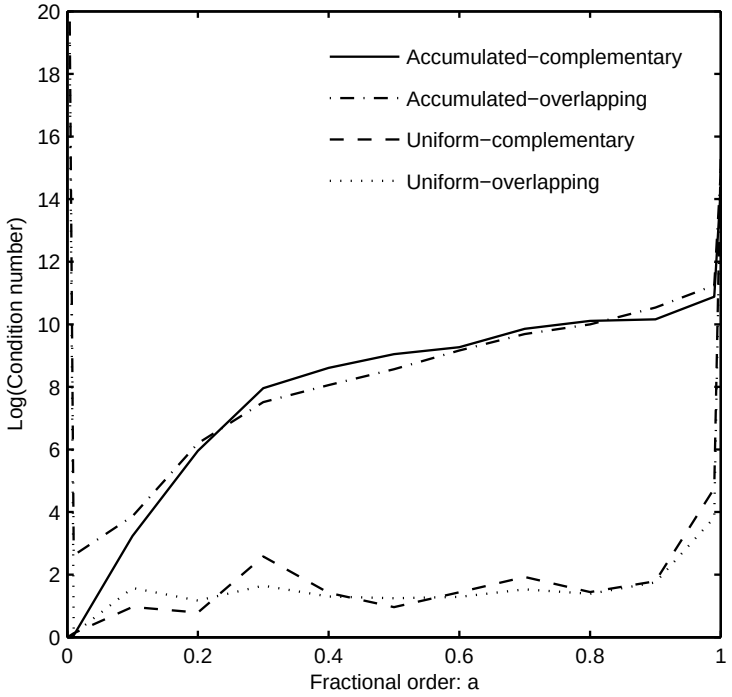

Figure 7.6: Condition number vs a for all distributions when $m_1 = 16$ and $m_2 = 240$

of m_1 to $N/2$. However, for different m_1 values that are close to $N/2$, it looks like the curves saturate to the same level for large values of a. In fact, this is not true because saturation is due to the precision limits of Matlab. If we had enough high precision, the levels would be seperated for each different value of m_1. We have checked that when we have lower precision, the condition number for lower values of m_1 also saturates to the same level with the higher m_1 values. Thus, as m_1 increases, condition number increases only within the precision limits.

Now, let us also investigate the accumulated-overlapping case. In this case, for the values of m_1 that are close to $N/2$ (more precisely, for $m_1 > 32$), the condition number is not within precision limits for any value of fractional order a. We can obtain condition numbers which are within the precision limits only for considerably uneven distributions (more precisely, for $m_1 \leq 32$). As we have discussed before, there is a lower limit for redundancy, which depends on the

maximum number of known samples in one domain. For $a = 0$ case, we have strict redundancy and the known information is at its lower limit. For considerably uneven distributions, this lower limit is still close to N. For this reason, even when a increases slightly from 0, it can get out of strict redundancy situation quickly since the additional information given by known samples in the other domain can fill much of this information gap. However, for nearly even distributions, the difference between the lower limit and N is large, and thus the additional information from other known samples can not close this difference since the relative dependency between these points is high as discussed before. Moreover, as the order increases, this relative dependency also increases slightly due to having more similar effects. In fact, for larger values of a, overlapping case gives similar results with the complementary case. This result is expected since for large values of a, the domains are far apart from each other and the content of the overlaps between the cones starts to be similar in terms of both common known and unknown samples. Thus, being complementary or overlapping does not create much difference on the dependency between known points when a is large. But note that the complementary case performs better than the overlapping case for small values of a. We can generalize this result such that shifts in known points in one domain does not affect much the amount of information they carry when two domains are not very close to each other. For the accumulated-complementary distribution, we finally note that since the discrete FRT has a periodic nature, the effect of one sample at the edge continues at the other edge, which adds complementarity to the problem in contrast to defining it as an overlapping distribution. Although this behaviour does not exist in the continuous case, here we obtain better results in the discrete case compared to the real physical situation due to this behaviour.

As clearly seen from figure 7.6, uniform distribution gives better condition numbers than the accumulated distribution. Thus, measurements that spread all over the plane carries more information than the same number of measurements

that are concentrated in a particular region. To see this, consider our usual cones from knowns in the domain with fewer number of known samples. For small values of a, there is only one unknown inside each cone, which corresponds to the optimal case, and thus there is no dependency between the known samples. However, if we increase a further, depending on the value of m_1, after some point each cone starts to contain common unknowns with the other cones. This will cause a small increase in the condition number until each cone contains all the unknowns in the other domain. This increase is very small compared to the accumulated case because, since known samples are apart from each other, dependency of each known point to unknown points in the other domain is different for different known points. That is, each known point is affected by one unknown sample dominantly and since this dominant unknown sample is different for each known sample, there is still less dependency between known points. As we take known samples more closely to each other (or equivalently, as $m_1 \to N/2$), this relative dependency will be larger and so will the condition number. If we increase a beyond the point where each cone contains all the unknowns, slight changes in the condition number can be observed due to the equalization of the effects as $a \to 1$. In the uniform case, there is strict redundancy at $a = 1$ since the matrix is rank deficient in this case (see the appendix for a proof). Thus, the values at $a = 1$ are not much meaningful due to numerical limitations since it should be theoretically infinite in this case. But, note that the values at these points are also not much relevant for our interpretations. As similar with the accumulated case, the uniform-overlapping case will be similar with the uniform-complementary case after it gets rid of the strict redundancy at $a = 0$.

7.4.2 Case where total number of knowns are more than the number of unknowns

This experiment investigates the improvement in the condition number when $m_1 + m_2 \geq N$, or equivalently when we increase the total number of known samples beyond N. The curves in figure 7.7 and 7.8 are obtained by starting with the $m_1 = 16$ and $m_2 = 240$ case and doubling m_1 each time. We see that as we increase the number of known samples in one domain, the large condition numbers in the accumulated case improves very quickly while considerably small condition numbers in the uniform case get better. Thus the amount of information that will be used for the recovery of the signal becomes better. Also observe that for accumulated distributions, even when we exceed N considerably, the condition number is not small enough for large values of a. The behaviour of the curves can be understood with similar cone investigations. For instance, for accumulated-complementary case, the sharp increase in the condition number will start when the overlap between each two cones contains at least one unknown since this will create dependency between known samples.

We modify the previous investigation such that m_2 also increases while m_1 doubles. As seen from figures 7.9 and 7.10, improvement is observed for the accumulated distribution compared to the previous case. For the accumulated distribution, the increase in the condition number starts later, which is because, the overlap between each two cones starts to contain at least one unknown for a larger value of a. Moreover, the condition number saturates to lower values for all m_1 and m_2 pairs. This is because, since maximum number of known samples in one domain has increased, the lower limit to how much redundancy involved has also increased.

Lastly, we investigate the case when there are equal number of samples in both domains. As seen from figures 7.11 and 7.12, condition number is very small for

most of the distributions. However, for accumulated-overlapping distribution, even considerably large number of known samples do not give small condition numbers for relatively small values of a. That is, it can not quickly move away from the strict redundancy case. We can see the reason from the cones easily. For small values of a, there are unknowns which are not covered by any of the cones originating from knowns in the other domain. Thus, roughly speaking, all of the knowns in one domain say nothing about some unknowns in the other domain. This situation is overcomed when every unknown is covered by at least one cone. Up to this point, condition number will get better quickly and after this point, smaller changes will occur on the condition number.

7.4.3 Case when partial information is given in four domains

Up to this point, we have considered the problem of recovering signals from partial fractional Fourier domain information when two domains are involved. Generalization of this investigation to multiple domains is desired. A preliminary work is performed on this subject. For this, we consider four FRFDs and the order of each domain is chosen such that they are equally separated equal with intervals of Δa. We investigate the case when all the known samples are equally distributed between each domain for different distributions. Without loss of generality, we can say that the 0th order plane does not contain any known sample so that we can choose it as our reference plane. Since we choose an empty plane as reference, the formulation will be an extended version of the one given in (7.13). The condition number for different values of Δa and for different distributions is obtained as shown in table 7.1. One can also investigate the condition number for random distribution of known points to multiple domains.

Δa	Accumulated-Complementary	Accumulated-Overlapping	Uniform-Complementary	Uniform-Overlapping)
0.125	2.2076	1.4002e+003	2.4315	1.4711e+017
0.25	4.0786	175.9445	7.7509	2.7279e+017

Table 7.1: Condition number for four domain case

7.5 Future Work

It may be possible to derive the condition number explicitly for arbitrary sample distributions by using the discrete FRT given in [4], since this matrix has a closed form expression. One can also find optimal or suboptimal measurement places for the signal recovery problem by using minimum condition number criteria. This approach has been used in different areas in the literature [67, 68] and is here left as a subject for future study. It may be also interesting to recover real physical signals with the approach given in this work and compare the recovery error vs. fractional order with our condition number plots. Applicability of this work to phase retrieval problems and to other parametric transforms different than FRT are also left for future work.

For future research, we also note that the definition of the condition number used in this work is affected by the row and column scaling [66], which is not consistent with its interpretation as the measure of dependent information. The definition in [69] given by

$$\text{cond}(\mathbf{A}) = |||\mathbf{A}^{-1}||\mathbf{A}||| \tag{7.20}$$

is invariant under row scaling, and thus may be more appropriate for our purposes. After some preliminary work performed on this issue, we have observed that both definitions give similar curves, only with the small difference that the latter has a little more smoother variations compared to the former. This indicates that we typically do not encounter with poorly scaled matrices in this work.

7.6 Appendix

Let us first consider the complementary case such that multiples of P are unknown in the time domain and multiples of P are known in the frequency domain. Assume that N is a multiple of P^2. We want to prove the rank deficiency of the system matrix $\mathbf{F}^a(\mathbf{n}, \bar{\mathbf{k}})$. As is well-known, the elements of the lth row of the DFT matrix are $e^{-j\frac{2\pi}{N}ln}$ where the sample index n is an integer running from 0 to $N-1$. We can obtain the system matrix from the DFT matrix by choosing its rows and columns that are multiples of P. The size of this submatrix is $\frac{N}{P} \times \frac{N}{P}$. The entry that lies in the kth row and the mth column of the submatrix is given by $e^{-j\frac{2\pi}{N}(Pk)(Pm)}$. Rank deficiency can occur when some rows of the matrix are repeated, or equivalently when

$$e^{-j\frac{2\pi}{N}(Pk)(Pm)} = e^{-j\frac{2\pi}{N}(P(k+T))(Pm)} \tag{7.21}$$

$$1 = e^{-j\frac{2\pi}{N}P^2Tm} \tag{7.22}$$

The above equality is satisfied for all values of m (for all elements in a row) if and only if $T = \frac{N}{P^2}$. As a result, the first $\frac{N}{P^2}$ rows are repeated P times inside the system matrix, and thus the number of independent rows is $\frac{N}{P^2}$, which gives the rank of the matrix. Thus, the rank is $1/P$th of the matrix size. That is, N/P^2 known samples carry the same information as the N/P known samples in the frequency domain.

Another way to see this result is to write the equations for the known samples in the frequency domain in terms of the unknown samples in the time domain. Let us denote the signal and its Fourier transform as x and X, and divide the known samples in the frequency domain to P equal intervals as $X[Pk], X[N/P+$

$Pk], ..., X[N - N/P + Pk]$ with $k = 0, 1, ..., \frac{N}{P^2} - 1$. Then, we have

$$\begin{aligned} X\left[\frac{N}{P}m + Pk\right] &= \frac{1}{\sqrt{N}} \sum_{n=0}^{N-1} x[n] e^{-j\frac{2\pi}{N}(\frac{N}{P}m+Pk)n} \\ &= \frac{1}{\sqrt{N}} \sum_{n=0}^{N/P-1} x[Pn] e^{-j\frac{2\pi}{P}Pmn} e^{-j\frac{2\pi}{N}P^2kn} + \text{Additional terms} \\ &= \frac{1}{\sqrt{N}} \sum_{n=0}^{N/P-1} x[Pn] e^{-j\frac{2\pi}{N}P^2kn} + \text{Additional terms} \end{aligned} \tag{7.23}$$

where $m = 0, 1, \ldots, P-1$, and the additional terms depend on known samples in the time domain. Here, again the rows of the system matrix will be repeated P times with each repetition being of length N/P^2. Here, unorganized DFT with nonnegative indices is used, but the result can be easily extended to the samples with negative indices by using the periodicity of the DFT.

As proved in section 7.3, the condition number remains the same when we exchange the known and unknown samples between two domains. As a result, the above result for rank deficiency is also valid when multiples of P are known in the time domain and multiples of P are unknown in the frequency domain.

Let us now investigate the overlapping case, which corresponds to the case when all samples in the frequency domain are shifted by the same amount. Let multiples of P be unknown in the time domain and $X[Pk + c]$ are given in the frequency domain where c is an arbitrary integer. Then, the rank-deficiency result will still be valid since all equations will be multiplied with the same constant. Shifting the known points in the time domain will also give the same result from the equivalence of the problems. Thus, we can conclude that if known samples in one domain and unknown samples in the other domain goes with equal intervals of length P, then rank deficiency always occurs regardless of their starting point.

We can generalize the above rank deficiency result for the following signal recovery problem: Multiples of P or a shifted version of this are unknown (known) in the time domain and arbitrary samples are known (unknown) in the frequency

domain. In this more general case, the known samples in the frequency domain can be categorized into P different subsequences of the interval $[0, N-1]$, each going with intervals of P:

$$\begin{array}{cccc} 0, & P, & 2P, & 3P & \dots \\ 1, & 1+P, & 1+2P, & 1+3P & \dots \\ 2, & 2+P, & 2+2P, & 2+3P & \dots \\ \vdots & \vdots & \vdots & \vdots & \\ P-1, & 2P-1, & 3P-1, & 4P-1 & \dots \end{array} \tag{7.24}$$

We know from previous investigation that each different sequence will give N/P^2 independent rows and the matrix will be repeated after N/P^2 rows. Since we have totally P sequences, when all of the N samples are given, the matrix will have $P(N/P^2) = N/P$ independent rows, and thus will have full rank. However, we do not need all of the N samples in the frequency domain to achieve full-rank, indeed N/P samples will be sufficient. In order to obtain a full rank matrix for the signal recovery problem, we should choose N/P samples as following: Take N/P^2 samples from each sequence, but the distance between any two sample should never be a multiple of N/P^2. As a final remark, we note that this approach is only for obtaining full-rank matrices and may not guarantee that it has a small condition number.

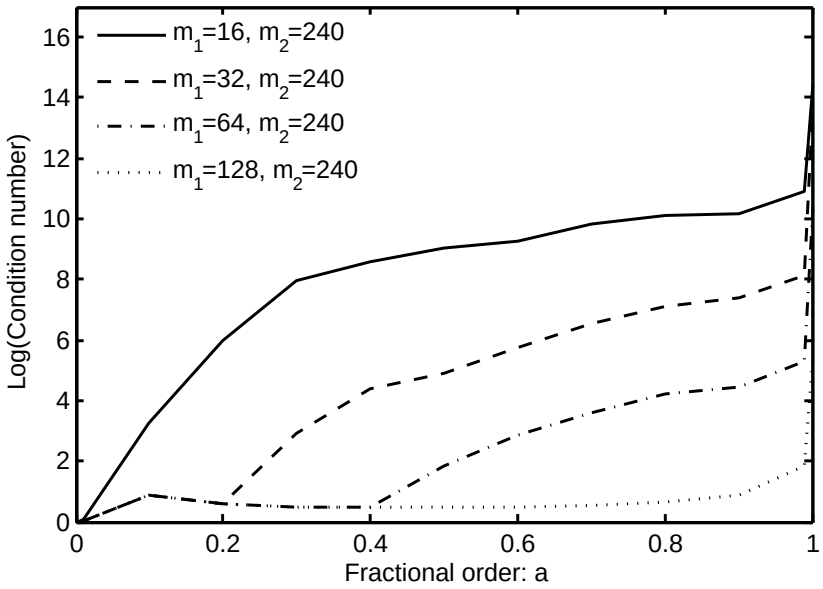

(a) Accumulated-complementary distribution

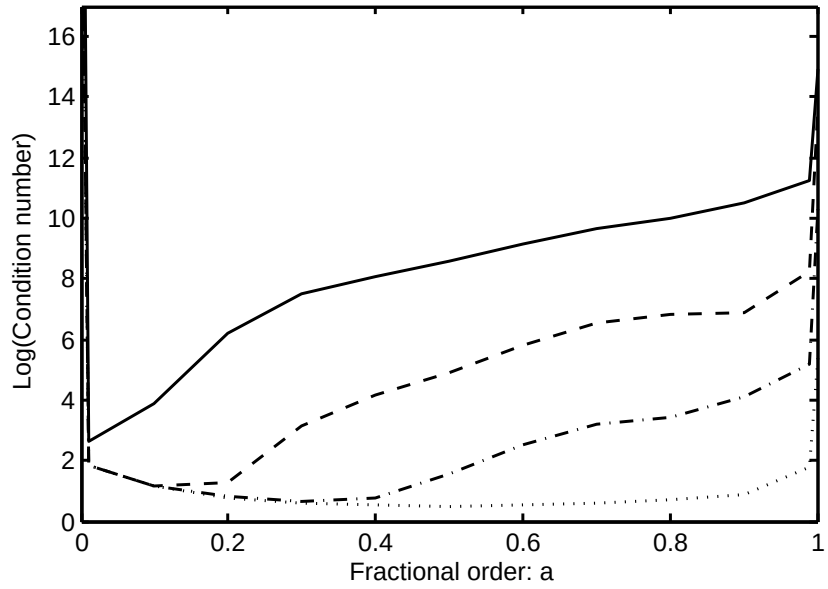

(b) Accumulated-overlapping distribution

Figure 7.7: Condition number vs a for accumulated distribution when $m_1+m_2 \geq N$ and m_1 is doubled each time (The legend is valid for both plots)

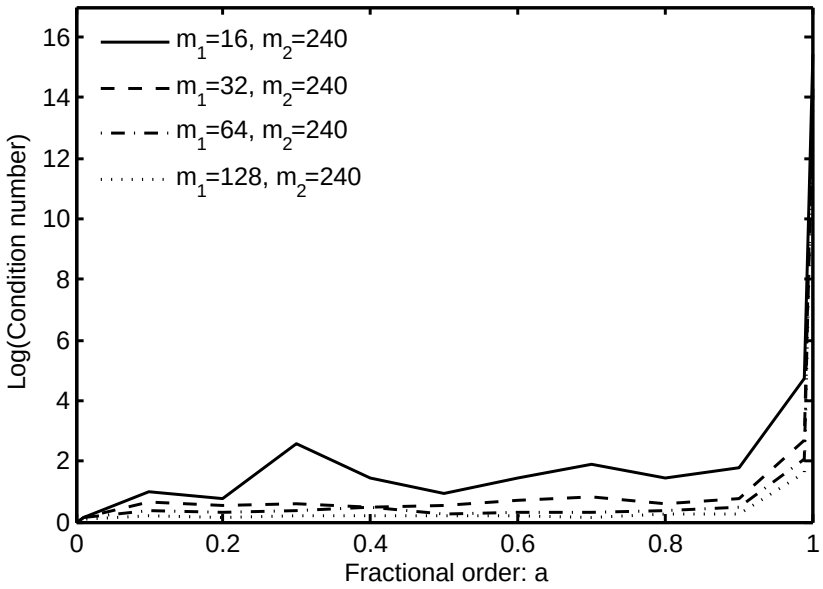

(a) Uniform-complementary distribution

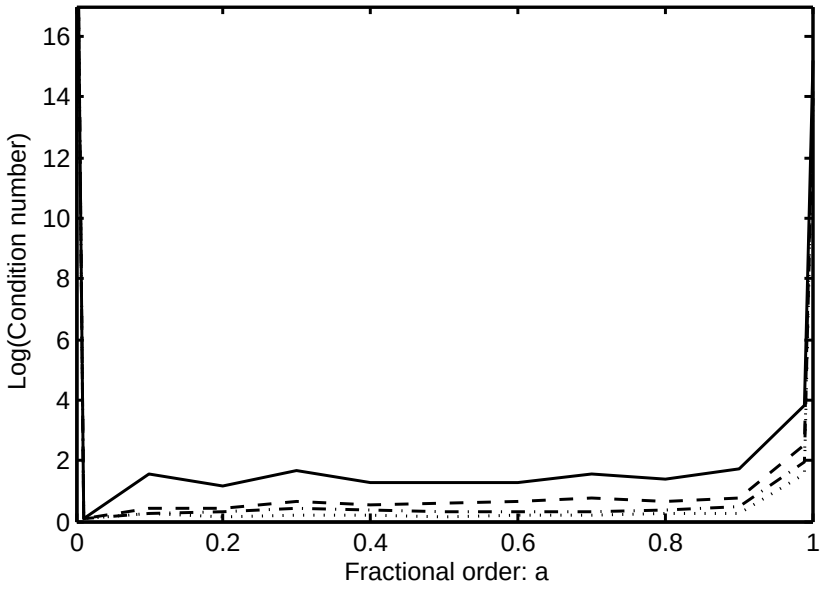

(b) Uniform-overlapping distribution

Figure 7.8: Condition number vs a for uniform distribution when $m_1 + m_2 \geq N$ and m_1 is doubled each time (The legend is valid for both plots)

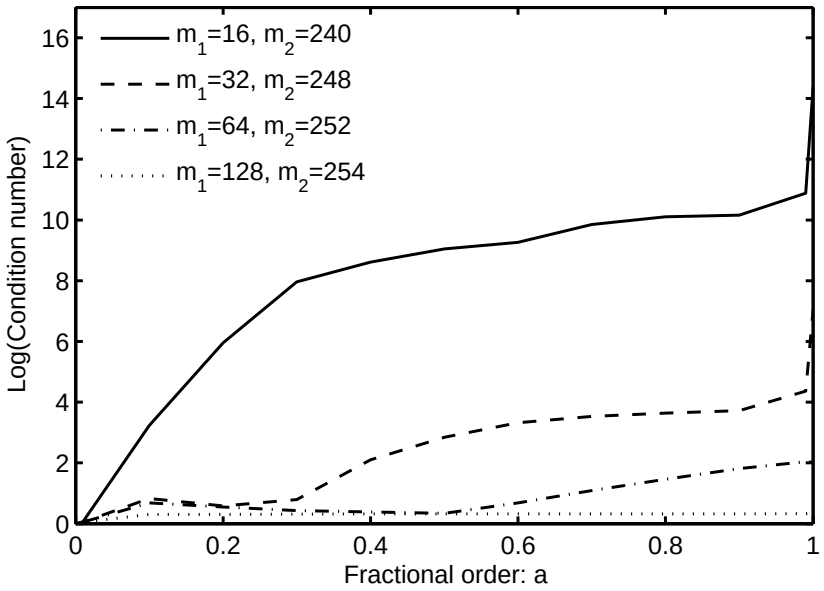

(a) Accumulated-complementary distribution

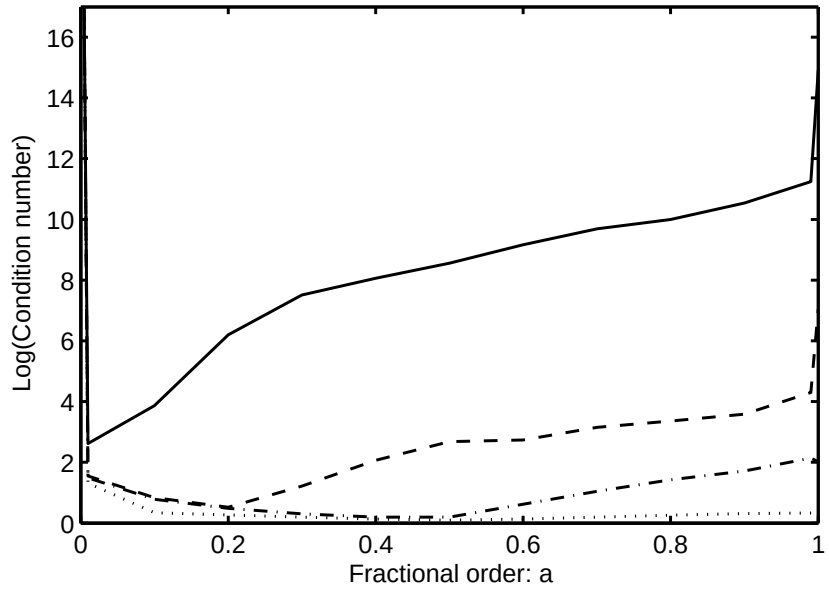

(b) Accumulated-overlapping distribution

Figure 7.9: Condition number vs a for accumulated distribution when $m_1+m_2 \geq N$ with m_1 doubled and m_2 increased each time (The legend is valid for both plots)

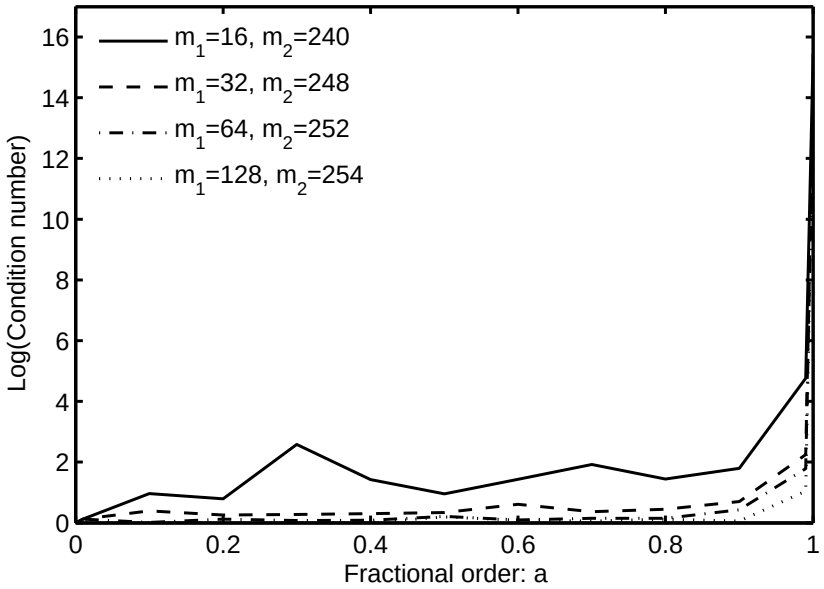

(a) Uniform-complementary distribution

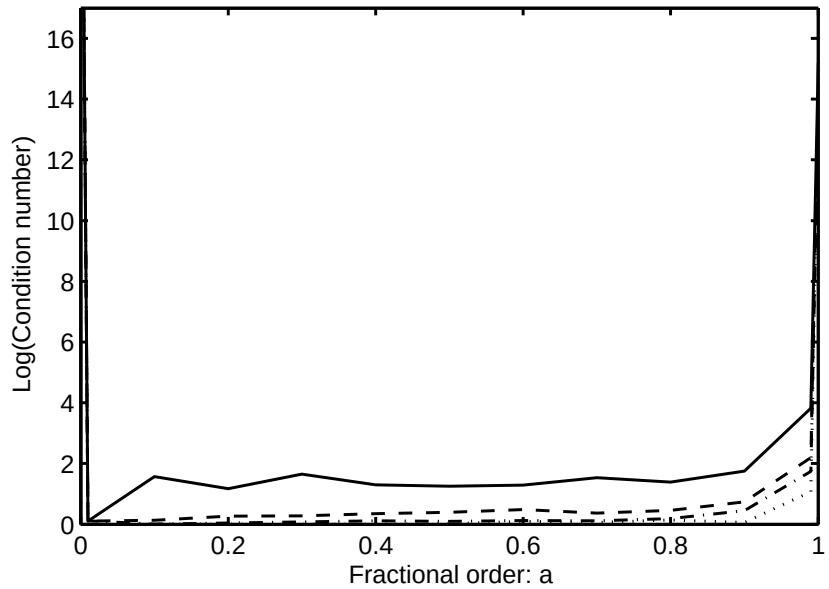

(b) Uniform-overlapping distribution

Figure 7.10: Condition number vs a for uniform distribution when $m_1 + m_2 \geq N$ with m_1 doubled and m_2 increased each time (The legend is valid for both plots)

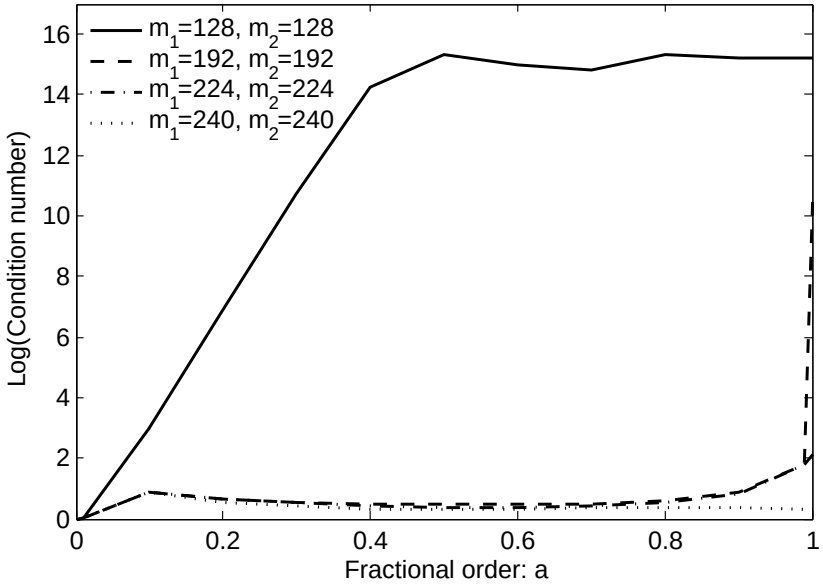

(a) Accumulated-complementary distribution

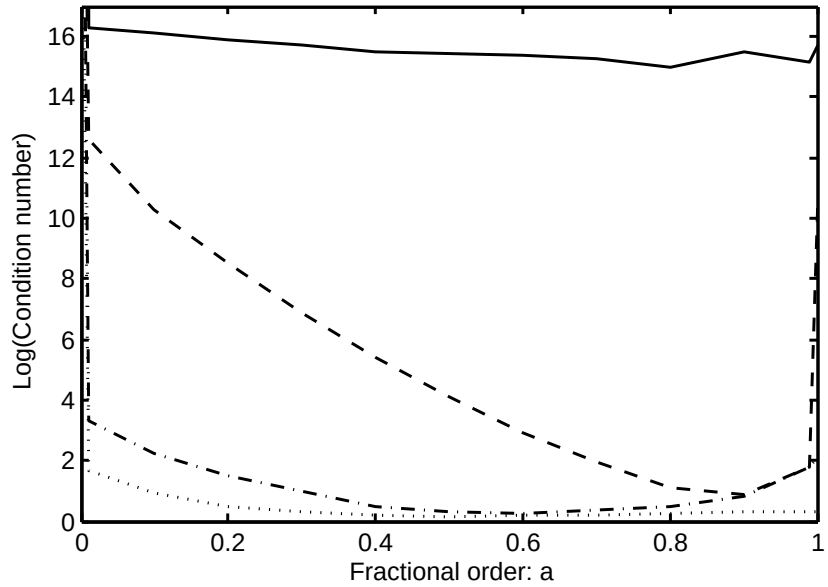

(b) Accumulated-overlapping distribution

Figure 7.11: Condition number vs a for accumulated distribution when $m_1+m_2 \geq N$ and $m_1 = m_2$ (The legend is valid for both plots)

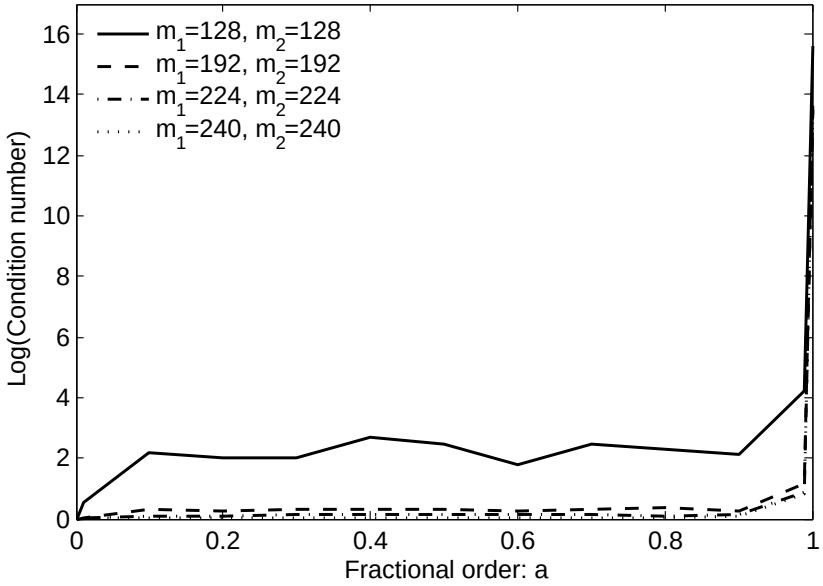

(a) Uniform-complementary distribution

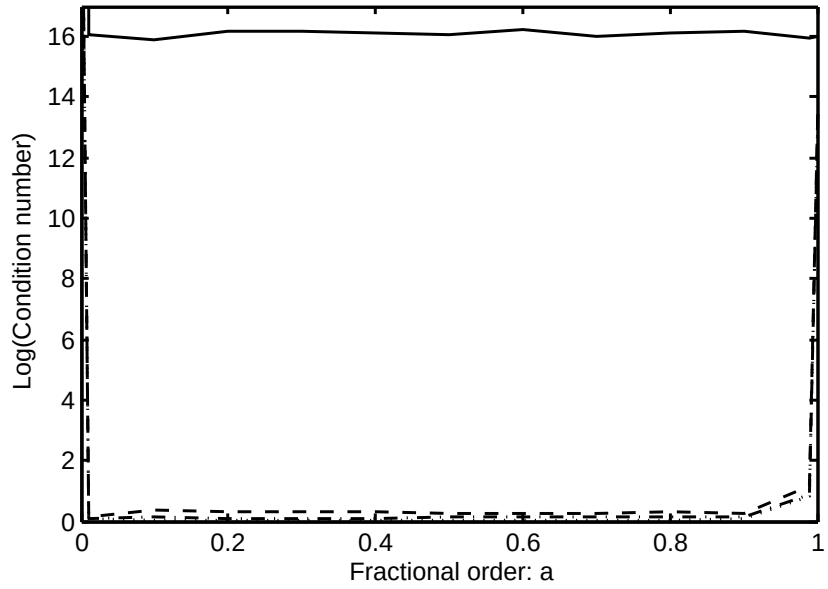

(b) Uniform-overlapping distribution

Figure 7.12: Condition number vs a for uniform distribution when $m_1 + m_2 \geq N$ and $m_1 = m_2$ (The legend is valid for both plots)

Chapter 8

CONCLUSIONS

In the first part of the thesis, we have studied a number of fundamental issues associated with signal representation under finite extent contraints in the FRT or LCT domains. First of all, we have developed the notion of the bicanonical width product, which is the number of degrees of freedom of the set of signals which are confined to finite intervals in two arbitrary LCT domains. This result is significant since it constitutes a generalization of the ordinary time-bandwidth product. Moreover, we have showed that the bicanonical width product is the area of the time-frequency support of this set of signals, which is simply given by a parallelogram. Furthermore, these signals can be represented in these two LCT domains with the minimum number of samples, given by the bicanonical width product.

In addition, we have addressed to the problem of finding the minimum number of samples to represent arbitrary signals based on the LCT sampling criteria and figured out the LCT domains in which we can represent the signal with that minimum number of samples, given by the bicanonical width product. We have showed that this problem reduces to a simple geometrical problem, which aims to find the smallest parallelogram enclosing a given time-frequency support.

By using this equivalence, we have seen that the bicanonical width product will provide a better fit to the actual number of degrees of freedom of an arbitrary signal as compared to the time-bandwidth product. Thus, it allows us to represent the signal with fewer numbers of samples. Theoretical bounds on the representational efficiency of this approach have been also provided. With this, we have showed that for an arbitrary convex polygonal space-frequency support, the number of samples to represent the signal with this approach is at most two times the actual number of degrees of freedom of the signal.

Furthermore, we extend this approach and its equivalent geometrical problem to the problem of representing signals at a specific domain. In this case, the bicanonical width product provides fewer number of samples than the time-bandwidth product, with the difference being substantial in some cases.

In the process, we have accomplished to relate LCT domains to the time-frequency plane. We have showed that each LCT domain is essentially a scaled FRT domain, and thus any LCT domain can be labeled only by its associated fractional order a. As a result, throughout an optical system, we can label any plane with only one parameter a even though LCTs have three parameters. Thus the puzzling aspects of a three-parameter family of domains, especially the problem of how these domains are sequenced or structured, is eliminated and instead, we can view them them as FRT domains of monotonicly increasing order.

We have also presented the exact relation between the continuous LCT and the discrete LCT, which provides the underlying foundation for approximately computing the samples of the LCT of a continuous signal with the DLCT. We have showed that, provided N is chosen to be at least equal to the bicanonical width product of the set of signals we are dealing with, the DLCT which can be efficiently computed by taking $N \log N$ time can be used to obtain a good approximation to the continuous LCT. With this, we have accomplished to use

the DLCT such that the number of samples in both domains are equal to each other regardless of the LCT parameters, and this number of samples is the minimum possible for both domains, for the given extents. In addition, we have showed that an interval independent definition of the DLCT can be used to approximately compute continuous LCTs. This new definition would be useful in studies which are formulated in a purely discrete setting and in developing fast transform algorithms. In the process, we have also defined the linear canonical series, which is the generalization of the ordinary Fourier series.

We have lastly analyzed arbitrary quadratic-phase optical systems with arbitrary numbers of apertures. The number of degrees of freedom of the system has been found both as a region and as a number in terms of the system parameters, and the redundant and effective apertures have been investigated. Moreover, we have developed a method to investigate the change in the extent of an arbitrary input signal throughout the system. Based on this method, we have also derived formulas to directly trace the extent from the given extents of the input signal. These extents are useful to find the minimum number of samples to represent the wave at an arbitrary plane and to simulate the optical system with discrete-time systems with the same degree of accuracy compared to continuous systems.

In the second part, we have turned our attention to signal recovery problems under partial and redundant information in multiple transform domains. We have proposed a novel linear algebraic approach to these problems and used the condition number as a measure of the redundant information in given samples. By analyzing the effect of the number of known samples and their distributions on the condition number, we have explored the redundancy and information relations between the given data under different partial information conditions.

We have observed that distributing known samples equally to each domain causes the largest amount of redundant information in the given data. Moreover, measurements that spread all over the planes carry more information than

the same number of measurements that are concentrated in a particular region. Roughly speaking, as a increases, the amount of redundant information increases. Besides, being complementary or overlapping does not create much difference on the dependency between known points when a is not very small. However, for small values of a, the complementary distribution is better conditioned than the overlapping case.

In the process, we have found the effectiveness region of an input point and the dependency region of an output point. We have showed that these regions expand as the fractional order increases for both continuous-time and discrete-time FRT systems. That is, for small values of a, there is only local dependency and as $a \to \infty$, the contribution of all points are equalized. These concepts have been used to interpret the simulation results.

Bibliography

[1] H. M. Ozaktas and M. F. Erden, "Relationships among ray optical, gaussian beam, and fractional fourier transform descriptions of first-order optical systems," *Opt. Commun.*, vol. 143, no. 1–3, pp. 75–86, 1997.

[2] H. M. Ozaktas, Z. Zalevsky, and M. A. Kutay, *The Fractional Fourier Transform with Applications in Optics and Signal Processing.* New York: Wiley, 2001.

[3] B. Barshan, M. A. Kutay, and H. M. Ozaktas, "Optimal filtering with linear canonical transformations," *Opt. Commun.*, vol. 135, pp. 32–36, 1997.

[4] S.-C. Pei and J.-J. Ding, "Closed-form discrete fractional and affine fourier transforms," *IEEE Trans. Signal Process.*, vol. 48, no. 5, pp. 1338–1353, May 2000.

[5] B. M. Hennelly and J. T. Sheridan, "Generalizing, optimizing, and inventing numerical algorithms for the fractional fourier, fresnel, and linear canonical transforms," *J. Opt. Soc. Am. A*, vol. 22, no. 5, pp. 917–927, 2005.

[6] A. Papoulis, *Signal Analysis.* New York: McGraw-Hill, 1977.

[7] F. S. Oktem and H. M. Ozaktas, "Exact relation between continuous and discrete linear canonical transforms," *IEEE Signal Process. Lett.*, vol. 16, no. 8, pp. 727–730, Aug. 2009.

[8] K. B. Wolf, *Integral Transforms in Science and Engineering.* Plenum Press, 1979.

[9] T. Erseghe, P. Kraniauskas, and G. Carioraro, "Unified fractional fourier transform and sampling theorem," *IEEE Trans. Signal Process.*, vol. 47, no. 12, pp. 3419–3423, Dec 1999.

[10] C. Candan, M. Kutay, and H. Ozaktas, "The discrete fractional fourier transform," *IEEE Trans. Signal Process.*, vol. 48, no. 5, pp. 1329–1337, May 2000.

[11] T. Erseghe, N. Laurenti, and V. Cellini, "A multicarrier architecture based upon the affine fourier transform," *IEEE Trans. Commun.*, vol. 53, no. 5, pp. 853–862, May 2005.

[12] J. J. Ding, "Research of fractional fourier transform and linear canonical transform," Ph.D. dissertation, National Taiwan Univ., Taipei, Taiwan, 2001.

[13] A. Stern, "Sampling of linear canonical transformed signals," *Signal Process.*, vol. 86, no. 7, pp. 1421–1425, 2006.

[14] B. Deng, R. Tao, and Y. Wang, "Convolution theorems for the linear canonical transform and their applications," *Sci. China Ser. F Inform. Sci.*, vol. 49, no. 5, pp. 592–603, 2006.

[15] C. Candan and H. M. Ozaktas, "Sampling and series expansion theorems for fractional fourier and other transforms," *Signal Process.*, vol. 83, pp. 1455–1457, 2003.

[16] S.-C. Pei, M.-H. Yeh, and T.-L. Luo, "Fractional fourier series expansion for finite signals and dual extension to discrete-time fractional fourier transform," *IEEE Trans. Signal Process.*, vol. 47, no. 10, pp. 2883–2888, Oct 1999.

[17] H. Ozaktas and U. Sumbul, "Interpolating between periodicity and discreteness through the fractional fourier transform," *IEEE Trans. Signal Process.*, vol. 54, no. 11, pp. 4233–4243, Nov. 2006.

[18] J. J. Healy and J. T. Sheridan, "Cases where the linear canonical transform of a signal has compact support or is band-limited," *Opt. Lett.*, vol. 33, no. 3, pp. 228–230, 2008.

[19] A. Koc, H. M. Ozaktas, C. Candan, and M. A. Kutay, "Digital computation of linear canonical transforms," *IEEE Trans. Signal Process.*, vol. 56, no. 6, pp. 2383–2394, June 2008.

[20] H. M. Ozaktas, B. Barshan, D. Mendlovic, and L. Onural, "Convolution, filtering, and multiplexing in fractional fourier domains and their relation to chirp and wavelet transforms," *J. Opt. Soc. Am. A*, vol. 11, no. 2, pp. 547–559, 1994.

[21] X.-G. Xia, "On bandlimited signals with fractional fourier transform," *IEEE Signal Process. Lett.*, vol. 3, no. 3, pp. 72–74, Mar 1996.

[22] A. Zayed, "On the relationship between the fourier and fractional fourier transforms," *IEEE Signal Process. Lett.*, vol. 3, no. 12, pp. 310–311, Dec 1996.

[23] R. Torres, P. Pellat-Finet, and Y. Torres, "Sampling theorem for fractional bandlimited signals: A self-contained proof. application to digital holography," *IEEE Signal Process. Lett.*, vol. 13, no. 11, pp. 676–679, Nov. 2006.

[24] R. Tao, B. Deng, W.-Q. Zhang, and Y. Wang, "Sampling and sampling rate conversion of band limited signals in the fractional fourier transform domain," *IEEE Trans. Signal Process.*, vol. 56, no. 1, pp. 158–171, Jan. 2008.

[25] J. J. Healy, B. M. Hennelly, and J. T. Sheridan, "Additional sampling criterion for the linear canonical transform," *Opt. Lett.*, vol. 33, no. 22, pp. 2599–2601, 2008.

[26] J. J. Healy and J. T. Sheridan, "Sampling and discretization of the linear canonical transform," *Signal Process.*, vol. 89, pp. 641–648, 2009.

[27] A. W. Lohmann, *Optical Information Processing.* lecture notes. Optik+Info, Post Office Box 51, Uttenreuth, Germany, 1986.

[28] A. W. Lohmann, R. G. Dorsch, D. Mendlovic, Z. Zalevsky, and C. Ferreira, "Space-bandwidth product of optical signals and systems," *J. Opt. Soc. Am. A*, vol. 13, no. 3, pp. 470–473, 1996.

[29] D. Gabor, "Light and information," in *Progress In Optics*, E. Wolf, Ed. Elsevier, 1961, vol. I, ch. 4, pp. 109–153.

[30] F. Gori, "Sampling in optics," in *Advanced Topics in Shannon Sampling and Interpolation Theory.* New York: Springer, 1993, ch. 2, pp. 37–83.

[31] F. Gori and G. Guattari, "Effects of coherence on the degrees of freedom of an image," *J. Opt. Soc. Am.*, vol. 61, no. 1, pp. 36–39, 1971.

[32] ——, "Shannon number and degrees of freedom of an image," *Opt. Commun.*, vol. 7, no. 2, pp. 163–165, February 1973.

[33] ——, "Degrees of freedom of images from point-like-element pupils," *J. Opt. Soc. Am.*, vol. 64, no. 4, pp. 453–458, 1974.

[34] F. Gori, S. Paolucci, and L. Ronchi, "Degrees of freedom of an optical image in coherent illumination, in the presence of aberrations," *J. Opt. Soc. Am.*, vol. 65, no. 5, pp. 495–501, 1975.

[35] F. Gori and L. Ronchi, "Degrees of freedom for scatterers with circular cross section," *J. Opt. Soc. Am.*, vol. 71, no. 3, pp. 250–258, 1981.

[36] L. Ronchi and F. Gori, "Degrees of freedom for spherical scatterers," *Opt. Lett.*, vol. 6, no. 10, pp. 478–480, 1981.

[37] G. Francia, "Resolving power and information," *J. Opt. Soc. Am.*, vol. 45, no. 7, pp. 497–499, 1955.

[38] T. Alieva and M. J. Bastiaans, "Alternative representation of the linear canonical integral transform," *Opt. Lett.*, vol. 30, no. 24, pp. 3302–3304, 2005.

[39] M. J. Bastiaans and T. Alieva, "Synthesis of an arbitrary abcd system with fixed lens positions," *Opt. Lett.*, vol. 31, no. 16, pp. 2414–2416, 2006.

[40] J. A. Rodrigo, T. Alieva, and M. L. Calvo, "Optical system design for orthosymplectic transformations in phase space," *J. Opt. Soc. Am. A*, vol. 23, no. 10, pp. 2494–2500, 2006.

[41] H. M. Ozaktas and O. Aytur, "Fractional fourier domains," *Signal Process.*, vol. 46, no. 1, pp. 119–124, 1995.

[42] O. Aytur and H. M. Ozaktas, "Non-orthogonal domains in phase space of quantum optics and their relation to fractional fourier transforms," *Opt. Commun.*, vol. 120, no. 3–4, pp. 166–170, 1995.

[43] H. Zhao, Q.-W. Ran, J. Ma, and L.-Y. Tan, "On bandlimited signals associated with linear canonical transform," *IEEE Signal Process. Lett.*, vol. 16, no. 5, pp. 343–345, May 2009.

[44] G.-X. Xie, B.-Z. Li, and Z. Wang, "Identical relation of interpolation and decimation in the linear canonical transform domain," in *Proc. Int. Conf. Signal Process.*, Oct. 2008, pp. 72–75.

[45] K. Sharma and S. Joshi, "Uncertainty principle for real signals in the linear canonical transform domains," *IEEE Trans. Signal Process.*, vol. 56, no. 7, pp. 2677–2683, July 2008.

[46] B. Evans, J. Teich, and C. Schwarz, "Automated design of two-dimensional rational decimation systems," in *Proc. IEEE Asilomar Conf. Signals, Systems, and Computers*, vol. 1, Oct. 31 - Nov. 2 1994, pp. 498–502.

[47] V. Isler and R. Bajcsy, "The sensor selection problem for bounded uncertainty sensing models," in *Proc. IEEE Int. Symp. Information processing in sensor networks*, 2005, pp. 151–158.

[48] A. D. Vainshtein, "Construction of the minimal enclosing parallelogram," *Diskretnaya Matematika*, vol. 2, no. 4, pp. 72–81, 1990.

[49] C. Schwarz, J. Teich, E. Welzl, and B. Evans, "On finding a minimal enclosing parallelogram," International Computer Science Institute, Berkeley, CA, Tech. Rep. tr-94–036, Feb. 1994.

[50] R. L. Graham, "An efficient algorithm for determining the convex hull of a finite planar set," *Information Processing Lett.*, vol. 1, no. 4, pp. 132–133, 1972.

[51] H. S. M. Coxeter, "The classification of zonohedra by means of projective diagrams," *Journal de Math. Pures Appl.*, vol. 41, pp. 137–156, 1962.

[52] L. Durak and O. Arikan, "Generalized time-bandwidth product optimal short-time fourier transformation," in *Proc. IEEE Int. Conf. Acoustics, Speech, and Signal Process.*, vol. 2, 2002, pp. 1465–1468.

[53] ——, "Short-time fourier transform: two fundamental properties and an optimal implementation," *IEEE Trans. Signal Process.*, vol. 51, no. 5, pp. 1231–1242, May 2003.

[54] A. J. E. M. Janssen, "On the locus and spread of pseudo-density functions in the time-frequency plane," *Philips J. Res.*, vol. 37, pp. 79–110, 1982.

[55] L. Cohen, *Integral Time-Frequency Analysis.* Englewood Cliffs, NJ: Prentice-Hall, 1995.

[56] C. H. Dowker, "On minimum circumscribed polygons," *Bull. Amer. Math. Soc.*, vol. 50, no. 4, pp. 120–122, 1944.

[57] J. E. Boyce, D. P. Dobkin, R. L. Drysdale, and L. J. Guibas, "Finding extremal polygons," *SIAM Journal on Computing*, vol. 14, no. 1, pp. 134–147, 1985.

[58] A. Aggarwal, J. S. Chang, and C. K. Yap, "Minimum area circumscribing polygons," *The Visual Computer: Int. J. Graphics*, vol. 1, no. 2, pp. 112–117, 1985.

[59] J. Zhao, R. Tao, and Y. Wang, "Sampling rate conversion for linear canonical transform," *Signal Process.*, vol. 88, no. 11, pp. 2825–2832, 2008.

[60] H. M. Ozaktas and D. Mendlovic, "Fractional fourier optics," *J. Opt. Soc. Am. A*, vol. 12, no. 4, pp. 743–751, 1995.

[61] A. E. Cetin, H. Özaktaş, and H. M. Ozaktas, "Resolution enhancement of low resolution wavefields with POCS algorithm," *Electronics Lett.*, vol. 39, pp. 1808–1810, 2003.

[62] H. E. Guven, H. M. Ozaktas, A. E. Cetin, and B. Barshan, "Signal recovery from partial fractional fourier domain information and its applications," *IET Signal Process.*, vol. 2, pp. 15–25, 2008.

[63] M. Ertosun, H. Atli, H. Ozaktas, and B. Barshan, "Complex signal recovery from multiple fractional fourier-transform intensities," *Appl. Opt.*, vol. 44, no. 23, pp. 4902–4908, 2005.

[64] G. B. Esmer, V. Uzunov, L. Onural, H. M. Ozaktas, and A. Gotchev, "Diffraction field computation from arbitrarily distributed data points in space," *Signal Process.: Image Commun.*, vol. 22, pp. 178–187, 2007.

[65] A. Ozcelikkale, H. M. Ozaktas, and E. Arikan, "Optimal measurement under cost constraints for estimation of propagating wave fields," in *Proc. IEEE Int. Symp. Information Theory*, June 2007, pp. 696–700.

[66] M. T. Heath, *Scientific Computing: An Introductory Survey.* New York: Mc Graw Hill, 2002.

[67] C. Madtharad, S. Premrudeepreechacharn, N. Watson, and R. Saeng-Udom, "An optimal measurement placement method for power system harmonic state estimation," *IEEE Trans. Power Del.*, vol. 20, no. 2, pp. 1514–1521, April 2005.

[68] C. Rakpenthai, S. Premrudeepreechacharn, S. Uatrongjit, and N. Watson, "Measurement placement for power system state estimation by decomposition technique," in *Proc. Int. Conf. Harmonics and Quality of Power*, Sept. 2004, pp. 414–418.

[69] R. D. Skeel, "Scaling for numerical stability in gaussian elimination," *J. ACM*, vol. 26, no. 3, pp. 494–526, 1979.